

THESIS
2
2004
5455005

LIBRARY
Michigan State
University

This is to certify that the
dissertation entitled

Functional Analysis of OmtA and Subcellular Localization of
Aflatoxin Enzymes in *Aspergillus parasiticus*

presented by

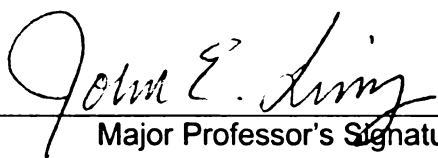
Li-Wei Lee

has been accepted towards fulfillment
of the requirements for the

Doctoral

degree in

Food Science and
Environmental Toxicology



Major Professor's Signature

11-25-03

Date

PLACE IN RETURN BOX to remove this checkout from your record.
 TO AVOID FINES return on or before date due.
 MAY BE RECALLED with earlier due date if requested.

DATE DUE	DATE DUE	DATE DUE
MAY 29 2007 JUN 24 10		
		.

FUNCTIONAL ANALYSIS OF *OMTA* AND SUBCELLULAR LOCALIZATION OF
AFLATOXIN ENZYMES IN *ASPERGILLUS PARASITICUS*

By

Li-Wei Lee

A DISSERTATION

Submitted to
Michigan State University
in partial fulfillment of the requirements
for the degree of

DOCTOR OF PHILOSOPHY

Department of Food Science and Human Nutrition

2003

ABSTRACT

FUNCTIONAL ANALYSIS OF *OMTA* AND SUBCELLULAR LOCALIZATION OF AFLATOXIN ENZYMES IN *ASPERGILLUS PARASITICUS*

By

Li-Wei Lee

Biosynthesis of aflatoxin is a complex process that involves the activities of at least 17 pathway enzymes. The distribution of these enzymes within fungal colonies and location within fungal cells are not known. The objective of this study was to investigate the distribution and sub-cellular location of Nor-1, Ver-1 and OmtA that represent early, middle and late enzymatic activities, respectively, in the aflatoxin biosynthetic pathway. My initial goal was to determine if OmtA is necessary and sufficient to catalyze the conversion of the aflatoxin pathway intermediate sterigmatocystin to O-methylsterigmatocystin *in vivo* and if this reaction is necessary for aflatoxin synthesis. I generated *A. parasiticus omtA* null mutant LW1432 and a maltose binding protein-OmtA fusion protein expressed in *Escherichia coli*. Enzyme activity analysis of OmtA fusion protein *in vitro* confirmed the reported catalytic function of OmtA. Feeding studies conducted on LW1432 demonstrated a critical role for OmtA and the reaction catalyzed by this enzyme in aflatoxin synthesis *in vivo*. Because of a close regulatory link between aflatoxin synthesis and asexual sporulation (conidiation), I hypothesized a spatial and temporal association between OmtA expression and conidiospore development. I developed a novel time-dependent colony fractionation protocol to analyze the accumulation and distribution of OmtA in fungal colonies grown on a solid medium that supports both toxin synthesis and conidiation. Using Western blot analysis, OmtA was

detected in all fractions of a 72h old colony including cells (0 to 24h) in which little conidiophore development was observed. OmtA in older fractions of the colony (24 to 72h) was partly degraded. Fluorescence-based immunohistochemical analysis demonstrated that OmtA is evenly distributed among different cell types and is not concentrated in conidiophores. These data suggest that OmtA is present in newly formed fungal tissue and then is proteolytically cleaved as cells in that section of the colony age.

Western blot analysis and immuno-fluorescence microscopy demonstrated the highest abundance of Nor-1, Ver-1 and OmtA in colony fraction 2 (24 to 48h) of SU1. Fungal tissues in this fraction were subjected to freeze-substitution, immuno-gold labeling with highly specific polyclonal antibodies, and analysis by transmission electron microscopy. Nor-1 and Ver-1 were primarily localized to the cytoplasm suggesting that they are cytosolic enzymes. OmtA was also detected in the cytoplasm. However, in cells located near the basal (substrate) surface of colony fraction 2 of SU1, large quantities of OmtA were detected in organelles identified as vacuoles. The role of this organelle in toxin biosynthesis is unclear. Based on data from this and previous studies, it is reasonable to assign two potential roles for the vacuole in aflatoxin synthesis: 1) as a means to reduce or limit aflatoxin synthesis, OmtA is transported to and inactivated in vacuoles via proteolytic cleavage; 2) as a means to shield the cell from the potential toxic effects of aflatoxin in the mycelium, OmtA is transported to the vacuole together with the late aflatoxin pathway intermediate ST. In the vacuole, OmtA is activated and ST is converted to OMST and further converted to AFB₁ by OrdA localized in or on the same vacuole. These hypotheses form the basis for my future studies on aflatoxin synthesis.

Copyright by

Li-Wei Lee

2003



ACKNOWLEDGMENTS

I would like to thank my major professor, Dr. John Linz. Without him, this dissertation would not have been possible.

I also would like to thank my committee members, Dr. James Pestka, Dr. Karen Klomparans, Dr. Gale Strasburg and Dr. Jay Schroeder.

Several people in the Linz laboratory provided a great deal of help including Ching-Hsun Chiou, Dr. Michael Miller, Matt Rarick, Dr. Shun-Hsin Liang and Dr. Ren-Qing Zhou. This help was greatly appreciated.

TABLE OF CONTENTS

LIST OF TABLES.....	ix
LIST OF FIGURES.....	x
CHAPTER 1	
Literature Review	1
Impact of aflatoxin contamination on health and the economy	1
Environmental factors affecting toxin production on crops - Temperature and Humidity	3
Aflatoxin biosynthesis and asexual sporulation	4
Aflatoxin biosynthesis	7
Aflatoxin gene cluster	7
Aflatoxin genes	9
<i>AflR</i>	9
<i>AflJ</i>	9
<i>fas1</i> , <i>fas2</i> and <i>pks</i>	10
<i>nor-1</i>	10
<i>avnA</i>	10
<i>adhA</i> and <i>norA</i>	11
<i>avfA</i>	11
<i>estA</i>	11
<i>vbs</i> and <i>verB</i>	12
<i>ver-1</i> and <i>moxY</i>	12
<i>omtB</i>	13
<i>omtA</i>	13
<i>ordA</i>	14
Organelles involved in secondary metabolism in filamentous fungi- the microbody and vacuole	15
Microbody	16
Vacuole	19
Compartmentalization of penicillin	25
REFERENCES	28
CHAPTER 2	
Genetic Disruption of <i>omtA</i> in <i>Aspergillus parasiticus</i>	36
INTRODUCTION	36
MATERIALS AND METHODS	37
Fungal strains	37
Construction of <i>omtA</i> disruption vector pLW14	37
Transformation and screening for <i>omtA</i> gene-disruption strains	38
Southern hybridization analysis	40
Northern hybridization analysis	40

Feeding studies of <i>omtA</i> gene disruption strains.....	41
RESULTS	41
Generation of <i>omtA</i> disruption mutants	41
<i>In vivo</i> feeding experiments	46
DISCUSSION	46
REFERENCES	50

CHAPTER 3

Expression/Distribution of the OmtA Protein in Colonies of <i>Aspergillus parasiticus</i>	52
INTRODUCTION	52
MATERIALS AND METHODS	53
Fungal strains	53
Construction of OmtA expression vector pLW12	53
Conversion of sterigmatocystin to O-methylsterigmatocystin by maltose binding protein–OmtA	54
OmtA antibody production and purification	55
Western blot analysis	56
Time-dependent fractionation of colonies grown on solid medium	57
Immunolocalization of OmtA protein.....	58
Preparation of paraffin-embedded fungal sections	58
Immunolabeling	59
Confocal Laser Scanning Microscopy (CLSM)	59
RESULTS	60
Western bolt analysis and protein localization using Pab against native OmtA	60
Purification of Maltose Binding Protein-OmtA	60
Enzymatic conversion of sterigmatocystin to O-methylsterigmatocystin by Maltose Binding Protein–OmtA	61
Production of PAb against OmtA fusion protein	61
Western blot analysis of OmtA in colonies grown on solid medium	67
Confocal Laser Scanning Microscopy	67
DISCUSSION	74
ACKNOWLEDGEMENTS	80
REFERENCES	81

CHAPTER 4

Sub-cellular Localization of Aflatoxin Biosynthetic Enzymes in Time-Dependent Fractionated Colonies of <i>Aspergillus parasiticus</i>	84
INTRODUCTION	84
MATERIALS AND METHODS	86
Fungal strains and time-dependent fractionation of fungal colonies	86
Western blot analysis of proteins isolated from colony fractions	86
Immuno-fluorescence labeling and confocal laser scanning microscopy (CLSM)	87
Quantitative fluorescence intensity analysis	87

Sample preparation for immuno-electron microscopy	88
Immuno-gold labeling and electron microscopy	88
RESULTS	89
DISCUSSION	105
ACKNOWLEDGEMENTS	109
REFERENCES	110

CHAPTER 5

Detection of Aflatoxin in Fungal Spores and Colonies	113
INTRODUCTION	113
MATERIALS AND METHODS	116
Fungal strains	116
Aflatoxin distribution in time-dependent fractionated colonies of SU1 grown on solid medium	116
Spores harvested by water (wet conditions)	116
Binding of AFB ₁ , AFG ₁ , OMST, and VA in water by spores	120
Spores harvested by cotton-tipped applicators	120
RESULTS	121
Aflatoxin distribution in time-dependent fractionated colonies of SU1 grown on solid medium	121
Binding of AFB ₁ and pathway intermediates in water by spores	124
AFB ₁ concentrations in spores harvested under dry condition	130
DISCUSSION	130
REFERENCES	134

CHAPTER 6

Future Studies	135
Model 1	135
Model 2	135
Model 3	136

LIST OF TABLES

Table 4.1. Quantative fluorescence intensity analysis of <i>A. parasiticus</i> SU1 and AFS10 immuno-fluorescence labeled with Nor-1, Ver-1 and OmtA antibodies.....	94
Table 5.1. Fractionation of fungal colonies at different ages	118
Table 5.2. Total aflatoxin detected in the colony, agar and membrane from different aged colonies	122
Table 5.3. Dry weight (g) of fractionated mycelium from different aged colonies	122
Table 5.4. Total aflatoxin (μg) in fractionated mycelium from different aged colonies.	123
Table 5.5. Normalized aflatoxin levels (μg of aflatoxin/g dry weight mycelium) in fractionated mycelium from different aged colonies	123
Table 5.6. Aflatoxin detected in conidiospores isolated under wet and dry conditions from <i>A. parasiticus</i> grown on YES and PDA agar	125

LIST OF FIGURES

Figure 1.1. A model for genetic control of <i>Aspergillus</i> growth, asexual sporulation and sterigmatocystin biosynthesis	6
Figure 1.2. Schematic presentation of the aflatoxin gene cluster	8
Figure 1.3. A schematic presentation of the peroxisomal-targeting sequence-dependent protein-import pathway for proteins destined for the peroxisomal matrix	20
Figure 1.4. PSORT (Prediction of Protein Localization Sites version 6.4) prediction for the protein targeting sequences (PTS1 and PTS2) in (A) Aflatoxin enzymes, AflJ, Nor-1, AvnA, VBS, Ver-1, OmtA and OrdA from <i>A. parasiticus</i> , and (B) 6-aminopenicillanic acid acyltransferase from <i>Penicillium chrysogenum</i> and <i>A. nidulans</i>	21
Figure 2.1. Restriction endonuclease map of plasmid pLW14	39
Figure 2.2. Southern hybridization analysis of <i>omtA</i> gene disruption strains	42
Figure 2.3. Northern blot analysis of <i>omtA</i> gene disruption strains	44
Figure 2.4. Thin layer chromatography of extracts of CS10 and <i>omtA</i> -disruption strains LW1418 and LW1432	47
Figure 3.1. Western blot analysis and fluorescence microscopy using polyclonal antibodies raised against partially purified fungal OmtA proteins.....	62
Figure 3.2. Western blot analysis of fungal protein extracts using subtraction-purified PAb raised against native OmtA.	64
Figure 3.3. Conversion of ST to OMST by affinity purified MBP-OmtA fusion protein	65
Figure 3.4. Western blot analysis of fungal protein extracts using affinity purified OmtA PAb	68
Figure 3.5. OmtA protein localization in time-fractionated colonies of <i>A. parasiticus</i> SU1, AFS10 (<i>AfR</i> knockout), CS10 and LW1432 (<i>omtA</i> knockout) grown on YES agar for 72 h.	71
Figure 3.6. Protein localization using OmtA PAb and anti-SKL, and detection of nuclei using SYTOX Green.	73

Figure 4.1. Western blot analysis of fungal protein extracts using Ver-1 and Nor-1 polyclonal antibodies.	90
Figure 4.2. Immuno-fluorescence confocal microscopy of Nor-1 and Ver-1 in <i>A. parasiticus</i> SU1 and AFS10 (<i>aflR</i> knockout mutant) grown on YES agar for 72 h	92
Figure 4.3. Immuno-gold labeling of <i>A. parasiticus</i> SU1 and AFS10	95
Figure 4.4. Immuno-gold labeling of OmtA in <i>Aspergillus parasiticus</i> AFS10 and SU1	98
Figure 4.5. Immuno-gold labeling of OmtA in <i>Aspergillus parasiticus</i> SU1	100
Figure 4.6. Immuno-gold labeling using anti-SKL and anti-Ver-1 in <i>A. parasiticus</i> AFS10 and SU1.	103
Figure 5.1. Mutants in the aflatoxin biosynthetic pathway	115
Figure 5.2. Diagram of colony fractionation	117
Figure 5.3. Thin layer chromatography of aflatoxin and OMST in water used for spore harvest	126
Figure 5.4. Thin layer chromatography of RHN1 spore extracts	127
Figure 5.5. Thin layer chromatography of SU1 and ATCC36537 spore extracts	128
Figure 5.6. Thin layer chromatography of SU1 and RHN1 spore extracts after binding with water used to harvest ATCC36537 spores	129
Figure 6.1. Proposed models for synthesis and export of aflatoxin from fungal cells ...	138
Figure 6.2. Western blot analysis of fungal protein extracts using affinity-purified OrdA PAb	139
Figure 6.3. Production of MBP-AflJ fusion protein and AflJ antibody	140

CHAPTER 1

Literature Review

1.1. Impact of aflatoxin contamination on health and economy.

Ingestion of aflatoxins by humans and animals can cause acute and chronic aflatoxicosis. The effects vary depending on the dose of aflatoxin ingested, time of exposure and nutritional status of patients (CAST, 2003). Aflatoxins were identified as the cause of thousands of turkey deaths in 1960 (known as Turkey X disease) (Asao *et al.*, 1963). Chronic toxicity can cause lowered levels of reproduction, feed efficiency, weight gain, meat and egg production, and enhance liver cancer in animals.

Immunosuppression resulting from chronic toxicity can lower animal resistance to bacterial, fungal and parasitic infection. Aflatoxins can cause acute hepatitis in humans. AFB₁ was detected in liver tissues of deceased patients (CAST, 2003) and patients suffering two childhood diseases, Kwashiorkor and Reye's syndrome (Becroft and Webster, 1972).

Chronic aflatoxicosis in humans is usually associated with liver cancer. Epidemiological studies showed a positive correlation between dietary aflatoxins and liver cell cancer (LCC) in Asia and Africa (Eaton and Gallagher, 1994). Humans exposed to both hepatitis B virus (HBV) and aflatoxin increased the possibility of developing liver cancer. The synergism between the two factors was also observed in experimental studies in HBV transgenic mice and woodchucks (Sell *et al.*, 1991; Bannasch *et al.*, 1995). The mechanism of interaction between aflatoxin and HBV is still not clear. Two hypotheses were suggested (Wild and Turner, 2002). One possibility is that HBV infection alters the

expression of aflatoxin metabolizing enzymes and consequently increases the binding of aflatoxin to DNA. The second hypothesis is that aflatoxin exposure enhances viral infection and replication. HBV may also inhibit DNA excision repair enzyme activity and increase AFB₁ adduct persistence.

The role of aflatoxin in liver cancer may be associated with mutations in the tumor suppressor gene p53. p53 is known to regulate several cell activities such as cell cycle, apoptosis, and DNA repair. Mutations in p53, therefore, may render a selective growth advantage to the cell (Smela *et al.*, 2001). In liver cells, aflatoxin B₁ can be activated to the 8,9-epoxy AFB₁ by Cytochrome P450 mono-oxygenase enzymes. This epoxy AFB₁ is particularly reactive with the guanine in the third position of codon 249 (AGG) of p53 and forms a DNA adduct. It was proposed that the DNA composition surrounding codon 249 of p53 favors this reaction. It has been shown that aflatoxins prefer to bind a guanine base with a guanine or cytosine as an adjacent 5' base (Smela *et al.*, 2001; Wild and Turner, 2002). After DNA repair, mutation with a G to T transversion occurs and results in an Arg (AGG) to Ser (AGT) alteration in the p53 protein. This mutation may disable the normal function of p53 protein (Smela *et al.*, 2001). The 249^{Ser} mutant is insufficient to immortalize human liver cells but confers a growth advantage to previously immortalized cells (Wild and Turner, 2002).

The economic impact of aflatoxin contamination is huge. The potential economic cost resulting from the loss of crops and livestock contaminated with aflatoxins was estimated and reported by the Council for Agricultural Science and Technology (CAST, 2003). The mean simulated potential value of crops lost because of aflatoxin contamination was \$ 47 million per year in food crops (corn and peanuts) and \$ 225 million per year in feed corn. The potential value of livestock lost was \$ 4 million per

year (CAST, 2003). As a result of human and economic issues, a standard to restrict aflatoxin levels in food and feed for human and animal safety was set by the U.S. Food and Drug Administration. The action levels of aflatoxin are 20 p.p.b. (0.5 p.p.b. for milk) for food for human consumption and 20-300 p.p.b. for animal feeds (CAST, 2003).

1.2. Environmental factors affecting toxin production on crops- Temperature and Humidity.

The colonization of crops and production of aflatoxins by *A. flavus* are known to be affected by environmental factors (CAST, 2003). Among them, temperature and humidity are two of the most important factors affecting aflatoxin contamination in the field and during storage of crops. It has been observed that abnormally high temperatures and below average moisture (drought) are highly associated with the incidence of aflatoxin contamination in corn and peanuts (Payne, 1998). This can be explained by the fact that, under high temperature and drought conditions, *A. flavus* can grow better than other fungi on crops with low water activity. Conditions for aflatoxin production are more restrictive than those for fungal growth. *A. flavus* can grow in the temperature range from 12 to 48°C with the optimal temperature at 37°C. *Asperigillus* species grow at water activity above 0.85 (Wilson and Payne, 1994). The optimum conditions for colonization are a temperature between 25 to 35°C with a substrate water activity at 0.90. However, the optimal conditions for the fungus to produce aflatoxin are 30°C with a water activity of 0.996 (Gqaleni *et al.*, 1997). At temperatures of 20 and 37°C, *A. parasiticus* did not produce aflatoxin (Feng and Leonard, 1998).

Another important factor that has a positive effect on aflatoxin production is insect infestation. Insect damage in crops provides the fungus entry through the hard hull

of pistachios, cotton bolls and corn, and allows to successful infection of crops (CAST, 2003).

The interaction between environmental factors (temperature and humidity) and crop species (which provides nutrient and water activity) are the most critical determinants for successful colonization and aflatoxin production by *A. flavus*. In addition, the nutrient composition of crops and their effects on aflatoxin production have been reported (Luchese and Harrigan, 1993 and Calvo *et al.*, 2002). Simple sugars such as sucrose, glucose, fructose and sorbitol support aflatoxin production (Luchese and harrigan, 1993). The seed oil, linoleic acid, also supports aflatoxin production (Calvo *et al.*, 2002).

1.3. Aflatoxin biosynthesis and asexual sporulation.

It has been shown that fungal cells after a period of vegetative growth (at least 18 h) become competent to receive developmental signals (conidiation). The signals include carbon and nitrogen starvation. In *A. nidulus*, asexual sporulation and sterigmatocystin (ST) production are coordinately up-regulated by FluG and FlbA, and down- regulated by a G-protein-mediated signaling pathway (FadA-dependent proliferation signaling) (Hicks *et al.*, 1997; Adams and Yu, 1998). FluG is involved in the production of an extracellular factor(s) required for initiation of the developmental pathway (D'Souza et al., 2001). An extracellular factor(s) can bind to receptors on the cell surface and transmit a positive signal for asexual sporulation by activating transcription factor *brlA* (an early regulator of development), and by activating transcription factor FlbA (fluffy low *brlA*). Activated FlbA then represses the FadA-dependent signal for proliferation by inactivating the α -subunit (FadA, fluffy autolytic dominant) of a hereterotrimeric G-protein. Both inactive

FadA and active FlbA result in induction of ST production possibly through activating transcription factor AflR (Adams and Yu, 1998 and Figure 1.1).

The proposed relationship between fungal growth, aflatoxin production and sporulation in *A. parasiticus* is similar to that in *A. nidulus* but the genetic evidence is not yet clear. The following observations, however, suggest that they are closely associated.

1) The chemicals, fluoroacetic acid and diaminobutanone, which inhibit sporulation also reduce aflatoxin accumulation (Reiss, 1982). Using a concentration that had little effect on growth, fluoroacetic acid could greatly reduce the accumulation of aflatoxin. When the concentration was adjusted to allow sporulation, toxin accumulation returned to normal levels (Reiss, 1982). Added after spore germination, diaminobutanone could completely suppress sporulation and aflatoxin production (Guzman-de-Pena *et al.*, 1997). 2) In submerged shake culture, no sporulation was observed, and a much lower concentration of aflatoxin was produced than that in solid culture (Guzman-de-Pena *et al.*, 1997). 3) Two mycotoxins, Aurasperone C (in *A. niger*) and Fumigaclavine C (in *A. fumigatus*), were found mainly in spores but not in mycelia (Palmgren *et al.*, 1986). Aflatoxin concentrations in spores isolated from *A. parasiticus* and *A. flavus* were reported (Wicklow and Shotwell, 1983; Palmgren *et al.*, 1986). Wicklow (1983) reported that the aflatoxin concentration in spores (harvested in water) ranged from 1,106 to 54,300 ppb, and in sclerotia from 109 to 73,200 ppb in *Aspergillus parasiticus*. Using a vacuum method, Palmgren *et al.* reported that 161,000 ppb of aflatoxin was detected in the spores and 245,000 ppb in the mycelia in *Aspergillus parasiticus* (Palmgren *et al.*, 1986). In the same report, norsolorinic acid in a *nor-1* mutant (mutation in the *nor-1* gene) was mainly detected in mycelia (730,000 ppb) and only 280 ppb in the spores (compared with

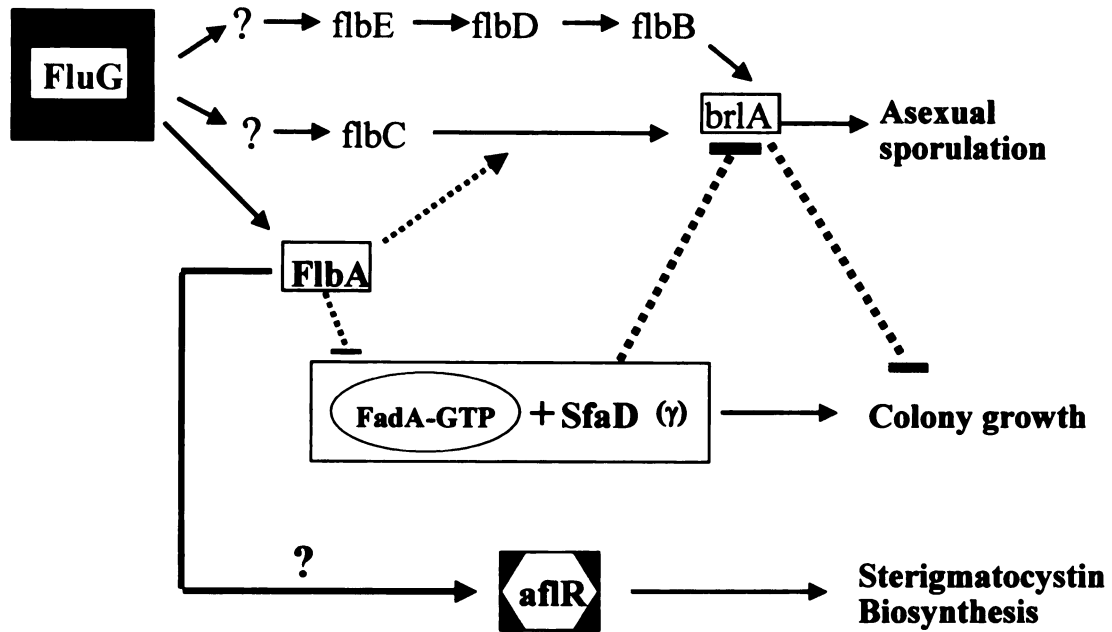


Figure 1.1. A model for genetic control of *Aspergillus* growth, asexual sporulation and sterigmatocystin biosynthesis.

161,000 ppb of aflatoxin in wild-type spores) (Palmgren *et al.*, 1986). This result implied that aflatoxin is synthesized mainly in mycelia. The question of whether aflatoxin is synthesized in spores or requires transport to spores remains unanswered.

1.4. Aflatoxin biosynthesis.

Aflatoxin gene cluster. Aflatoxins are secondary metabolites produced by filamentous fungi, including *A. flavus*, *A. parasiticus*, *A. nomius* and *A. pseudotamarii* (Ito *et al.*, 2001). More than 17 enzymes are involved in aflatoxin biosynthesis and the genes encoding these proteins are found clustered in a 75 kb genomic DNA fragment (Figure 1.2; and Bhatangar *et al.*, 2003). Recently, it was demonstrated that location within the aflatoxin cluster plays an essential role in the regulation of aflatoxin gene expression. When *nor-1* was relocated to other chromosomal positions outside the cluster (*pyrG* and *niaD*), the expression of this gene was highly reduced (Chiou *et al.*, 2002). An enhancer element is proposed to be located inside or surrounding the cluster to positively regulate aflatoxin gene expression. In addition, clustering of secondary metabolite genes may provide an advantage for horizontal gene transfer and, therefore, favor cluster dispersal and survival as a unit (Walton, 2000). Dispersed pathway genes can be transmitted vertically but do not favor horizontal transfer because a single pathway gene has no advantage to the recipient host. The synthesis of secondary metabolites may be subject to the natural selection to benefit the producing fungi. A dothistromin gene cluster, homologous to the aflatoxin and sterigmatocystin clusters, was isolated from the pine needle pathogen *Dothistroma pini* (Bradshaw *et al.*, 2002). Dothistromin is a difuranoanthraquinone toxin with structure similar to versicolorin B. However,

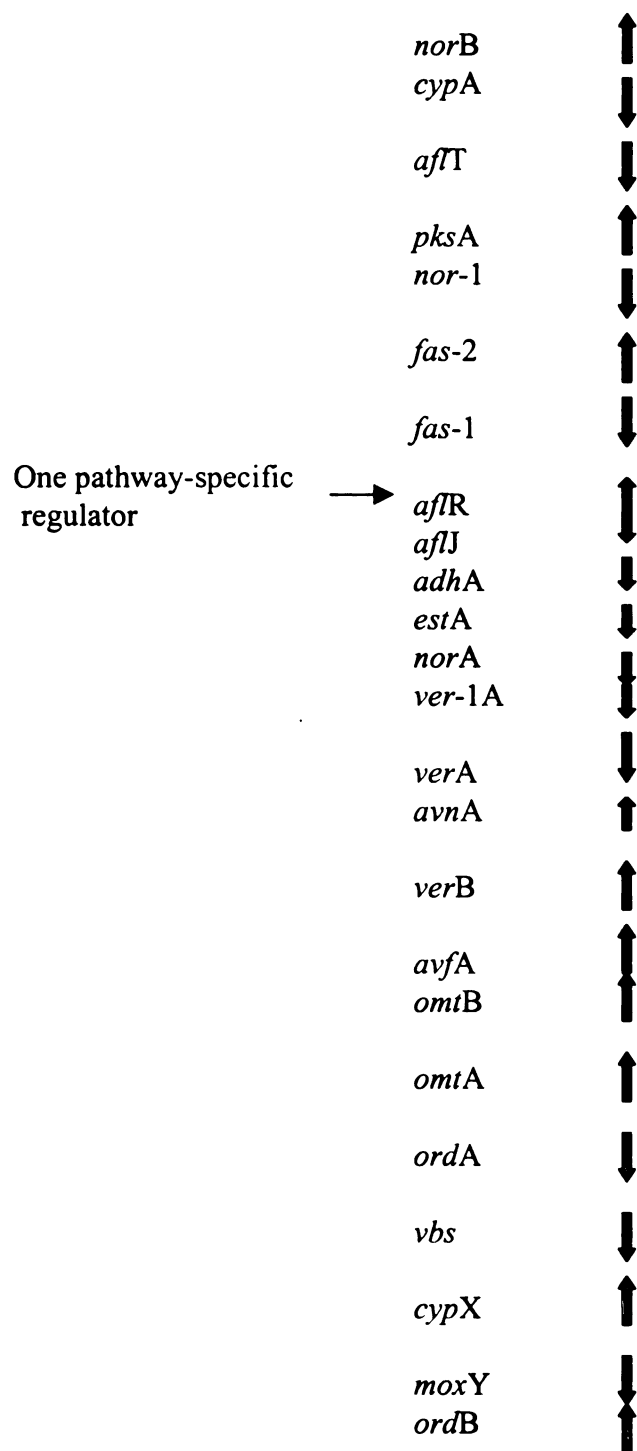


Figure 1.2. Schematic presentation of the aflatoxin gene cluster. Arrows indicate the direction of gene transcription.

dothistromin can not be converted to aflatoxin by *A. parasiticus*, suggesting that *A. parasiticus* has no enzyme to convert this toxin to an aflatoxin intermediate. One DNA fragment containing four biosynthetic genes, *dotA*, B, C and D was cloned from *D. pini*. The amino acid sequences of *dotA* and *dotC* have 80.2 and 31.2% identity to *ver-1* and *aftT* (toxin transporter), respectively. Because dothistromin is a phytotoxin targeted to mature pine embryos and leaf callus, DotC was proposed to transport dothistromin out to the target in host plant. This proposed general secretion mechanism may protect fungal cells from this toxin.

Aflatoxin genes.

***aflR*.** *aflR* encodes a pathway-specific regulator for many genes in the aflatoxin gene cluster. AflR can bind to a consensus DNA sequence, 5'-TCG N₅ CGA-3' (consensus AFLR binding site) in the promoters of regulated genes. Disruption of *aflR* eliminated accumulation of aflatoxin and pathway enzymes (Cary *et al.*, 2002) except for the transcript from *aflJ* (Chang and Yu, 2002). The function of AflR may be necessary but not sufficient to activate certain pathway genes whose promoters do not contain perfect AflR binding site, for example, *avfA*. Other transcription factors may be also involved in the regulation of aflatoxin genes and responsible for basal level of aflatoxin gene expression.

***aflJ*.** *aflJ* is located adjacent to *aflR* in the aflatoxin gene cluster. A gene disruption experiment showed *aflJ* is involved in Aflatoxin biosynthesis. No aflatoxin was detected in *aflJ* mutant while other aflatoxin gene transcripts including *pksA*, *nor-1*, *ver-1* and *omtA* were detected (Meyers *et al.*, 1998). The actual function of this gene is not clear. No *aflJ* homolog can be found in DNA/protein sequence databases to date. Based on the Peroxisomal Targeting Sequence 2 (PTS2) found in this gene, one proposed

function of AflJ is the transport of Aflatoxin proteins into microbodies (Meyers *et al.*, 1998). Recently, several reports suggested that AflJ may function to regulate early-pathway gene transcription (Du, ASM Meeting 2000) possibly through interaction with AflR as demonstrated in a yeast two hybrid system (Bhatangar, 2000; Chang, 2003).

fas1, fas2 and pks. The structural genes involved in aflatoxin biosynthesis include *pksA*, *fas-1A*, *fas-2A*, *nor-1*, *avnA*, *avfA*, *ver-1*, *omtB*, *omtA*, *ordA* and *vbs* (Figure 1.2; Bhatangar *et al.*, 2003). The 6-carbon compound hexanoyl-CoA is the starter unit in aflatoxin biosynthesis and is generated by fatty acid synthases Fas1 and Fas2 using one acetyl-CoA and two malonyl-CoA molecules (Mahanti *et al.*, 1996; Watanabe *et al.*, 1996). Malonyl-CoA and acetyl-CoA are first converted to hexanoyl-CoA by these two enzymes. The hexanoyl-CoA is further extended to noranthrone (NA) by polyketide synthase (PKS) using 7 molecules of malonyl-CoA (Minton and Townsend, 1997).

nor-1. Norsolorinic acid (NOR) is the first stable intermediate in aflatoxin biosynthesis. NOR is converted to averantin (AVN) by the enzyme Nor-1 (Zhou and Linz, 1999). Mutation of the *nor-1* gene in *A. parasiticus* greatly reduced aflatoxin production and resulted in accumulation of the red pigment, NOR (Trail *et al.*, 1994). A low level of aflatoxin production remained suggesting that an alternative pathway or enzyme(s) could substitute Nor-1 function but with lower enzymatic efficiency.

avnA. The reaction to convert AVN to 5'-hydroxyaverantin (HAVN) is catalyzed by the enzyme AvnA. Disruption of *avnA* in *A. parasiticus* resulted in a non-aflatoxin producing strain and accumulation of the aflatoxin precursor AVN (Yu *et al.*, 1997). AvnA is a cytochrome P-450 monooxygenase and contains 495 amino acids with a calculated molecular mass of 56.3 kDa.

***adhA* and *norA*.** HAVN can be converted to averufin (AVR) by AdhA and NorA (Bhatangar *et al.*, 2003). An *adhA* mutant was reported to produce trace amounts of aflatoxins (Chang, ASM Meeting 2000). Based on the observation that *adhA* and *nor-1* mutants still produced aflatoxins, it seems likely that enzymes involved in the early stages of secondary metabolism share some activities with other primary metabolic enzymes.

***avfA*.** AVR is converted to versiconal hemiacetal acetate (VHA) by AvfA (Yu *et al.*, 2000) and may also involve CypX (Bhatangar *et al.*, 2003). *avfA* is located downstream of *omtB* and upstream of *verB*. AvfA contains 285 amino acid with a calculated molecular mass of 30.9 kDa (Yu *et al.*, 2000). The function of AvfA has not been determined yet but it may function as a dehydrogenase based on its amino acid sequence.

***estA*.** The conversion of VHA to versiconal (VAL) is catalyzed by an esterase (Anderson and Green, 1994). The gene thought to encode this esterase is *estA*, located downstream of *adhA* and upstream of *norA* in the gene cluster (Yu, et al., 2002). Based on the cDNA sequence, this enzyme has a putative molecular mass of 34 kDa (Yu, et al., 2002). In the native form, however, this enzyme may form a dimer of 60 kDa as shown by gel filtration (Kusumoto and Hsieh, 1996). The expression pattern of *estA* may differ from other aflatoxin genes based on its ability to be expressed in non-aflatoxin inducing medium (PMS) (Anderson and Green, 1994; Yu, et al., 2002). However, this conclusion was based on RT-PCR; additional data generated from different methods such as Western blot analysis or Northern blot analysis may be required to confirm this statement. The second copy of this gene, *estA2*, located outside of this gene cluster, however, was not expressed in either inducing or non-inducing media (Yu, et al., 2002). This provides

additional evidence for a positional effect on the aflatoxin gene cluster reported previously (Chiou et al. 2002).

vbs and verB. The side-chain of Versiconal (VAL) is cyclized by Versicolorin B synthase (VBS) to generate Versicolorin B (VERB) (Lin and Anderson, 1992; Silva, 1996 and 1997). The bisfuran ring structure of AFB₁ is formed at this step. VBS may require glycosylation to obtain enzyme activity (Silva, 1996 and 1997). The native VBS purified from *A. parasiticus* has a molecular mass of 78 kDa. Compared to the deduced molecular mass of 70.3 kDa, a post-translational modification (glycosylation) of the native protein was suggested. A double bond is introduced into the bifuran structure of VERB by a desaturase called VerB (*verB*) to generate versicolorin A (VERA). The bifuran ring is responsible for the mutagenic nature of aflatoxin AFB₁.

ver-1 and moxY. The conversion of versicolorin A (VERA) to demethyl sterigmatocystin (DMST) may require several steps (oxidation, keto-reduction, and decarboxylation) and several enzymes (Keller *et al.*, 1995). Ver-1, a keto-reductase, was confirmed to be involved in this conversion (Liang, 1996 and 1997). Based on similarity with a polyhydroxynaphthalene reductase (66% identity and 82% similarity) which is involved in melanin biosynthesis in *Magnaporthe grisea*, the proposed function for Ver-1 is to catalyze a deoxygenation of VA to 6-deoxy VA. Disruption of the *ver-1* gene in *Aspergillus parasiticus* NR-1 (NiaD⁻) resulted in a non-aflatoxin producing strain, VAD-102 (Liang *et al.*, 1996). The *moxY* gene, located in the aflatoxin gene cluster, also was suggested to be involved in conversion of VERA to DMST (Bhatnagar *et al.*, 2003). However, no specific data were presented to support this idea. In *A. nidulans*, *stcS*, which encodes a monooxygenase, was demonstrated to be involved in VERA to DMST conversion (Keller *et al.*, 1995).

omtB. The conversion of DMST to sterigmatocystin (ST) is carried out by OmtB (Yaba *et al.*, 1989 and Yu *et al.*, 2000). The calculated molecular mass of OmtB is 43.1 kDa. OmtB as well as OmtA are the only two methyl-transferases utilized in the aflatoxin biosynthetic pathway. *omtB* is located downstream of *omtA* and upstream of *avfA* in the aflatoxin gene cluster. The promoter of *omtB* contains an AflR binding site but the downstream gene, *avfA*, does not. The intergenic region between the *omtB* translation stop codon and the start codon of *avfA* is only 173 bp. Yu *et al.* (2000) suggested that *avfA* may be co-transcribed with *omtB* from the *omtB* promoter and subsequently the transcript is processed into two mRNAs.

omtA. OmtA is a methyltransferase that catalyzes the conversion of ST to O-methyl-sterigmatocystin (OMST) by transferring a methyl group from the cofactor S-adenosyl-methionine (SAM) (Bhatnagar *et al.*, 1987 and Cleveland *et al.*, 1987). Although the molecular structure of OMST is close to ST, several chemical characteristics of OMST are more similar to AFB₁. Under UV illumination, the fluorescence emitted from ST shows a weak brick-red color while emission is pale blue from OMST and blue from AFB₁. The migration rate (R_f) in TLC analysis showed that the R_f of ST is 0.97, OMST is 0.44, and AFB₁ is 0.37 using ether-methanol-water (96:3:1) as a development system. In a chloroform-acetone (95:5) development system, the R_f of ST is 0.74, OMST is 0.24 and AFB₁ is 0.22 (Bhatnagar *et al.*, 1987).

The first native OmtA purified from a cell-free extract of *A. paraciticus* showed one band on a non-denaturing gel with a molecular mass of 168 kDa. This protein was shown to contain two subunits, 110 and 58 kDa, by SDS-PAGE (Bhatnagar *et al.*, 1988). This large enzyme was extremely unstable and displayed a low reaction rate *in vitro*. Therefore, Bhatnagar *et al.* suggested that a (hydrophobic) environment is required to

stabilize the hydrophobic ST (substrate), SAM (cofactor), OMST (product) and this enzyme (Bhatnagar *et al.*, 1988). However, using a similar method, a different protein (OmtA) was purified with the same O-methyl-transferase activity. The second purified protein had a smaller molecular mass of 40 kDa (Keller *et al.*, 1993; Liu *et al.*, 1993). Antisera raised against the 40 kDa purified protein was used to screen a cDNA expression library resulting in the cloning of *omtA* (Yu *et al.*, 1993). The molecular mass derived from the OmtA cDNA is 46 kDa. Comparing the N-terminal sequence of the purified protein (40 kDa) with the deduced amino acid sequence (46 kDa), Yu *et al.* suggested that OmtA might contain a leader sequence of 41 amino acids. This leader sequence may function to translocate OmtA across a membrane structure (Yu *et al.*, 1993). To explain the relationship between the two purified enzymes, 40 kDa and 168- kDa, Yu *et al.* suggested that OmtA subunits were posttranslationally modified and polymerized to become the large protein (Yu *et al.*, 1993). However, the antibody generated from the large protein (168- kDa) has very little reactivity with the 40 kDa OmtA protein, suggesting that these two enzymes are different proteins (Keller, 1993). No further study was carried out on this large purified protein. In the current study, we conducted a knockout of the *omtA* gene in *A. paraciticus* CS10 and conducted an *in vivo* feeding experiment. Our results suggested that OmtA (46 kDa) plays a major role in conversion of ST to OMST *in vivo* (Lee *et al.*, 2002).

ordA. OrdA is the final enzyme involved in the aflatoxin biosynthetic pathway. The proposed reactions for the conversion of OMST to AFB₁ include parahydroxylation, demethylation, reduction, ring cleavage, and conversion of a six-membered ring to a five-membered ring (Bhatnagar *et al.*, 1991). Therefore, more than one enzyme was proposed to be involved in this conversion. In one early study, the partially purified oxidoreductase

showed four major bands on a non-denaturing gel with a molecular mass about 180 - 200 kDa and seven major proteins (165, 105, 88, 64, 43, 38, and 26 kDa) on SDS-PAGE (Bhatnagar *et al.*, 1991). However, none of the bands excised from the native gel showed enzymatic activity. Recently, *ordA* encoding an enzyme activity able to convert OMST to AFB₁ was cloned from *A. flavus* (Prieto and Woloshuk, 1997). The putative molecular mass of OrdA is 60.2 kDa. Based on the amino acid sequence, OrdA is predicted to function as a monooxygenase. Yeast transformed with a single *gal1-ordA* construct (*ordA* fused with inducible *gal1* promoter) were able to convert exogenous OMST to AFB₁ (Yu *et al.*, 1998). Because no other intermediates between OMST and AFB₁ were reported, it is possible that this final reaction step requires only OrdA. However, the possibility can not be ruled out that other enzymes may help OrdA in more general reactions rather than the specific step in both filamentous fungi and yeast. The co-purified proteins with oxidoreductase activity observed in the early study could represent these helper proteins (Bhatnagar *et al.*, 1991).

Two additional proteins were identified that are required for production of the G group aflatoxins and these are detected in microsomal and cytosolic fractions (Yabe *et al.*, 1999).

1.5. Organelles involved in secondary metabolism in filamentous fungi- the microbody and vacuole.

For most secondary metabolites including aflatoxin, the biological functions are not clear. Specific secondary metabolites (including penicillin and prehelminthosporol) are believed to enhance the survival of the producing organism by inhibition of other micro-organisms in the same growth environment (Calvo *et al.*, 2002; Akesson, et al.,

1996.). Characterization of the sub-cellular compartments of secondary metabolites can aid in understanding their biological functions; storage and secretion mechanism, and even efficient production via industrial fermentation.

Penicillin is perhaps the best-studied secondary metabolite (Van der Kamp *et al.*, 1999). The biosynthesis of penicillin in *Penicillium chrysogenum* involves three enzyme activities that are distributed in at least in two sub-cellular compartments. The major storage compartment for the substrates, α -aminoadipic acid, L-cysteine and L-valine, is the vacuole (Van der Kamp *et al.*, 1999). The first and second pathway enzymes were localized in the cytosol (Van der Lende, 2002). The final enzyme was localized in the microbody (Muller *et al.*, 1991; Van der Lende, 2002). It was suggested that penicillin is possibly synthesized and stored in this membrane-bound organelle (Muller *et al.*, 1991).

To have full enzyme activity, it is important for biosynthetic enzymes to be confined in the proper environment under conditions in which optimal pH, required cofactors and a transport system for substrate are provided. Based on these observations, I hypothesized that microbodies and vacuoles represent two compartments for aflatoxin synthesis. The biogenesis, protein import pathway and biological function of these two organelles are briefly reviewed in the following sections.

Microbody. Microbodies can be divided into two subgroups based on the enzymes they contain: peroxisomes (contain flavin-linked oxidase) and glyoxysomes (contain enzymes of the glyoxylate cycle). The specific function of microbodies also varies in different cell types. In hepatocytes, peroxisomes can catalyze several metabolic pathways including the biosynthesis of ether lipids, catabolism of long chain fatty acids and production of cholesterol (Faumgart and Baumgart, 1993). Unlike animals where β -

oxidation occurs primarily in the mitochondria, β -oxidation in plants and fungi is exclusively a peroxisomal function (Waterham and Cregg, 1997).

The biogenesis of peroxisomes can occur either by fission or budding from an existing peroxisome or proliferation independent of a pre-existing peroxisome (Markham *et al.*, 1994; Rapp *et al.*, 1996; Valenciano *et al.*, 1998). The proliferation of peroxisomes involves several maturation steps- from low-density organellar structures (pre-peroxisome) to mature peroxisomes (Hettema *et al.*, 1998). The low-density organellar structures (pre-peroxisome) contain several peroxisomal proteins including Pex10p and ScPex11p that are responsible for independent peroxisome proliferation in yeast (Waterham *et al.*, 1997). Pex10p (34-48 kDa) is a peroxisomal integral-membrane protein. ScPex11p (27 kDa) is a peroxisomal membrane-associated protein. Induction of both genes leads to an over-proliferation of peroxisomes.

Proteins targeted to the peroxisome are mainly dependent on the Peroxisomal Targeting Sequences (PTS) on the protein. Three kinds of PTS have been identified: PTS-1, 2 and internal PTS (Subramani, 1998). PTS-1 and PTS-2 are commonly found in peroxisomal proteins whereas the internal PTS is not yet clearly defined. PTS-1 is a tripeptide sequence, Ser-Lys-Leu (SKL) or conserved variants (S/A(/C))(K/R/H)L, located at the carboxyl-terminus (Waterham *et al.*, 1997). PTS-1 is not cleaved after import into the peroxisome. PTS-2 is an amino-terminal motif with a consensus sequence Arg-Leu-X₅-His/Gln-Leu (RLX₅H/QL). PTS-2 may be cleaved after import to the peroxisome (Waterham *et al.*, 1997). Internal PTS motifs may be contained in some peroxisomal matrix proteins with or without PTS-1 and/or PTS-2. For example, the yeast catalase A with PTS-1 deleted is still able to be imported into the peroxisome (Purdue and Lazarow, 1994). The potential position of internal PTS for this protein is located

between residues 104 and 126. Since the receptor for internal PTS has not been identified, a proposed function for internal PTS motifs is to associate and co-translocate with other PTS-1-containing proteins into the peroxisome (Subramani, 1998).

Unlike mitochondria and ER proteins that require an unfolded conformation for translocation, peroxisomal proteins can be imported in either extended monomeric conformation or large preassembled structures (Waterham and Cregg, 1997). The monomer without a PTS-2 sequence can be dimerized with a PTS-2-containing monomer and translocated into peroxisomes (Rachubinski and Subramani, 1995). Formation of large structures via PTS-1 receptor-PTS-2 receptor by protein-protein interaction has been demonstrated in a yeast system (Rachubinski and Subramani, 1995; Tabak *et al.*, 1999). The yeast (*Saccharomyces cerevisiae*) PTS-1 receptor (PTS-1Rs), Pex5p, contains a loosely conserved 34 amino acid repeat called the tetratricopeptide (TPR) domain. The yeast PTS-2 receptor (PTS2R), Pex7p, contains six copies of a motif of 40 amino acid residues (WD40 motif). WD is a Trp (W)-Asp (D) pair at the carboxyl terminus of the motif. The results from two-hybrid experiments indicate that the binding between Pex7p and Pex5p is mediated by interaction between the TPR domain and the WD motif (Rachubinski and Subramani, 1995). Other proteins such as Pex1p and Pex6p with AAA domain (ATPases associated with diverse cellular activities) are also involved in protein import (Tabak *et al.*, 1999). These proteins are associated with vesicles and interact in an ATP-dependent manner in *Pichia pastoris* (Tabak *et al.*, 1999).

A simple model for operation of a PTS-containing protein-import pathway is demonstrated in Figure 1.3 (modified from Tabak *et al.*, 1999). First, a PTS-containing protein forms a complex with its receptor in the cytosol. Second, this complex binds to docking proteins (translocon) in and on the peroxisomal membrane. Third, the PTS

protein is released into the peroxisomal matrix and the receptor is recycled. The docking proteins consist of three proteins, Pex13p (an integral peroxisomal membrane protein), Pex14p (a peroxisomal membrane-associated protein) and Pex17p (membrane-associated protein). Two additional helper proteins, hsp70-class cytoplasmic chaperones (Hsp70) and J-domain-containing proteins (Djp1p), are required in the recognition of PTS-containing proteins by PTS receptors and/or the formation of PTS-1 and PTS-2 receptors complex during the translocation process (Hettema *et al.*, 1998). Based on a PSORT search, the 6-aminopenicillanic acid acyltransferase from *Penicillium chrysogenum* and *Aspergillus nidulans* contain a carboxyl-terminal tripeptide ARL (PTS-1). The experiments also confirmed that 6-aminopenicillanic acid acyltransferase is localized in microbodies. A PSORT search suggested that several aflatoxin enzymes contain PTS-1 sequences but the locations of PTS-1 sequences in those enzymes are different from the suggested location (carboxyl-terminal). Among them, AflJ even contains both PTS-1 and 2, located at the appropriate sites in the protein. The PSORT report for aflatoxin enzymes is shown in Figure 1.4. So far, no published data have been obtained to confirm the functional significance of these targeting signals.

Vacuole. The origin of vacuoles is not clear. It was suggested that the endoplasmic reticulum may be involved directly in vacuole biogenesis and the Golgi complex involved in increasing vacuole size (Klionsky, 1990). In vacuole biogenesis, more than 40 proteins are required. Mutations in vacuole biosynthetic genes usually result in fragmentation of the vacuole into small vacuoles, or vesicles, or unusual membrane inclusions (Ohsumi *et al.*, 2002). Proteins such as newly synthesized hydrolytic enzymes destined for the vacuole are transported through the endoplasmic reticulum and Golgi

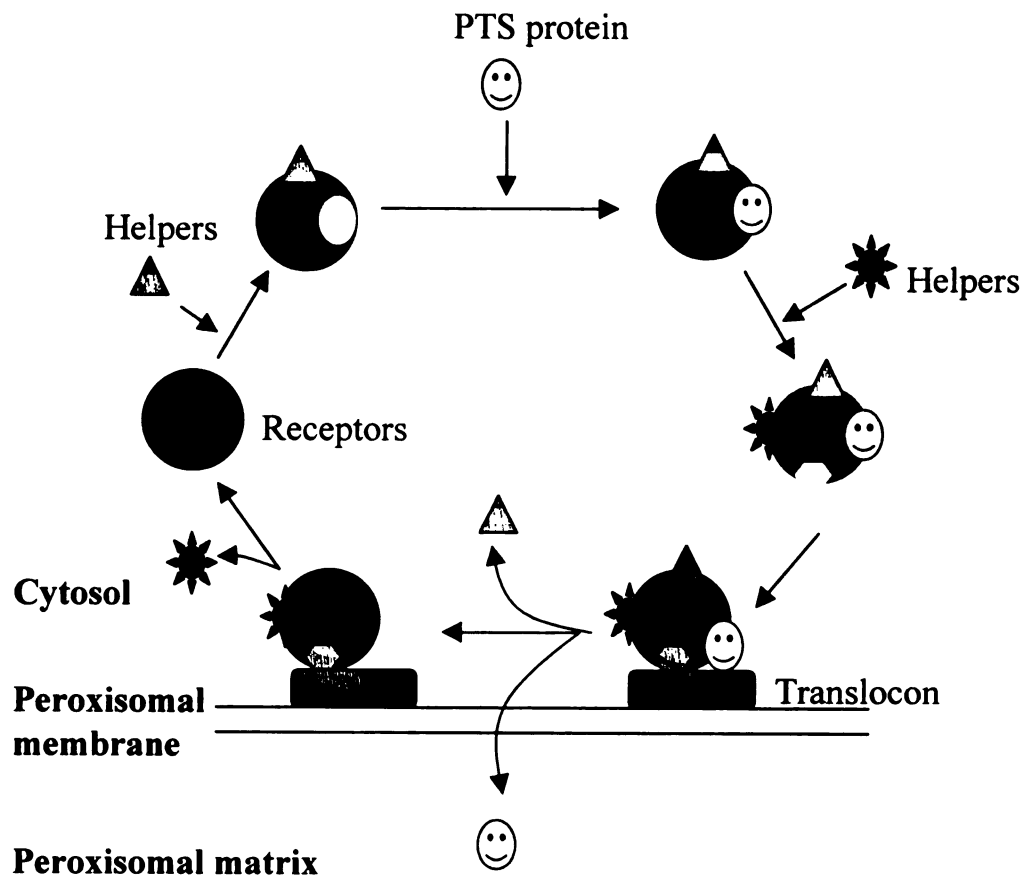


Figure 1.3. A schematic presentation of the peroxisomal-targeting sequence-dependent protein-import pathway for proteins destined for the peroxisomal matrix.

A.

AñJ

1. SKL motif (signal for peroxisomal protein): **ARL (a.a. 354; n.t. 438)**
2. SKL2: 2nd peroxisomal targeting signal: found [**KLASIPLHL** at **a.a. 286**]

Nor-1

SKL motif (signal for peroxisomal protein): **ARL (a.a. 225; n.t. 271)**

AvnA

1. SKL motif (signal for peroxisomal protein): **SHL (a.a. 211; n.t. 396)**
2. Peroxisomal proteins: Status: positive

VBS

SKL motif (signal for peroxisomal protein): **No.**

Ver-1

SKL motif (signal for peroxisomal protein): **AKL (a.a. 75; n.t. 262)**

OmtA

SKL motif (signal for peroxisomal protein): **SHL (a.a. 81; n.t. 418)**

OrdA

1. GvH: Examining signal sequence (von Heijne) Possible cleavage site: 23
2. Seems to have a cleavable N-term signal sequence.
3. SKL motif (signal for peroxisomal protein): **AHL (a.a. 84; n.t. 528)**

B.

Acyl coenzyme A: 6-aminopenicillanic acid acyltransferase (from *Penicillium chrysogenum* and *Aspergillus nidulans*)

1. SKL motif (signal for peroxisomal protein): SKL motif found at the C-terminus
2. Peroxisomal proteins: **positive**.

Figure 1.4. PSORT (Prediction of Protein Localization Sites version 6.4) prediction for the protein targeting sequences (PTS-1 and PTS-2) in (A) Aflatoxin enzymes, AflJ, Nor-1, AvnA, VBS, Ver-1, OmtA and OrdA from *A. parasiticus*, and (B) 6-aminopenicillanic acid acyltransferase from *Penicillium chrysogenum* and *A. nidulans*.

secretion pathway (Klionsky, 1990 and 1997). These proteins are carried by vesicles and finally released into the vacuole. The process is completed by fusion between vesicles and the vacuole with the help of small GTPases. The small GTPases recycle between donor (vesicle) and receptor (vacuole) membranes (Ohsumi *et al.*, 2002). GTP-bound GTPase directs the fusion of vesicle to the vacuole. Upon fusion, GTPase hydrolyzes GTP to GDP and is released from the membrane with the assistance of GTPase-activating protein. The GDP-bound GTPase then returns to the donor membrane and GDP is replaced by GTP with the assistance of guanine exchange factor.

The vacuole is a single-membrane bound organelle with highly dynamic structure (Markham, 1994). Morphological changes in the vacuole occur rapidly and may correspond to the growth stage (Markham, 1994; Paul, *et al.*, 1994). Hyphal vacuolation and fragmentation was only observed after a rapid growth phase during fungal fermentation (Paul, *et al.*, 1994). Recently, it was discovered that the vacuole is not just an empty space as its electron microscopic appearance suggests but an organelle with multiple possible functions (Markham, 1994). Therefore, vacuoles may consist of a series of functionally distinct subclasses of organelles to compartmentalize a variety of biological activities (Markham, 1994). The detailed functions of vacuoles in filamentous fungi are not completely understood but may be similar to those in yeast (Klionsky, 1990). Here, vacuoles are large storage sites for metabolites, ions and amino acids. Ions (Ca^{++} , Mg^{++} , Zn^{++} , Fe^{++}), including potential toxic ions (Sr^{++} , Co^{++} , Pb^{++}), and inorganic phosphorus (in the form of polyphosphate) (Markham, 1994). S-adenosyl-methionine (AdoMet) is an important methyl donor involved in a great variety of transmethylation reactions. In *S. cerevisiae*, S-adenosyl-methionine accumulates to high levels (about 60% of intracellular S-adenosyl-methionine) in vacuoles by a specific transport system

(Farooqui *et al.*, 1983; Schwencke *et al.*, 1976; Svihla *et al.*, 1969). S-adenosyl-methionine in vacuoles can be directly detected by microscopy under ultraviolet light (at a wavelength of 260 or 265 nm) (Farooqui *et al.*, 1983; Schwencke *et al.*, 1976; Svihla *et al.*, 1969). Results from subcellular fractionation revealed that two metabolically distinct S-adenosyl-methionine pools exist in yeast. The labile pool exists in the cytosol while the stable pool is in the vacuole (Farooqui *et al.*, 1983). The vacuole is also an important nitrogen reserve. Basic amino acids like arginine are concentrated in vacuole. The amino acids α -aminoadipic acid, L-cysteine and L-valine used in penicillin synthesis are also stored in vacuoles. Recently, the vacuole was found to be an important compartment for lipid degradation and glycerol production at a specific stage during appressoria formation in *Magnaporthe grisea*, suggesting that partial or complete enzymatic pathways may be compartmentalized in vacuoles (Weber *et al.*, 2001). Vacuoles control the intracellular pH homeostasis (Thumm, 2000). The pH in vacuoles is maintained at pH6 in *Neurospora crassa*. The membrane ATPase can pump H⁺ from the cytosol into the vacuole, generating a membrane potential of about 25-40 mV in *N. crassa*. This electron-chemical potential is the driving force to transport ions and amino acids across the vacuolar membrane. Vacuolar hydrolases (e.g. aminopeptidase I) mature in this organelle after cleavage of a signal peptide. Fungal vacuoles are an equivalent of mammalian lysosomes in that they can be involved in degradation and recycling of unneeded proteins and even whole organelles (Amor *et al.*, 2000). In *Saccharomyces*, cytoplasmic proteins can be transported into the vacuole by macroautophagy or the cytoplasm to vacuole targeting (cvt) pathway without involvement of receptors. These two pathways are regulated by nutrients (e.g. glucose or ethanol) and nutritional conditions (nutrition limitation) (Klionsky, 1997 and Thumm, 2000).

1.6. Compartmentalization of penicillin in *Penicillium chrysogenum*.

The biosynthesis of penicillin in *Penicillium chrysogenum* involves three enzyme activities and three amino acids (α -aminoadipic acid, L-cysteine and L-valine) (Van der Kamp *et al.*, 1999). In the first reaction, α -aminoadipic acid, L-cysteine and L-valine are condensed to a δ -(L- α -aminoadipyl)-L-cysteinyl-D-valine tripeptide (ACV) catalyzed by the enzyme δ -(L- α -aminoadipyl)-L-cysteinyl-D-valine synthetase (ACV synthetase). The substrate amino acids (α -aminoadipic acid, L-cysteine and L-valine) are stored in vacuoles. In early studies, ACV synthetase was localized in two subcellular compartments, a Golgi-like organelle (Kurylowicz *et al.*, 1987) and vacuoles (Lenderfeld *et al.*, 1993). Recently, ACV synthetase was also suggested to localize in the cytosol (Van der Lende *et al.*, 2002). The second reaction is conversion of ACV to isopenicillin N (IPN) by the enzyme, isopenicillin N-synthetase. This enzyme has been localized to Golgi-like organelles (Kurylowicz *et al.*, 1987) and the cytosol (Van der Lende *et al.*, 2002). Most evidence suggests that the cytosol is the true compartment for this enzyme (Müller *et al.*, 1991 and Van der Lende *et al.*, 2002). The final reaction entails the conversion of IPN to penicillin G by Acyl-coenzyme A: isopenicillin N acyltransferase (IAT). IAT was localized in peroxisomes (microbodies) (Müller *et al.*, 1991 and Van der Lende *et al.*, 2002). In this step, the aminoadipyl side-chain of IPN is substituted by phenylacetyl (PA) or phenoxyacetyl (POA) to yield penicillin G or penicillin V, respectively (van de Kamp *et al.*, 1999). Prior to this reaction, the PA and POA have to be activated to their thioesters (PA-CoA and POA-CoA) by acetyl-CoA synthetase (ACS) or PA-CoA ligase (PCL). ACS is a cytosolic enzyme. PCL contains a PTS-1 sequence,

suggesting that this enzyme may target to microbodies where it could function together with IAT (van de Kamp *et al.*, 1999). Based on localization results, Müller *et al.* suggested that penicillin is stored in the microbody together with IAT (Müller *et al.*, 1991). To summarize these studies, Van der Lende *et al.* suggested that the penicillin biosynthetic activities are likely confined to two major compartments, the cytosol and microbodies (Van der Lende *et al.*, 2002). Other compartments observed in earlier studies were proposed to be artifacts generated from the experimental procedures. A detailed discussion is presented in two publications (Müller *et al.*, 1991 and Van der Lende *et al.*, 2002). For the localization of ACV synthetase in vacuoles, van der Lende *et al.* suggested that this artifact occurred during the isolation of protoplasts and organelles (Van der Lende *et al.*, 2002). Because the procedure is time-consuming (one day) and is conducted under nutrition starvation conditions (cell wall digestion), this enzyme potentially could relocate from the cytosol into the vacuole for protein degradation. For the localization of ACV synthetase and isopenicillin N-synthetase in Golgi-like organelles, Müller *et al.* suggested that organelles would be disrupted during grinding of mycelia and subsequent fractionation procedure (Müller *et al.*, 1991). The broken organelles could be reformed into new organelles with morphology similar to other organelles.

To avoid potential artifacts introduced by vigorous cell disruption and time-consuming organelle isolation procedures, another strategy for *in situ* localization of protein is immuno-electron microscopy. In immuno-electron microscopic analysis, the sample is processed first by fixation to prevent protein relocation and organelle disruption. Therefore, the fixation method plays a crucial role in this analysis. In general, the sample can be fixed by chemical crosslinking (chemical fixation) or low temperature freezing (cryofixation). It is widely accepted that it is very difficult to obtain

simultaneously good preservation of both cellular ultrastructure and protein antigenicity.

For example, chemical fixation usually requires a longer incubation time because crosslinking will inhibit chemical penetration and slow down the fixation process.

Prolonged crosslinking with chemicals like glutaraldehyde may provide a good preservation of ultrastructure but result in loss of antigenicity. The cryofixation method is commonly considered superior to chemical fixation in preservation of ultrastructure and protein antigenicity. This method physically fixes cellular components in a very short time (ms) without any modification of protein antigenicity (Akesson *et al.*, 1996 and Müller *et al.*, 1991). However, membrane components are easily extracted during substitution of water with organic solvent. Although a low concentration of chemical fixative can be added in the substitution solvent to maintain the membrane structure, this may cause the loss of antigenicity.

REFERENCES

- Adams T. H., J. K. Wieser, and J-H. Yu.** 1998. Asexual sporulation in *Aspergillus nidulans*. Microbiol. Mol. Biol. Rev. **62**:35-54.
- Adams T. H. and J-H. Yu.** 1998. Coordinate control of secondary metabolite production and asexual sporulation in *Aspergillus nidulans*. Curr Opin Microbiol. **1**:674-677.
- Akesson, H., E. Carlemalm, E. Everitt, T. Gunnarsson, G. Odham, and H-B Jansson.** 1996. Immunocytochemical localization of phytotoxins in *Bioplaris sorokiniana*. Fungal Gene. Biol. **20**:205-216.
- Amor, C., A. I. Dominguez, J. R. D. Lucas, and F. Laborda.** 2000. The catabolite inactivation of *Aspergillus nidulans* isocitrate lyase occurs by specific autophagy of peroxisomes. Arch. Microbiol. **174**:59-66.
- Anderson, J. A., and L. D. Green.** 1994. Timing of appearance of versiconal hemiacetate esterase and versiconal cyclase activity in cultures of *Aspergillus parasiticus*. Mycopathologia. **126**:169-172.
- Asao, T., G. Buchi, M. M. Abdel-Kader, S.B. Chang, E. L. Wick, and G. N. Wongan.** 1963. Aflatoxin B and G. J. Am. Chem. Soc. **85**:1706-1707.
- Bannasch, P., N. I. Khoshkhou, and H. J. Hacker.** 1995. Synergistic hepatocarcinogenic effect of hepadnaviral infection and dietary aflatoxin B1 in woodchucks. Cancer Res. **55**:3318-3330.
- Becroft, D. M. O., and D. R. Webster.** 1972. Aflatoxins and Reye's disease. Br. Med. J. **4**:117.
- Bhatnagar D., S. P. McCormick, L. S. Lee, and R. A. Hill.** 1987. Identification of O-methylsterigmatocystin as an aflatoxin B1 and G1 precursor in *Aspergillus parasiticus*. Appl. Environ. Microbiol. **53**:1028-33.
- Bhatnagar D., A. H. Ullah, and T. E. Cleveland.** 1988. Purification and characterization of a methyltransferase from *Aspergillus parasiticus* SRRC 163 involved in aflatoxin biosynthetic pathway. Prep. Biochem. **18**:321-49.
- Bhatnagar D., T. E. Cleveland, and D. G. I. Kingston.** 1991. Enzymological evidence for separate pathways for aflatoxin B1 and B2 biosynthesis. Biochimie. **30**:4343-4350.

- Bhatnagar D., K. C. Ehrlich, and T. E. Cleveland.** 1992. Oxidation-reduction reactions in biosynthesis of secondary metabolites, p. 255-286. In D. Bhatnagar, E. B. Lillehoj, and D. K. Arora (ed.), Handbook of applied mycology, vol. 5. Mycotoxins in ecological systems. Marcel Dekker, Inc., New York.
- Bhatnagar D., K. C. Ehrlich, and T.E. Cleveland.** 2003. Molecular genetic analysis and regulation of aflatoxin biosynthesis. Appl. Microbiol. Biotechnol. **61**:83-93.
- Bradshaw, R. E., D. Bhatnagar, R. J. Ganley, C. J. Gillman, B. J. Monahan, and J. M. Seconi.** 2002. *Dothistroma pini*, a forest pathogen, contains homologs of aflatoxin biosynthetic pathway genes. Appl. Microbiol. Biotechnol. **68**:2885-2892.
- Calvo, A. M., R. A. Wilson, J. W. Bok, and N. P. Keller.** 2002. Relationship between secondary metabolism and fungal development. Microbiol. Mol. Biol. Rev. **66**:447-459.
- Cary, J. W., M. D. John, K. C. Ehrlich, M. S. Wright, S-H. Liang, and J. E. Linz.** 2002. Molecular and functional characterization of a second copy of the aflatoxin regulatory gene, AflR, from *Aspergillus parasiticus*. Biochim. Biophys. Acta. **1576**: 316-323.
- CAST.** 2003. Council for Agricultural Science and Technology. Mycotoxins: Risks in plant, animal, and human systems. Report 139.
- Chang P.-K., J. Yu, K. C. Ehrlich, S. M. Boue, B. G. Montalbano, D. Bhatnagar, and T. E. Cleveland.** 2000. Disruption of the aflatoxin biosynthetic gene *adhA* in *Aspergillus parasiticus* leads to accumulation of 5'-Hydroxyaverantin. ASM 100th Meeting.
- Chang P.-K., and J. Yu.** 2002. Characterization of a partial duplication of the aflatoxin gene cluster in *Aspergillus parasiticus* ATCC56775. Appl. Microbiol. Biotechnol. **58**:632-636.
- Chang P.-K.** 2003. The *Aspergillus parasiticus* protein AFLJ interacts with the aflatoxin pathway-specific regulator AFLR. Mol. Gen. Genomics. **268**:711-719.
- Chiou, C.-H., M. Miller, D. L. Wilson, F. Trail, and J. Linz.** 2002. Chromosomal location plays a role in regulation of aflatoxin gene expression in *Aspergillus parasiticus*. Appl. Environ. Microbiol. **68**:306-315.
- Cleveland T. E., A. R. Lax, L. S. Lee, and D. Bhatnagar.** 1987. Appearance of enzyme activities catalyzing conversion of sterigmatocystin to aflatoxin B1 in late-growth-phase *Aspergillus parasiticus* cultures. Appl. Environ. Microbiol. **53**:1711-3.
- D'Souza, C. A., B. N. Lee, and T. H. Adams.** 2001. Characterization of the role of the FluG protein in asexual development in *Aspergillus nidulans*. Microbiol. Genetic. **158**:1027-1036.

- Du W. L., and G. A. Payne.** 2000. Function of *afII* in regulating Aflatoxin Biosynthesis. ASM 100th General Meeting.
- Eaton D. L. and E. P. Gallagher.** 1994. Mechanisms of aflatoxin carcinogenesis. *Ann Rev. Pharmacol. Toxicol.* **34**:135-72.
- Farooqui, J. Z., H. W. Lee, S. Kim, and W. K. Paik.** 1983. Studies on the compartmentation of S-adenosyl-L-methionine in *Saccharomyces cerevisiae* and isolated rat hepatocytes. *Biochimica et Biophysica Acta.* **757**:342-352.
- Faumgart E. and E. Baumgart.** 1993. Electron Microscopic cytochemistry in biomedicine. Chapter 9. Cell Organelles. p 491-502. by CRC Press, Inc.
- Feng, G. H., and T. J. Leonard.** 1998. Culture conditions control expression of the genes for aflatoxin and sterigmatocystin biosynthesis in *Aspergillus parasiticus* and *Aspergillus nidulans*. *Appl. Environ. Microbiol.* **64**:2275-2277.
- Gqaleni, N., J. E. Smith, J. Lacey, and G. Gettinby.** 1997. Effects of temperature, water activity, and incubation time on production of aflatoxins and cyclopiazonic acid by an isolate of *Aspergillus flavus* in surface agar culture. *Appl. Environ. Microbiol.* **63**:1048-1053.
- Guzman-de-Pena, D., and J. Ruiz-Herrera.** 1997. Relationship between aflatoxin biosynthesis and sporulation in *Aspergillus parasiticus*. *Fungal Genet Biol.* **21**:198-205.
- Hettema E. H., C. C. M. Ruigrok, M. G. Koerkamp, M. van den Berg, H. F. Tabak, B. Distel, and I. Braakman.** 1998. The cytosolic DnaJ-like protein djplp is involved specifically in peroxisomal protein import. *J. Cell Biol.* **142**:421-34.
- Hicks J. K., J. H. Yu , N. P. Keller and T. H. Adams.** 1997. *Aspergillus* sporulation and mycotoxin production both require inactivation of the FadA G alpha protein-dependent signaling pathway. *EMBO J.* **6**:4916-23.
- Ito, Y., S. W. Peterson, D. T. Wicklow, and T. Goto.** 2001. *Aspergillus pseudotamarii*, a new aflatoxin producing species in *Aspergillus* section *Flavi*. *Mycol. Res.* **105**:233-239.
- Keller N. P., H. C. Dischinger, JR., D. Bhatnagar, T. E. Cleveland, and A. H. J. Ullah.** 1993. Purification of a 40-kDa methyltransferase activity in the aflatoxin biosynthetic pathway. *Appl. Environ. Microbiol.* **36**:270-273.
- Keller N. P., S. Segner, D. Bhatnagar, and T. E. Cleveland.** 1995. *stcS*, a putative P-450 monooxygenase, is required for the conversion of versicolorin A to sterigmatocystin in *Aspergillus nidulans*. *Appl. Environ. Microbiol.* **61**:3628-3632.
- Klionsky, D. J., P. K. Herman, and S. D. EMR.** 1990. Fungal vacuole: composition, function and biogenesis. *Microbiol. Rev.* **54**:266-292.

- Klionsky, D. J.** 1997. Protein transport from the cytoplasm into vacuole. *J. Membrane Biol.* **157**: 105-115.
- Kurylowicz, W., W. Kurzatkowski, and J. Kurzatkowski.** 1987. Biosynthesis of benzylpenicillin by in *Penicillium chrysogenum* and its golgi apparatus. *Arch. Immunol. Ther. Exp.* **35**:699-724.
- Kusumoto, K., and D. P. Hsieh.** 1996. Purification and characterization of the esterase involved in the aflatoxin biosynthesis in *Aspergillus parasiticus*. *Can. J. Microbiol.* **8**:804-810.
- Lee, L.-W., C.-H., Chiou, and J. E. Linz.** 2002. Function of native OmtA *in vivo* and expression and distribution of this protein in colonies of *Aspergillus parasiticus*. *Appl. Environ. Microbiol.* **68**:5718-5727.
- Lenderfeld, T., D. Ghali, M. Wolschek, E. M. Kubicek-Pranz, and C. P. Kubicek.** 1993. Subcellular compartmentation of penicillin biosynthesis in *Penicillium chrysogenum*. *J. Biol. Chem.* **268**:665-671.
- Liang S-H., C. D. Skory and J. E. Linz.** 1996. Characterization of the function of the *ver-1* and *ver-1B* genes, involved in aflatoxin biosynthesis in *Aspergillus parasiticus*. *Appl Environ Microbiol.* **62**:4568-4575.
- Liang S-H., T-S. Wu, R. Lee, F. S. Chu, and J. E. Linz.** 1997. Analysis of mechanism regulating expression of the *ver-1* gene, involved in aflatoxin biosynthesis. *Appl Environ Microbiol.* **63**:1058-1065.
- Lin, B.-K., and J. A. Anderson.** 1992. Purification and properties of versiconal cyclase from *Aspergillus parasiticus*. *Arch. Biochem. Biophys.* **293**:67-70.
- Liu B. H., N. P. Keller, D. Bhatnagar, T. E. Cleveland and F. S. Chu.** 1993. Production and characterization of antibodies against sterigmatocystin O-methyltransferase. *Food Agric. Immunol.* **5**:155-164.
- Luchese, R. H. and W. F. Harrigan.** 1993. Biosynthesis of aflatoxin- the role of nutritional factors. *J. Applied Bacteriology.* **74**: 5-14.
- Mahanti, N., D. Bhatnagar, J. W. Cary, J. Joubran, and J. E. Linz.** 1996. Structure and function of *fas-1A*, a gene encoding a putative fatty acid synthetase directly involved in aflatoxin biosynthesis in *Aspergillus parasiticus*. *Appl. Environ. Microbiol.* **62**:191-195.
- Markham, P.** 1995. Organelles of filamentous fungi. Pp. 75-98. *In* N. A. R. Gow, and G. W. Gooday (ed), *The growing fungus*, 1st ed. Chapman & Hall, London, UK.

- Meyers D. M., G. Obrian, W. L. Du, D. Bhatnagar, and G. A. Payne.** 1998. Characterization of *aflJ*, a gene required for conversion of pathway intermediates to aflatoxin. *Appl. Environ. Microbiol.* **64**:3713-7.
- Minto, R. E., and C. A. Townson.** 1997. Enzymology and molecular biology of aflatoxin biosynthesis. *Chem. Rev.* **97**:2537-2555.
- Müller W.H., T.P. van der Krift, A.J.J. Krouwer, H.A.B. Wosten, L.H.M. van der Voort, E.B. Smaal, and A.J. Verkleij.** 1991. Localization of the pathway of the penicillin biosynthesis in *Penicillium chrysogenum*. *EMBO Journal.* **10**:489-495.
- Ohsumi, K., M. Arioka, H. Nakajima, and K. Kitamoto.** 2002. Cloning and characterization of a gene (*avaA*) from *Aspergillus nidulans* encoding a small GTPase involved in vacuole biogenesis. *Gene.* **291**:77-84.
- Palmgren M.S., and L. S. Lee.** 1986. Separation of mycotoxin-containing sources in grain dust and determination of their mycotoxin potential. **66**:105-108.
- Paul, G. C., C. A. Kent, and C. R. Thomas.** 1994. Hyphal vacuolation and fragmentation in *Penicillium chrysogenum*. *Biotechnol. Bioeng.* **44**:655-660.
- Payne, G. A.** 1998. Process of contamination by aflatoxin-producing fungi and their impact on crops. Pp.279-306. In K. K. S. Sinha and D. Bhatnagar (Eds). *Mycotoxins in Agriculture and Food Safety*. Marcel Dekker, Inc., New York.
- Prieto R. and C.P. Woloshuk.** 1997. *ord1*, an oxidoreductase gene responsible for conversion of O-methylsterigmatocystin to aflatoxin in *Aspergillus flavus*. *Appl Environ. Microbiol.* **63**:1661-6.
- Purdue P.E. and P.B. Lazarow.** 1994. Peroxisomal biogenesis: Multiple pathways of protein import. *J. Biol. Chem.* **268**:30065-68.
- Rachubinski R.A., and S. Subraman.** 1995. How proteins penetrate peroxisomes. *Cell.* **83**:525-528.
- Rapp S., R. Saffrich, M. Anton, U. Jakle, W. Ansorge, K. Gorgas, and W.W. Just.** 1996. Microtubule-based peroxisome movement. *J. Cell Sci.* **109**:837-849.
- Reiss J.** 1982. Development of *Aspergillus parasiticus* and formation of aflatoxin B1 under the influence of conidiogenesis affecting compounds. *Arch. Microbiol.* **133**:236-8.
- Sell, S., J. M. Hunt, H. A. Dunsford, and F. V. Chisari.** 1991. Synergy between hepatitis B virus expression and chemical hepatocarcinogens in transgenic mice. *Cancer Res.* **51**:1278-1285.
- Schwencke, J., and H. De Robichon-Szulmajster.** 1976. The transport of S-adenosyl-L-methionine in the isolated yeast vacuoles and spheroplasts. *Eur. J. Biochem.* **65**:49-60.

- Silva, J. C., R. E. Minto, C. E. Barry, K. A. Holland, and C. A. Townsend.** 1996. Isolation and characterization of the versicolorin B synthase gene from *Aspergillus parasiticus*. J. Biol. Chem. **271**:13600-13608.
- Silva, J. C., and C. A. Townsend.** 1997. heterologous expression, isolation, and characterization of Versicolonin B Synthase from *Aspergillus parasiticus*. J. Biol. Chem. **272**:804-813.
- Smela, M. E., S. S. Currier, E. A. Bailey, and J. M. Essigmann.** 2001. The chemistry and biology of aflatoxin B1: from mutational spectrometry to carcinogenesis. Carcinogenesis. **22**:535-545.
- Subramani, S.** 1998. Components involved in peroxisome import, biogenesis, proliferation, turnover, and movement. Physiol. Rev. **78**:171-88.
- Svihla, G., J. L. Dainko, and F. Schlenk.** 1969. Ultraviolet micrography of penetration of exogenous cytochrome c into the yeast cell. J. Bacteriol. **100**:498-504.
- Tabak, H. F., I. Braakman, and B. Distel.** 1999. Peroxisomes: simple in the function but complex in maintenance. Trends in cell biology. **9**:447-453.
- Thumm, M.** 2000. Structure and function of the yeast vacuole and its role in autophagy. Microscopy Research and Technique. **51**: 563-572.
- Trail F., P-K. Chang, J. Cary, and J. E. Linz.** 1994. Structural and functional analysis of the nor-1 gene involved in the biosynthesis of aflatoxin by *Aspergillus parasiticus*. Appl. Environ. Microbiol. **60**:3315-3320.
- Valenciano, S., J.R. De Lucas, I. Van der Klei, M. Veenhuis, and F. Laborda.** 1998. Charatcerization of *Aspergillus nidulans* peroxisomes by immunoelectron microscopy. Arch. Microbiol. **170**:370-376.
- Van der Kamp, M., A. J. M. Driessen, and W. N. Konings.** 1999. Compartmentalization and transport in B-Lactam antibiotic biosynthesis by filamentous fungi. Antonie van Leeuwenhoek. **75**:41-78.
- Van der Lende, T. R., M. van de Kamp, M. van den Berg, K. Sjollema, R. A. L. Bovenberg, M. Veenhuis, W. N. Konings and A. J. M. Driessen.** 2002. δ -(L- α -aminoadipyl)-L-cysteinyl-D-valine synthetase, that mediates the first committed step in penicillin biosynthesis, is a cytosolic enzyme. Fungal Gene. Biol. **37**:49-55.
- Walton, J. D.** 2000. Horizontal gene transfer and the evolution of secondary metabolite gene cluster in fungi: a hypothesis. Fungal Gene. Biol. **30**:167-171.
- Watanabe, C. M. H., D. Wilson, J. E. Linz, and C. A. Townsend.** 1996. Demonstration of the catalytic roles and evidence for the physical association of the type

I fatty acid synthases and a polyketide synthase in the biosynthesis of aflatoxin B1. *Chem. Biol.* **3**:463-469.

Waterham H. R., and J. M. Cregg. 1997. Peroxisome biogenesis. *Bioessays*. **19**:57-66.

Weber, R. W. S., G. E. Wakley, E. Thines, and N. J. Talbot. 2001. The vacuole as element of the lytic system and sink for lipid droplets in maturing appressoria of *Magnaporthe grisea*. *Protoplasma*. **216**:101-112.

Wicklow, D. T., and O. L. Shotwell. 1983. Intrafungal distribution of aflatoxins among conidia and sclerotia of *Aspergillus flavus* and *Aspergillus parasiticus*. *Can. J. Microbiol.* **29**:1-5.

Wild, C. P., and P. C. Turner. 2002. The toxicology of aflatoxins as a basis for public health decisions. *Mutagenesis*. **17**:471-481.

Wilson, D. M., and G. A. Payne. 1994. Factors Affecting *Aspergillus flavus* Group Infection and Aflatoxin Contamination of Crops. In Eaton, D.L. and Groopman, J.D. (Eds), *The Toxicology of Aflatoxins*. Academic Press, SanDiego. pp309-346.

Yabe, K., Y. Ando, J. Hashimoto, and T. Hamasaki. 1989. Two distinct O-methyltransferases in aflatoxin biosynthesis. *Appl Environ Microbiol.* **55**:2172-7.

Yabe, K., M. Nakamura, and T. Hamasaki. 1999. Enzymatic formation of G-group aflatoxins and biosynthetic relationship between G- and B-group aflatoxins. *Appl. Environ. Microbiol.* **65**:3867-3872.

Yu J., J. W. Cary, D. Bhatnagar, T. E. Cleveland, N. P. Keller, and F. S. Chu. 1993. Cloning and characterization of a cDNA from *Aspergillus parasiticus* encoding an O-methyltransferase involved in aflatoxin biosynthesis. *Appl. Environ. Microbiol.* **59**:3564-71.

Yu J., P.-K. Chang, J. W. Cary, D. Bhatnagar, and T. E. Cleveland. 1997. AvnA, a gene encoding a cytochrome P-450 monooxygenase, is involved in the conversion of averantin to averrufin in aflatoxin biosynthesis in *Aspergillus parasiticus*. *Appl. Environ. Microbiol.* **63**:1349-1356.

Yu, J., P. K. Chang, K. C. Ehrlich, J. W. Cary, B. Montalbano, J. M. Dyer, D. Bhatnagar, and T. E. Cleveland. 1998. Characterization of the critical amino acids of an *Aspergillus parasiticus* cytochrome P-450 monooxygenase encoded by *ordA* that is involved in the biosynthesis of aflatoxins B1, G1, B2, and G2. *Appl. Environ. Microbiol.* **64**:4834-41.

Yu, J., C. P. Woloshuk, D. Bhatnagar, and T. E. Cleveland. 2000. Cloning and characterization of *avfA* and *omtB* genes involved in aflatoxin biosynthesis in three *Aspergillus* species. *Gene*. **248**:157-167.

Yu, J., P. K. Chang, D. Bhatnagar, and T. E. Cleveland. 2002. Cloning and functional expression of an esterase gene in *Aspergillus parasiticus*. Mycopathologia. **156**:227-234.

Zhou, R., and J. E. Linz. 1999. Enzymatic function of the Nor-1 protein involved in aflatoxin biosynthesis in *Aspergillus parasiticus*. Appl. Environ. Microbiol. **65**:5639-5641.

CHAPTER 2

Genetic Disruption of *omtA* in *Aspergillus parasiticus* CS10

INTRODUCTION

Aflatoxins, highly toxic and carcinogenic secondary metabolites produced by the filamentous fungi *Aspergillus parasiticus*, *A. flavus*, *A. nomius*, and *A. tamarii* (6,11), frequently contaminate food and feed crops such as corn, cotton, peanuts and tree nuts resulting in health risks to animals and humans (6). Most genes involved in aflatoxin biosynthesis are clustered in a 75-kb genomic DNA region that carries a positive regulator, AflR, and structural genes including *omtA* (17). Although much has been learned about the molecular biology and biochemistry of aflatoxin biosynthesis, little is known about the location of aflatoxin enzymes within a fungal colony or within a fungal cell.

Early studies identified two enzymes, a 168 kDa protein and a 40 kDa protein (OmtA), in *Aspergillus parasiticus* capable of converting sterigmatocystin to O-methylsterigmatocystin (3,5) *in vitro*; about 60% of the enzyme activity in cell extracts was associated with the 168 kDa protein and 40% of the activity was associated with OmtA (4). Both enzymes required the co-factor S-adenosylmethionine. The 168-kDa protein was purified to near homogeneity (3) and consisted of two subunits (58 and 110 kDa). OmtA (40 kDa) was also purified to homogeneity (8,9). The gene encoding OmtA (*omtA*) was cloned from a cDNA expression library using OmtA-specific polyclonal antibodies raised to OmtA protein expressed in *E. coli* (9, 16); *omtA* was later shown to

reside in the aflatoxin gene cluster (17) supporting its proposed role in aflatoxin synthesis. Because sterigmatocystin and O-methylsterigmatocystin could be converted to aflatoxin B₁ *in vivo* (2), they were generally accepted as aflatoxin pathway intermediates. Two important issues remained unresolved. 1) Although the 168 kDa protein and OmtA converted sterigmatocystin to O-methylsterigmatocystin *in vitro*, it was not clear which of these activities was necessary and sufficient to catalyze this reaction *in vivo* (7, 10, 11, 14). 2) Because the methyl group on O-methylsterigmatocystin is removed during the subsequent oxidoreduction reaction and because structurally related molecules are incorporated into AFB₁ in feeding experiments with similar or higher efficiency than sterigmatocystin (7), it was not clear if this reaction was necessary for aflatoxin synthesis. To address these issues, I generated an *omtA* gene disruption mutant (LW1432). Feeding studies conducted on LW1432 demonstrated a critical role for OmtA and the reaction catalyzed by this enzyme in aflatoxin synthesis *in vivo*.

MATERIALS AND METHODS

Fungal strains. *A. parasiticus* SU1(NRRL5862, ATCC 56775) is a wild-type, aflatoxin-producing strain. *A. parasiticus* CS10 (*ver-1 wh-1 pyrG*) was derived from *A. parasiticus* ATCC36537 (*ver-1 wh-1*) (13). LW1418 and LW1432 (*ver-1 wh-1 omtA*) were generated in this study by disrupting the *omtA* gene in CS10. AFS10 is a non-aflatoxin producing *aflR* knockout strain derived from *A. parasiticus* NR1 (*niaD*) derived from SU1 (provided by Dr. Jeff Cary, USDA, New Orleans, LA.).

Construction of *omtA* disruption vector pLW14. Plasmid pLW14 was constructed by inserting *pyrG*, which encodes orotidine monophosphate decarboxylase

(13), into the coding region of *omtA* at the *SphI* site (Figure 2.1). A plasmid carrying *omtA* genomic DNA was kindly provided by Dr. Fun Sun Chu (University of Wisconsin-Madison, WI). The 2.5kb *pyrG* fragment was generated by polymerase chain reaction (PCR) using plasmid pPG3J (12) as template. The primers used to amplify *pyrG* carried an *SphI* (GCATGC) restriction site to facilitate cloning (5'-GTAGAAGTTCAGCATGCTGATGG-3' and 5'-GAGTATCACAGTCAGGCATGCACGTC-3'). The reaction conditions for thermal cycling were: 95° C for 5 min followed by 35 cycles at 95° C for 1 min, 62° C for 1 min, and 72° C for 3 min. The reaction was completed by incubation at 72° C for 10 min.

Transformation and screening for *omtA* gene-disrupted strains. Circular or linear plasmid (8 µg) digested with *HindIII* was used in transformation experiments using *A. parasiticus* CS10 as the recipient strain (13). Protoplasts were generated by digestion of mycelium (harvested 17 h after initiation of germination) with Novozyme 234 and transformation was conducted by a PEG method as described previously (13). The selection of *omtA*-disrupted strains was achieved in four steps. 1) *pyrG*-positive clones (*pyrG*⁺; uridine prototrophs) were selected by growth on CZ agar (Czapek Dox Agar; DIFCO Laboratories, Detroit, MI), a minimal growth medium (13). 2) Spores from 3 to 4 day old transformant colonies grown on CZ plates were transferred by sterile toothpick to coconut agar medium (1) supplemented with sterigmatocystin at a concentration of 20 µg/ml and also to CZ agar medium. CS10 protoplasts regenerated and tolerated sterigmatocystin supplementation of the agar during active growth and then utilized sterigmatocystin to synthesize aflatoxin B1 as active growth slowed or ceased. 3) Colonies that did not fluoresce blue under long-wavelength UV light (254 nm) after a

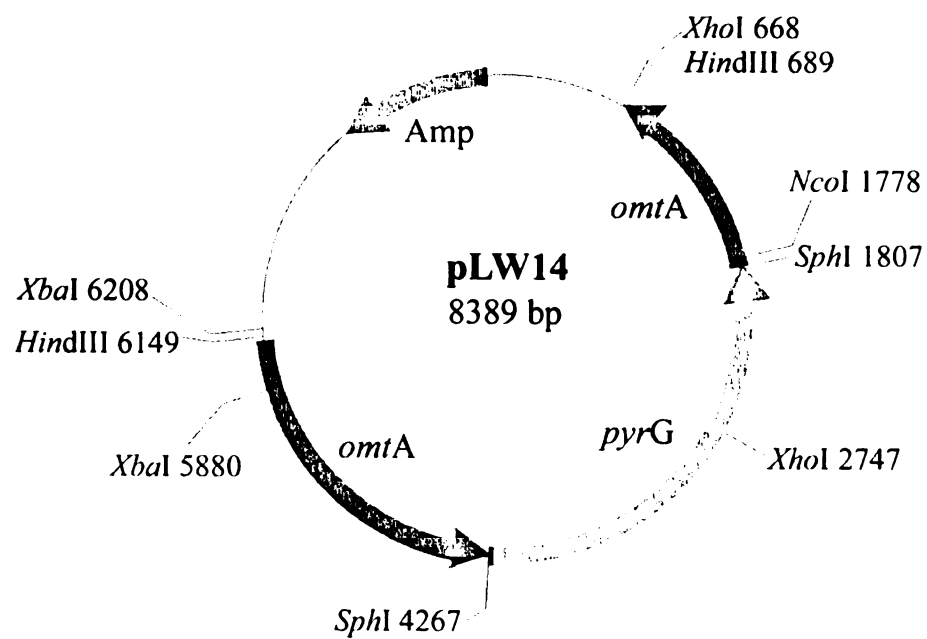


Figure 2.1. Restriction endonuclease map of plasmid pLW14.

3-day incubation at 29° C in the dark on coconut agar medium were selected and secondary metabolites extracted and analyzed by thin-layer chromatography by a previously published procedure (15). 4) The genotype of suspected *omtA*-disrupted strains was confirmed by Southern hybridization analysis. OmtA null mutants were further analyzed for ability to convert sterigmatocystin or O-methylsterigmatocystin to aflatoxin B₁ by a feeding experiment, as described below.

Southern hybridization analysis. Conidiospores (5×10^6) isolated from transformants were inoculated into 100 ml of YES and incubated with shaking at 150 rpm for 48 to 72 h at 29° C in the dark. One gram of freshly harvested mycelium was used for isolation of genomic DNA using a published procedure (13). Southern hybridization analysis was performed using a Non-Radioactive Hybridization Kit (Roche Molecular Biochemicals, Indianapolis, IN) and a procedure provided by the manufacturer. To identify the presence of *pyrG* sequences integrated within the chromosomal *omtA* gene, genomic DNA was digested with *Hind*III and *Eco*RI, separated by electrophoresis on a 1% agarose gel, transferred to Nytran membrane, and probed with digoxigenin-labeled 2.9 Kb *Hind*III fragment contained in the *omtA* gene.

Northern hybridization analysis. Conidiospores (5×10^6) isolated from LW1418, LW1432, CS10 and SU1 were inoculated into 100 ml of YES and incubated with shaking at 150 rpm for 48 h at 29° C in the dark. Total RNA was purified from freshly ground mycelium used TRIzol reagent (GibcoBRL, Rockville, MD). Northern hybridization analysis was performed using a Non-Radioactive Hybridization Kit (Roche Molecular Biochemicals, Indianapolis, IN) and a procedure provided by the manufacturer. The total RNA (35 µg) was separated by electrophoresis (60 V, 4 h) on a 1% formaldehyde-agarose gel, transferred to Nytran membrane, and probed with a

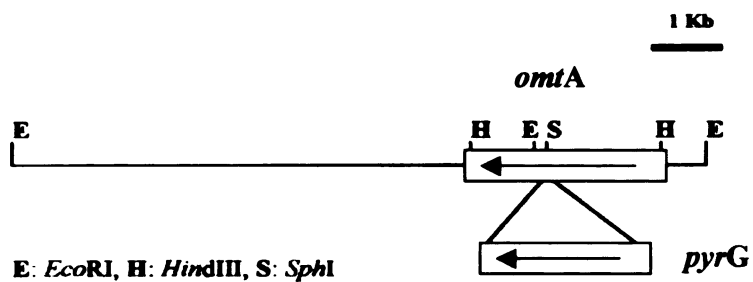
digoxigenin-labeled 2.9 Kb *Hind*III fragment contained in the *omtA* gene. The gel was stained with ethidium bromide (in 0.5 M ammonium acetate, at a final concentration of 0.5 µg per ml) for 40 min before the transferring procedure.

Feeding studies of *omtA* gene disruption strains. One gram of mycelia from the same culture as used in Southern hybridization analysis was inoculated into 10 ml of YES media supplemented with either sterigmatocystin or O-methylsterigmatocystin at a concentration of 20 µg per ml and incubated at 29° C for 24 h in the dark with shaking at 150 RPM. The fungal mycelium and culture medium were extracted with 10 ml of chloroform at 4° C for 16 h. The chloroform fraction was evaporated under N₂ gas and resuspended in 200 µl of acetone. Ten µl samples were analyzed by TLC using ether/methanol/water (96:3:1) as the solvent system.

RESULTS

Generation of *omtA* disruption mutants. TLC analysis of cell extracts from *pyrG*⁺ transformants tentatively identified 5 *omtA* gene disruption isolates. Two isolates (LW1418 and LW1432) were identified from among 41 *pyrG*⁺ colonies transformed with circular plasmid LW14. Southern hybridization analysis of genomic DNAs isolated from LW1418 and LW1432 detected a 2.5 kb *pyrG* DNA fragment within the *omtA* gene (Figure 2.2.). Northern hybridization analysis of total RNAs isolated from LW1418 and LW1432 did not detect any bands but a 1.6 kb band was detected in CS10 and SU1, confirming the gene disruption event in these isolates (Figure 2.3.).

Figure 2.2. Southern hybridization analysis of *omtA* gene disruption strains. A. Restriction endonuclease map of *omtA* locus in *omtA* disruption strains LW1418 and LW1432. B. Southern hybridization analysis. Genomic DNAs isolated from LW1418 and LW1432, CS10 (parent strain) and SU1 (wild-type) were digested with restriction enzymes *Hind*III and *Eco*RI. DNAs were resolved and hybridized to a digoxigenin-labeled 2.9 kb *Hind*III *omtA* DNA fragment using standard methods. Strains with *omtA*-disruption were predicted to contain a 5.4 kb *Hind*III fragment consisting of the 2.5 kb *pyrG* selectable marker inserted into the *omtA* locus. A 5.2 kb fragment in the *omtA*-disrupted strains was also predicted to replace the wild-type *Eco*RI fragment (2.7 kb). Numbers to the right of the blot represent the approximate size of the detected fragments in Kilobase pairs.

A**B**

Probe: 2.9 Kb *HindIII* fragment

Digestion: *Hind III* *EcoRI*

Wild type: 2.9 Kb 8 Kb + 2.7 Kb

Mutant: 5.4 Kb 8 Kb + 5.2 Kb

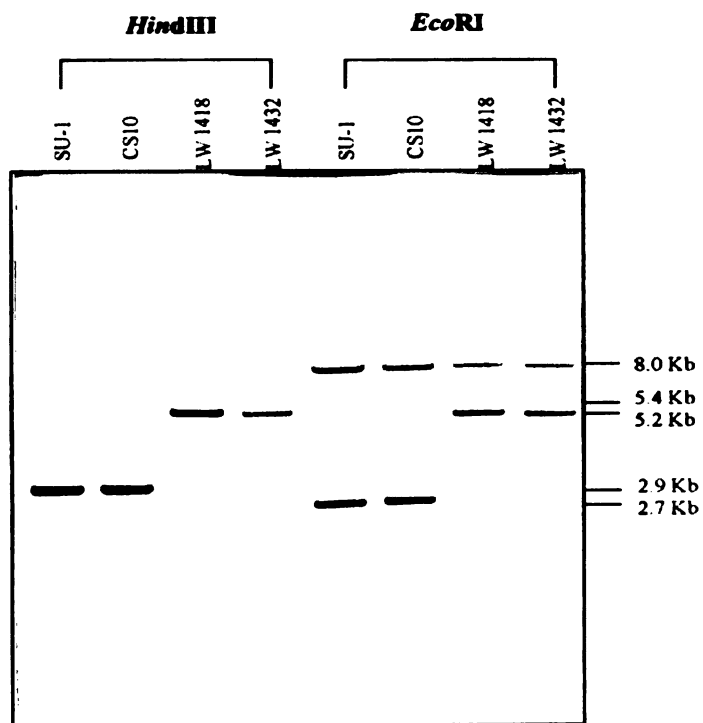
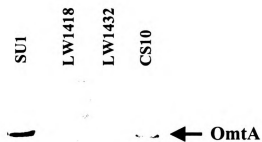


Figure 2.2.

Figure 2.3. Northern blot analysis of *omtA* gene disruption strains. (A) *omtA* transcript accumulation assessed by Northern hybridization analysis. Total RNAs isolated from LW1418 and LW1432, CS10 (parent strain) and SU-1 (wild-type) were resolved and hybridized to a digoxigenin-labeled 2.9 kb *HindIII* *omtA* DNA fragment using standard methods. Strains with *omtA*-disruption were predicted to contain no *omtA* transcript and a 1.6 kb transcript was predicted to be detected in both CS10 and SU-1. Equal loading of RNA is demonstrated by Ethidium bromide staining of RNA as shown in panel (B). Numbers to the left of the gel represent the approximate size of standard molecular fragments in Kilobase.

A.

Northern Blot Analysis



B.

EtBr Stain

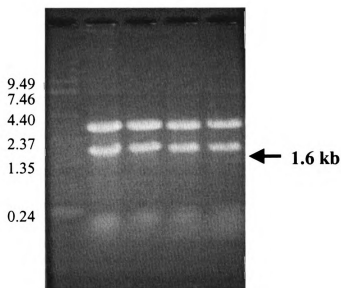


Figure 2.3.

***In vivo* feeding experiments.** No O-methylsterigmatocystin or aflatoxin B₁ could be detected in LW1418 or LW1432 supplied with (fed) exogenous sterigmatocystin; in contrast, each isolate converted exogenously supplied O-methylsterigmatocystin to aflatoxin B₁ (Figure 2.4.B). The parental strain CS10 converted either sterigmatocystin or O-methylsterigmatocystin to aflatoxin B₁ (Figure 2.4.A). These data suggest that LW 1418 and LW1432 carry mutant copies of *omtA*, but the genes encoding later pathway enzymes and the regulatory genes involved in aflatoxin biosynthesis are still functional.

DISCUSSION

The initial goal of this study was to determine if OmtA is necessary and sufficient to convert sterigmatocystin to O-methylsterigmatocystin *in vivo* and if this reaction is necessary for aflatoxin synthesis. When the same concentration of either sterigmatocystin or O-methylsterigmatocystin was fed to the parent strain CS10 (wild type OmtA and OrdA activities) nearly equal concentrations of O-methylsterigmatocystin and aflatoxin B₁ were generated. This observation could result for one of at least three potential reasons. 1) The intermediates were fed in excess of the capacity of the pathway enzyme to carry out complete conversion in the 24 hour period allotted. 2) The entry of the intermediates into the cell or into the enzyme active sites was rate-limiting. 3) The intermediates stimulate a feedback repression system downregulating activities of one or both enzymes. Nevertheless, it was clear that CS10 could convert either sterigmatocystin or O-methylsterigmatocystin to aflatoxin B₁ while LW1432 and LW1418 could convert

Figure 2.4. Thin layer chromatography of extracts of CS10 and *omtA*-disruption strains LW1418 and LW1432.

(A) Thin layer chromatography of extracts of CS10 supplied with (fed) exogenous sterigmatocystin (ST) or *O*-methylsterigmatocystin (OMST). Lane 1 and 7, AFB₁, AFB₂, AFG₁ and AFG₂ standard mixture. Lane 2 and 6, OMST standard. Lane 3, CS10 fed no pathway intermediate. Lane 4, CS10 fed sterigmatocystin. Lane 5, CS10 fed *O*-methylsterigmatocystin. Ten µl samples were analyzed using chloroform/acetone (95: 5) as the solvent system.

(B) Thin layer chromatography of extracts of *omtA*-disrupted strains LW1418 and LW1432 supplied with (fed) exogenous sterigmatocystin (ST) or *O*-methylsterigmatocystin (OMST). Metabolic scheme for aflatoxin biosynthesis in strain LW1418 and LW1432 is shown at the top of the thin layer chromatograph. The *ver-1* and *omtA* genes involved in aflatoxin biosynthesis are non-functional in LW1418 and 1432. Lanes 1 and 8, OMST standard. Lanes 2 and 7, AFB₁, AFB₂, AFG₁ and AFG₂ standard mixture. Lane 3, LW1418 fed OMST. Lane 4, LW1418 fed ST. Lane 5, LW1432 fed OMST. Lane 6, LW1432 fed ST. Abbreviations: VA, versicolorin A; DMST, demethylsterigmatocystin. Ten µl samples were analyzed using ether/methanol/water (96: 3:1) as the solvent system.

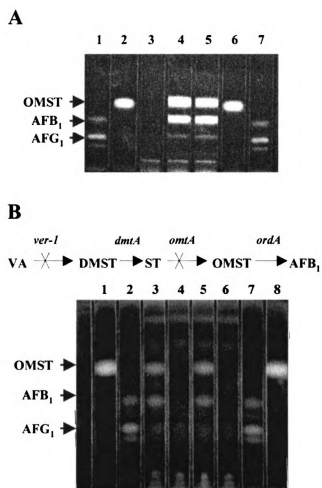


Figure 2.4.

O-methylsterigmatocystin to aflatoxin B₁ but were unable to convert sterigmatocystin to either O-methylsterigmatocystin or aflatoxin B₁. These data clearly demonstrate that OmtA is necessary for efficient conversion of sterigmatocystin to O-methylsterigmatocystin *in vivo* in *A. parasiticus* CS10 under the specified growth and assay conditions. The data also demonstrate that this reaction is necessary for aflatoxin biosynthesis. It is not yet clear if OmtA alone is sufficient to carry out this reaction *in vivo*. We cannot rule out the possibility that the 168 kDa protein contributes to this reaction, but its contribution appears negligible compared to OmtA. In support of this idea, LW1432 (*omtA* disruption) could not convert exogenously supplied sterigmatocystin to detectable levels of either O-methylsterigmatocystin or aflatoxin B₁ but could convert O-methylsterigmatocystin to aflatoxin B₁ *in vivo*. In contrast, CS10 (parent of LW1432) converted either sterigmatocystin or O-methylsterigmatocystin to aflatoxin B₁. These data demonstrate that the *omtA* disruption is gene-specific and does not affect the activity of late pathway enzymes or regulators of aflatoxin synthesis.

REFERENCES

1. **Arseculeratne, S. N., L. M. De Silva, S. Wijesundera, and C. H. S. R. Bandunatha.** 1969. Coconut as a medium for the experimental production of aflatoxin. *Appl. Microbiol.* **18**:88-94.
2. **Bhatnagar, D., S. P. McCormick, L. S. Lee, R. A. Hill.** 1987. Identification of O-methylsterigmatocystin as an aflatoxin B1 and G1 precursor in *Aspergillus parasiticus*. *Appl. Environ. Microbiol.* **53**:1028-33.
3. **Bhatnagar, D., A. H. Ullah, and T. E. Cleveland.** 1988. Purification and characterization of a methyltransferase from *Aspergillus parasiticus* SRRC 163 involved in aflatoxin biosynthetic pathway. *Prep. Biochem.* **18**:321-49.
4. **Bhatnagar, D., T. E. Cleveland, and E. B. Lillehoj.** 1989. Enzymes in aflatoxin B1 biosynthesis: Strategies for identifying pertinent genes. *Mycopathologia.* **107**:75-83.
5. **Cleveland, T. E., A. R. Lax, L. S. Lee, and D. Bhatnagar.** 1987. Appearance of enzyme activities catalyzing conversion of sterigmatocystin to aflatoxin B1 in late-growth-phase *Aspergillus parasiticus* cultures. *Appl. Environ. Microbiol.* **53**:1711-3.
6. **Eaton, D. L. and J. D. Groopman (eds.).** 1994. The toxicology of aflatoxins: human health, veterinary, and agricultural significance. San Diego, CA: Academic.
7. **Gengan R. M., A. A. Chuturgoon, D. A. Mulholland and M. F. Dutton.** 1999. Synthesis of sterigmatocystin derivatives and their biotransformation to aflatoxins by a blocked mutant of *Aspergillus parasiticus*. *Mycopathologia* **144**:115-122.
8. **Keller, N. P., H. C. Dischinger, JR., D. Bhatnagar, T. E. Cleveland and A. H. J. Ullah.** 1993. Purification of a 40-kDa methyltransferase activity in the aflatoxin biosynthetic pathway. *Appl. Environ. Microbiol.* **59**:479-484.
9. **Liu, B. H., N. P. Keller, D. Bhatnagar, T. E. Cleveland and F. S. Chu.** 1993. Production and characterization of antibodies against sterigmatocystin O-methyltransferase. *Food Agric. Immunol.* **5**:155-164.
10. **Mito, R. E. and C. A. Townsend.** 1997. Enzymology and molecular biology of aflatoxin biosynthesis. *Chem. Rev.* **97**:2537-2555.
11. **Payne, G. A. and M. P. Brown.** 1998. Genetics and physiology of aflatoxin biosynthesis. *Annu. Rev. Phytopathol.* **36**:329-362.

12. **Reichard, U., G. T. Cole, T. W. Hill, R. Ruchel and M. Monod.** 2000. Molecular characterization and influence on fungal development of ALP2, a novel serine proteinase from *Aspergillus fumigatus*. *Int. J. Med. Microbiol.* **290**:549-558.
13. **Skory, C. D., J. S. Horng, J. J. Pestka, and J. E. Linz.** 1990. Transformation of *Aspergillus parasiticus* with the homologous gene (*pyrG*) involved in pyrimidine biosynthesis. *Appl. Environ. Microbiol.* **56**:3315-3320.
14. **Sweeney, M. J. and A. D. W. Dobson.** 1999. Molecular biology of mycotoxin biosynthesis. *FEMS Microbiology Letters.* **175**:149-163.
15. **Trail, F., P-K. Chang, J. Cary and J. E. Linz.** 1994. Structural and functional analysis of the *nor-1* gene involved in the biosynthesis of aflatoxin by *Aspergillus parasiticus*. *Appl. Environ. Microbiol.* **60**:3315-3320.
16. **Yu, J., J. W. Cary, D. Bhatnagar, T. E. Cleveland, N. P. Keller, F. S. Chu.** 1993. Cloning and characterization of a cDNA from *Aspergillus parasiticus* encoding an O-methyltransferase involved in aflatoxin biosynthesis. *Appl. Environ. Microbiol.* **59**:3564-71.
17. **Yu, J., P-K. Chang, J. W. Cary, M. Wright, D. Bhatnagar, T. E. Cleveland, G. A. Payne, and J. E. Linz.** 1995. Comparative mapping of aflatoxin pathway gene clusters in *Aspergillus parasiticus* and *Aspergillus flavus*. *Appl. Environ. Microbiol.* **61**:2365-2371.

CHAPTER 3

Expression/Distribution of the OmtA Protein in Colonies of *Aspergillus parasiticus*

INTRODUCTION

Previous studies on accumulation of aflatoxin enzymes and expression of aflatoxin genes including *omtA* were conducted primarily in liquid medium using submerged shake culture (batch fermentation) (6,22,25); these conditions induce aflatoxin synthesis but do not support asexual sporulation (conidiation). Because a close regulatory association has been demonstrated between aflatoxin synthesis and conidiation (5,7,9) we hypothesized a spatial and temporal association between *omtA* expression and conidiospore development. Our goal was to develop a growth model that would closely mimic regulation of toxin synthesis in soil and on the host plant. We developed a novel time-dependent colony fractionation protocol to study OmtA accumulation in fungal colonies grown on solid medium; these conditions support toxin synthesis and conidiation. This protocol also allowed analysis of OmtA distribution to different cell types in fungal colonies. OmtA-specific polyclonal antibodies were generated against OmtA fusion protein (MBP-OmtA) and purified by affinity chromatography using a LW1432 protein extract. OmtA was not detected in 24 h old colonies but was detected in 48 h old colonies using Western blot analysis; the protein accumulated in all regions of a 72 h old colony including cells (0 to 24 h old near the colony margin) in which little conidiophore development was observed. OmtA in older parts of the colony (24 to 72 h) was partly degraded. Fluorescence-based immuno-histochemical analysis conducted on

thin sections of paraffin-embedded fungal cells from time-fractionated fungal colonies demonstrated that OmtA is evenly distributed among different cell types and is not concentrated in conidiophores. These data suggest that OmtA accumulates in newly formed fungal tissue and then is proteolytically cleaved as cells in that section of the colony age. The data also suggest that OmtA is localized to specific areas within a fungal cell but it is not yet clear if these areas correspond to specific sub-cellular organelles. The pattern of labeling using anti-OmtA was not consistent with localization of OmtA only to nuclei, peroxisomes, or Woronin bodies.

MATERIALS AND METHODS

Fungal strains. *A. parasiticus* SU1(NRRL5862, ATCC 56775) is a wild-type, aflatoxin-producing strain. *A. parasiticus* CS10 (*ver-1 wh-1 pyrG*) was derived from *A. parasiticus* ATCC36537 (*ver-1 wh-1*) (21). LW1418 and LW1432 (*ver-1 wh-1 omtA*) were generated in this study by disrupting the *omtA* gene in CS10. AFS10 is a non-aflatoxin producing *afIR* knockout strain derived from *A. parasiticus* NR-1 (*niaD*) which in turn was derived from SU1.

Construction of OmtA expression vector pLW12. An *omtA* cDNA was generated by reverse transcriptase- PCR (RT-PCR). Template RNA was isolated from *A. parasiticus* strain SU1 cultured in YES media for 48 to 72 h using Trizol reagent and a procedure supplied by the manufacturer (GibcoBRL, Rockville, MD). For first strand cDNA synthesis, 48 µg of total RNA were incubated in the RT-PCR mix at 37° C for 2 h. All chemicals used in the RT-PCR were purchased from GibcoBRL (Rockville, MD).

The 20 µl reaction mixture contained: 4 µl of 5 X first strand buffer, 2 µl of 0.1 M DTT, 1 µl of 10 mM dNTP, 2 µl of M-MLV Reverse Transcriptase (200 U per µl), and 1 µl of Oligo (dT) primer (0.5 µg per µl). One primer for *omtA* amplification contained a *Hind*III (AAGCTT) restriction site and the other primer an *Xba*I (TCTAGA) restriction site to facilitate cloning (5'-CCCTCTAGAATG GCACTACCGAGCAAAG-3' and 5'-TGCAAGCTTCTACTTGCGCAAACGCAGT-3'). One µl of the resulting cDNA mixture was used as template for PCR. The cycling conditions were: 95° C for 5 min followed by 35 cycles of 95° C for 1 min; 55° C for 1 min, and 72° C for 2 min. The mixture was incubated at 72° C for 10 min to complete the reaction. The *omtA* PCR fragment (1260 bp) was digested with restriction enzymes *Xba*I and *Hind*III and cloned into plasmid pMAL-c2 (New England Biolabs, Beverly, MA) digested with the same enzymes. The resulting plasmid construct, pLW12, was transformed into *E. coli* DH5α. The proper construction of pLW12 in clones expressing MBP-OmtA was confirmed by restriction enzyme analysis of purified plasmid DNA isolated by the Qiagen mini prep plasmid kit (Qiagen, Valencia, CA). The size of the fusion protein was determined by small-scale expression studies. *E. coli* DH5 α carrying pLW12 was incubated in 5 ml of LB broth containing Ampicillin (100 µg per ml) for 16 h. One ml of bacterial culture was saved as non-induced control. The remaining 4 ml of culture was induced to express fusion protein by addition of 0.3 mM of IPTG for 3 h.

Conversion of sterigmatocystin to O-methylsterigmatocystin by maltose binding protein -OmtA. The pMAL Protein Fusion and Purification System from New England Biolabs (Beverly, MA) was utilized to express and purify Maltose Binding Protein-OmtA. Large-scale preparation of Maltose Binding Protein-OmtA was conducted

for the study of enzymatic activity and antigen purification. *E. coli* DH5 α carrying pLW12 was grown in 500 ml of rich media (10 g tryptone, 5 g yeast extract, 5 g NaCl, 2% glucose) containing ampicillin (100 μ g per ml). Fusion protein synthesis was induced by addition of IPTG (0.3 mM), cells were sonicated (Sonifier cell disrupter W-350; Fisher Scientific, Pittsburgh, PA) and the fusion protein was purified by amylose affinity column chromatography according to a protocol supplied by the manufacturer (New England Biolabs, Beverly, MA).

Amylose resin-purified Maltose Binding Protein and Maltose Binding Protein - OmtA were used for analysis of enzyme activity. In a time-course experiment, three 1-ml reactions were prepared. Each reaction mixture contained 100 μ g of Maltose Binding Protein-OmtA, 20 μ g of sterigmatocystin, and 600 μ g of S-adenosylmethionine. Sterigmatocystin, O-methylsterigmatocystin and S-adenosylmethionine were purchased from Sigma (St. Louis, MO). The reaction mixtures were incubated at room temperature for appropriate times (20-min time points for 60 min; one tube per time point). Three control reactions were also incubated for 60 min. Each contained the same reagents as above except the Maltose Binding Protein-OmtA or sterigmatocystin or S-adenosylmethionine were omitted. Reactions were stopped by extraction with 4 volumes of chloroform. Chloroform extracts were dried under nitrogen gas and resuspended in 100 μ l of acetone. Five μ l of extract was analyzed by TLC using chloroform /acetone (95:5) as a development system (23).

OmtA antibody production and purification. OmtA polyclonal antibodies were generated in rabbits using purified MBP-OmtA as antigen. Each of 2 rabbits (New Zealand White) was injected subcutaneously with 300 μ g of protein in TitreMax adjuvant

(CytRx, Norcross, GA) at 1: 1 (V/V) ratio. After 35 days, the animals received one booster injection with 200 µg of protein in TitreMax adjuvant. Serum was obtained 4 weeks after the boost. The IgG fraction was purified from rabbit serum by precipitation with ammonium sulfate using standard procedures (2).

The IgG fraction of OmtA antibodies was further purified by affinity chromatography using a protein extract prepared from LW1432 grown in YES media for 48 h. This column was prepared by conjugating 11 mg of total protein to 2 ml of Aminolink coupling gel (coupling efficiency approximately 80%) using a procedure supplied by the manufacturer (Pierce Chemical Company, Rockford, IL). For antibody purification, one ml of IgG (8 mg) was loaded onto the gel bed in this column and an additional 2 ml of PBS was loaded to cover the gel bed. The column with antibodies was incubated at room temperature for 1.5 h at room temperature. After incubation, PBS was allowed to flow-through and antibody-containing fractions were identified by absorbance at 280nm. The protein concentration was determined by a BIO-RAD protein assay (Hercules, CA) using Dye Reagent and BSA (Fraction V, Sigma, St. Louis, MO) as standard. This highly purified antibody preparation (3 mg per ml) was used in Western blot analysis and immuno-fluorescence microscopy.

Western blot analysis. To determine specificity of anti-OmtA antibodies, fungal proteins were extracted from mycelia for Western blot analysis. Fungal strains including SU1, CS10, LW1418, LW1432, LW1468 and LW1470 were grown in the dark at 29°C (shaking at 150RPM) in 100 ml of YES liquid media for 24, 48 and 72 h or only 48 h. The mycelia were harvested, pulverized under liquid nitrogen and the fungal proteins were extracted in TSA buffer (2 mM Tris-Cl, pH8.0; 40 mM NaCl and 0.025 % sodium azide) containing complete protease inhibitors (Roche Molecular Biochemicals,

Indianapolis, IN). Proteins were resolved by SDS polyacrylamide gel electrophoresis using standard methods (2). For Western blot analysis, each lane on the 12% SDS-PAGE contained 30µg protein. The primary Ab was column-purified anti-OmtA IgG (1 µg per ml) and the secondary Ab consisted of a 10,000-fold dilution of goat anti-rabbit IgG alkaline phosphate conjugate (Schleicher & Schuell, Keene, NH). A BCIP/NBT colorimetric detection system was utilized (Roche Molecular Biochemicals, Indianapolis, IN).

The antibody against native OmtA was kindly provided by Dr. Fun Sun Chu (University of Wisconsin-Madison, WI). This antibody was also subtraction-purified with a LW1432 strain (*omtA* gene disrupted) protein extract before use in Western blot analysis (Figure 3.2.). 1.4 µl of antibody preparation was incubated with 100 µl (800 µg) of LW1432 protein extract for 1 h at 4° C. After incubation, the preparation was centrifuged at 12,000 x g for 15 min at 4° C to pellet cross-reactive antibodies. The supernatant was mixed with 14 ml of blocking reagent and used in Western blot analysis.

Time-dependent fractionation of colonies grown on solid medium. To determine the accumulation and distribution of OmtA in fungal colonies grown on solid culture media, conidiospores (2×10^5) of *A. parasiticus* SU1, AFS10, CS10, and LW1432 were inoculated onto the center of YES agar or PDA agar (for SU1 only) overlaid with sterile cellophane membranes and incubated at 29° C in the dark. Some colonies were analyzed after 24 or 48 h of growth. 72 h-old colonies were fractionated into three concentric rings based on area covered at three time points (72, 48 and 24 h). For example (Fig. 5D), a SU1 colony with a diameter of 4.2 cm was fractionated to S1 which contained mycelia from the colony center out to a distance of 0.8 cm (ages 48 to 72

h), S2 which contained mycelia from 0.8 to 2.5 cm (24 to 48 h) and S3 which contained mycelia from 2.5 to 4.2 cm (0 to 24 h). The harvested mycelia from appropriate sections of the colony were pulverized under liquid nitrogen and the fungal proteins were extracted in TSA buffer containing complete protease inhibitors. Western blot analysis was performed as described above.

Immuno-localization of OmtA protein. Immuno-localization of OmtA protein was conducted on SU1 colony fractions. In addition, AFS10, CS10, and LW1432 colonies were fractionated following the same scheme to generate analogous fractions R1, R2, R3, C1, C2, C3, and L1, L2, L3, respectively.

Preparation of paraffin-embedded fungal sections. Samples from fungal colony fractions were embedded in paraplast (Sigma, St. Louis, MO) using a published procedure (2) with the following modifications. Fungal tissues were fixed with Streck tissue fixative (Streck Laboratory Inc., Omaha, NE) at 4° C overnight, and then dehydrated in a graded series of ethanol: 30% (30 min, room temperature); 50% (30 min, room temperature); 70% (overnight, 4° C); 85% (30 min, room temperature, 2 times); 95% (30 min, room temperature, 2 times); 100% (30 min, 4° C, 2 times), followed by incubation in 100% xylene (10 min, room temperature, 3 times). Fungal tissues were then incubated in paraffin/xylene mixture (1:1; v/v) for 15 min, 60 min and overnight at 60°C and finally for 8 h in 100% paraffin at 60° C (three changes of paraffin during incubation). The paraffin embedded sample blocks were hardened in a plastic mold (VWR Scientific, Detroit, MI) at RT. Sample blocks were cut into 4 µm thick sections

using a tissue section microtome (AO Spencer 820 microtome, Fisher Scientific). The sections were attached to poly-L-Lysine (Sigma) coated coverslips (22 mm square).

Immuno-labeling. Coverslips with paraffin-embedded fungal sections were placed in a coverslip holder (EMS, Fort Washington, PA) for de-paraffinization and antigen retrieval. Sections were de-paraffinized twice in 100% xylene for 10 min, then rehydrated with a decreasing concentration of ethanol: twice in 100% for 10 min, once in 95%, 70%, 50% for 5 min each, and finally in deionized distilled H₂O. Antigen retrieval was performed by heating the sections in 10 mM citrate buffer (pH 6.0) at 95° C for 5 min followed by cooling at room temperature for 20 min. Coverslips were rinsed with TBS (Tris buffer saline, pH 7.5) and incubated in blocking solution (1% BSA with 0.1% saponin in TBS) at 4° C overnight. The samples were immuno-labeled with primary antibody (purified anti-OmtA IgG; 20 µg/ml) or anti-SKL (1:500, Zymed, So. San Francisco, CA) at room temperature for 1.5 h, followed by secondary antibody conjugated with fluorescent probe (goat anti-rabbit IgG-Alexa 488 conjugate [5 µg/ml]; Molecular Probes; Eugene, OR), at room temperature for 1 h. Coverslips were washed after each antibody treatment with TBS containing 1% BSA and 0.1% saponin followed by two washes with TBS for 10 min. Fungal nuclei were detected using SYTOX Green fluorescence dye (Molecular Probes). The samples were mounted onto microscopic slides with Prolong anti-fade mounting media (Molecular Probes, Eugene, OR).

Confocal Laser Scanning Microscopy (CLSM). Fluorescence image detection was performed on a Zeiss 210 Laser scanning microscope with 488 nm laser line. The 40 X oil objective lens (Zeiss Plan-NeoFlura, NA= 1.3) was used to acquire all images. The

Alexa 488 fluorescence probe (Abs 495 nm/ Em 519 nm) was detected using LP 520 or BP 520-560 barrier filters. Fluorescence image analysis of SU1, AFS10, CS10 and LW1432 was conducted under the same instrument parameter settings.

RESULTS

Western blot analysis and protein localization using PAb against native

OmtA. The antibodies against purified native OmtA were kindly provided by Dr. Fun Sun Chu (University of Wisconsin-Madison, WI). The specificity of this PAb was tested on SU1 (wild type) cultured in YES liquid medium for 24, 48 or 72 h. One primary band (larger than 45 kDa) was detected in Western blot analysis of protein extracts prepared from 24 h culture and three primary bands were detected in 48 or 72 h cultures (Figure 3.1.A). Protein localization using a slide-culture method (12) showed the primary signal was detected in conidiophores and conidiospores (Figure 3.1.B). This antibody was further purified by subtraction with a protein extract from LW1432 (*omtA* gene disruption strain) and the specificity was tested by Western blot analysis. Two primary bands were detected in SU1 and CS10 and one intense band was detected in all *omtA* knock-out strains, suggesting that this purified antibody still cross-reacted with one protein (Figure 3.2.).

Purification of Maltose Binding Protein-OmtA. Maltose Binding Protein-OmtA in DH5 α cell extracts (Figure 3.3.A) was purified by amylose column chromatography. Most of the purified Maltose Binding Protein-OmtA fusion protein was approximately 88 kDa in mass (Figure 3.3.B); this is consistent with a mass calculated

from the fusion of 42 kDa MBP and 45 kDa OmtA predicted using nucleotide sequence data. Very little proteolytic cleavage of the protein was detected by this analysis. The fusion protein remained soluble in the bacterial cytoplasm allowing purification of 39 mg of MBP-OmtA per liter of bacterial culture.

Enzymatic conversion of sterigmatocystin to O-methylsterigmatocystin by Maltose Binding Protein-OmtA. Purified OmtA fusion protein efficiently converted sterigmatocystin to O- methylsterigmatocystin in the presence of *S*-adenosylmethionine (Figure 3.3.C) within 60 min. The cofactor, *S*-adenosylmethionine, was required for this conversion. Without exogenous *S*-adenosylmethionine, no O-methylsterigmatocystin could be detected in the presence of the Maltose Binding Protein-OmtA. As expected, no O-methylsterigmatocystin was detected in the reaction that contained *S*-adenosylmethionine without substrate (sterigmatocystin), in a reaction without added Maltose Binding Protein-OmtA, or in a reaction with Maltose Binding Protein but without the Maltose Binding Protein-OmtA (data not shown).

Production of PAb against OmtA fusion protein. To obtain highly specific anti-OmtA polyclonal antibodies (PAb), amylose-purified MBP-OmtA was used as antigen to produce polyclonal antibodies in two rabbits. The IgG fraction of the rabbit serum was further purified by affinity chromatography using a protein extract from LW1432 (*omtA* gene disruption strain). The specificity of anti-OmtA PAb was tested on SU1 (wild type) cultured in YES liquid medium for 24, 48 or 72 h. No OmtA could be detected in Western blot analysis of protein extracts prepared from SU1 grown on YES liquid medium for 24 h while one primary band (approximately 45 kDa) could be

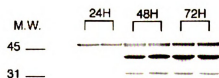
Figure 3.1. Western blot analysis and fluorescence microscopy using polyclonal antibodies raised against partially purified fungal OmtA proteins. The native OmtA antibody was kindly provided by Dr. Fun Sun Chu (University of Wisconsin-Madison, WI).

(A) Analysis of SU1 crude protein extracts isolated at three time points (24, 48 and 72 h) from fungal cultures grown in YES liquid medium. The approximate mass of the primary signal (45 kDa) is shown to the right of the blots.

(B) OmtA protein localization in a colony of *A. parasiticus* SU1 grown on YES agar for 48 h. Fungal tissue from slide-culture was digested with Novezyme and probed with OmtA PABs (20 µg/ml) followed by FITC-conjugated goat anti-rabbit IgG (1:50). The protein localization method used was reported previously (12).

A.

Western Blot Analysis: anti-OmtA



B.

Bright Field



OmtAFITC



Figure 3.1.

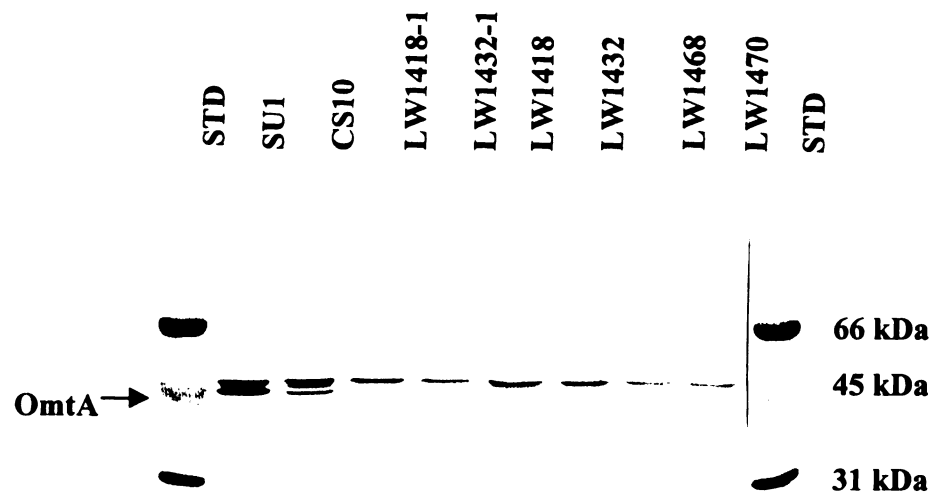


Figure 3.2. Western blot analysis of fungal protein extracts using subtraction-purified PAb raised against native OmtA. Crude protein extracts were isolated from wild-type aflatoxin-producing strain SU1, parent strain CS10, and *omtA* knock-out strains, LW1418-1, LW1432-1, LW1418, LW1432, LW1468 and LW1470, grown in YES liquid medium for 48 h. LW1418-1 and LW1432-1 are single spore isolates of LW1418 and LW1432, respectively. The native OmtA antibodies used were subtraction-purified with LW1418 protein extract two times. The possible OmtA reactive band (45 kDa) is indicated by an arrow at the left of the blots. Lane STD contains molecular mass standards; mass of standards is shown at the right of the blot.

Figure 3.3. Conversion of ST to OMST by affinity purified MBP-OmtA fusion protein. (A) SDS-PAGE of IPTG- induced bacterial crude extracts containing MBP-OmtA or MBP. (B) SDS-PAGE of affinity purified MBP-OmtA. Lanes MW1 and MW2 represent molecular mass standards; molecular mass is indicated to the left and right of the gel. (C) Thin layer chromatography to catalyze the conversion of ST to OMST by affinity purified MBP-OmtA and controls. Five μ l of reaction mixture was analyzed after appropriate time periods by TLC using chloroform /acetone (95:5) as the developing system. Control reactions included all reagents except ST, SAM, or MBP-OmtA, respectively. OMST standards are located in lanes on both ends of the TLC (STD: OMST).

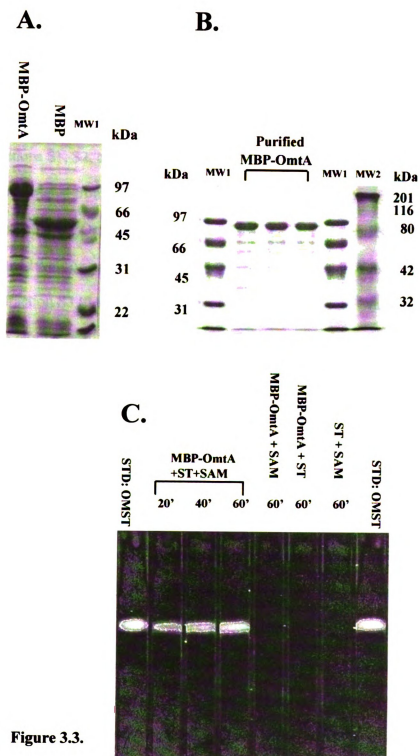


Figure 3.3.

detected in SU1 grown for 48 or 72 h in the same medium (Figure 3.4.A).

Western blot analysis of OmtA in colonies grown on solid medium. The accumulation and distribution of OmtA was analyzed in time-fractionated colonies grown on solid YES or PDA agar medium for 72 h (Figure 3.4.B, C and D). OmtA protein was detected in fractions S1, S2, and S3 of a 72 h old SU1 colony but not in corresponding colony fractions isolated from AFS10 (*aflR* knockout) (Figure 3.4.D) or LW1432 (*omtA* knockout) (Figure 3.4.C). OmtA in colony fractions S1 (48 to 72 h) and S2 (24 to 48 h) showed increased levels of smaller peptides and correspondingly less full-length protein. In contrast, in fraction S3 (0 to 24 h) of a 72 h old colony, full length OmtA was found at higher levels. A similar result was observed using SU1 grown on PDA medium and CS10 (parent strain of LW1432) grown on YES agar medium; very little OmtA protein could be detected in fraction S1 and C1 (48 to 72 h) while more full-length protein was detected in the youngest colony fraction (S3 and C3; 0 to 24 h) (Figure 3.4.C). No OmtA protein could be detected in any colony fraction of either LW1432 or AFS10.

Confocal Laser Scanning Microscopy. Immuno-fluorescence microscopy was conducted on samples prepared from fractionated colonies grown on YES solid media. To compare the fluorescence labeling intensity between SU1 and CS10 and their non-aflatoxin producing counterparts, AFS10 and LW1432, respectively, the samples were viewed under the lowest zoom level during the Confocal Laser Scanning Microscopy (zoom = 20) in order to acquire maximum cell number within a field. Under the same

Figure 3.4. Western blot analysis of fungal protein extracts using affinity purified OmtA PAb.

(A) Analysis of SU1 crude protein extracts isolated at three time points (24, 48 and 72 h) from fungal cultures grown in YES liquid medium. The approximate mass of the primary signal (45 kDa) is shown to the right of the blots in panels A and B, and to the left of blots in panels C and D. (B) Analysis of protein extracts from time-fractionated colonies of SU1 grown on PDA agar medium. 72 h-old colonies were fractionated into three concentric rings based on area covered at three time points. S1, 48 to 72 h; S2, 24 to 48 h; S3, 0 to 24 h. (C) Analysis of protein extracts from time-fractionated colonies of CS10 and LW1432 grown on YES agar medium. (D) Analysis of protein extracts from time-fractionated colonies of SU1 and AFS10 grown on YES agar medium. Lane STD contains molecular mass standards; mass of standards is shown at the right of panel C.

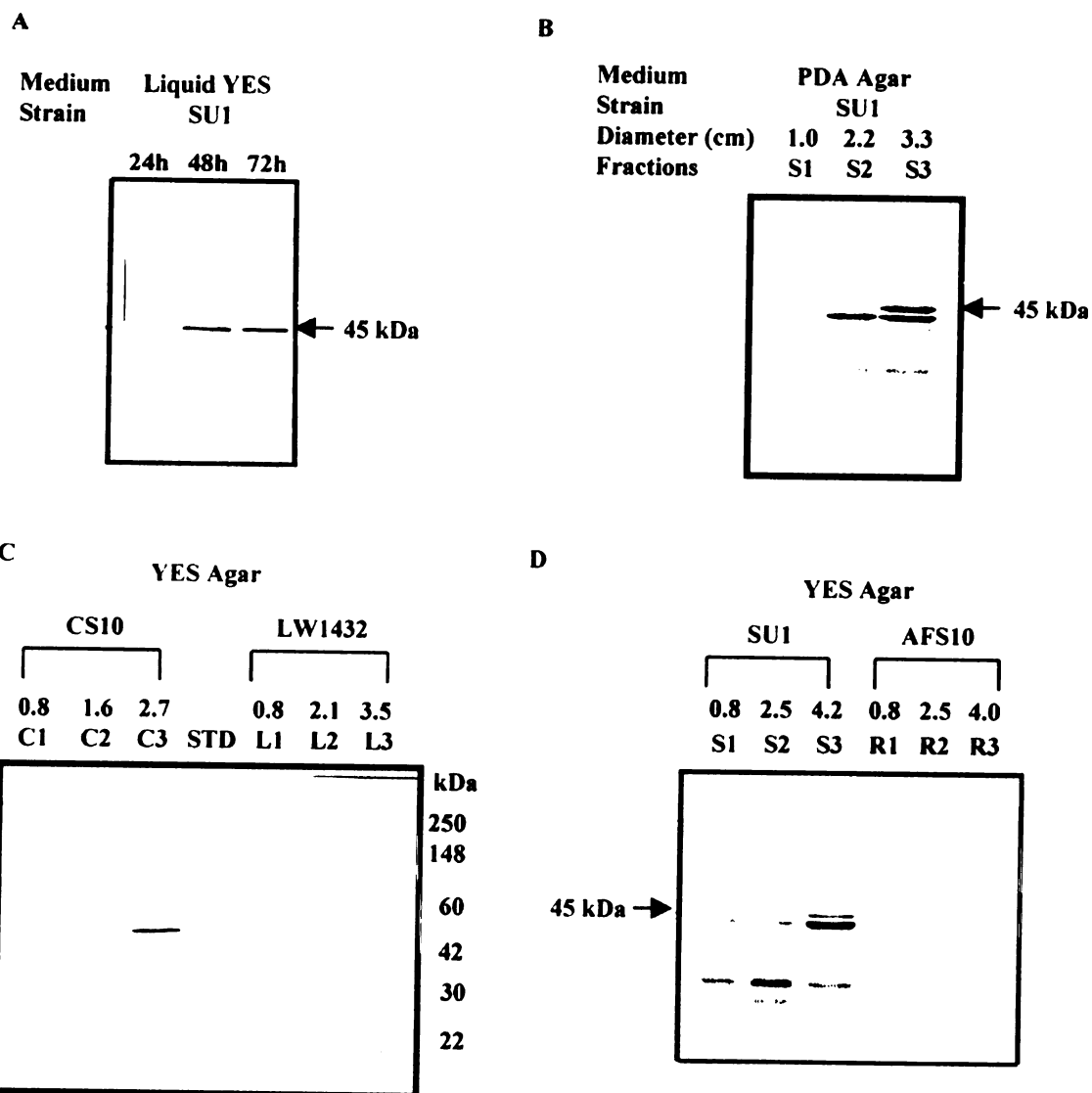


Figure 3.4.

contrast and brightness settings, the samples prepared from the control strain AFS10 (fractions R1, R2, and R3) and LW1432 (fractions L1, L2 and L3) did not show significant fluorescent signals compared to samples prepared from the same colony fractions from wild type SU1 (fractions S1, S2, and S3) or CS10 (fractions C1, C2 and C3) (Figure 3.5.). These data are consistent with Western blot analysis of protein extracts isolated from the same colony fractions (Figure 3.4.C and D; i.e., OmtA was only detected in SU1 and CS10 but not in AFS10 or LW1432). OmtA was observed in the substrate level mycelium throughout a 72 h old colony grown on YES media; the protein was also detected in the conidiospore-bearing structures (particularly in vesicles; Figure 3.6.B) located in fractions S1 and S2 at nearly equal intensity as in substrate level mycelium. The fluorescent signal was confined to discrete areas (patches) within cells (Figure 3.6.A). However, due to limitations in resolution of confocal laser scanning microscopy, it was not clear if these areas are associated with particular organelles. Similar samples were also probed with anti-SKL antibodies that are expected to detect proteins targeted to peroxisomes and Woronin bodies (Figure 3.6.C) (10,23). The observed fluorescent pattern was consistent with localization to these organelles. In addition, we used SYTOX Green to stain nuclei in fungal fractions (Figure 3.6.D); again the fluorescent pattern was consistent with the expected results. Neither anti-SKL nor SYTOX generated the same “patchy” pattern as anti-OmtA. In summary, the data suggest that OmtA protein is evenly distributed in all cell types in a fungal colony and does not accumulate to highest levels in conidiophores. The fluorescent signal is not consistent with localization of OmtA to only peroxisomes, Woronin bodies, or nuclei. However, the data do not rule out the possibility that OmtA is localized to other cell locations as well as these specific organelles.

Figure 3.5. OmtA protein localization in time-fractionated colonies of *A. parasiticus* SU1, AFS10 (*AfR* knockout), CS10 and LW1432 (*omtA* knockout) grown on YES agar for 72 h. Paraffin-embedded fungal sections were immuno-labeled with affinity purified OmtA PAb (20 µg/ml) followed by Alexa 488 conjugated goat anti-rabbit IgG.

(A) Fluorescence images of SU-1 (S1, S2, and S3) and AFS10 (R1, R2, and R3).

(B) Fluorescence images of CS10 (C1, C2 and C3) and LW1432 (L1, L2 and L3). All colony fractions were analyzed under the same instrument settings. Bar = 50 µm.

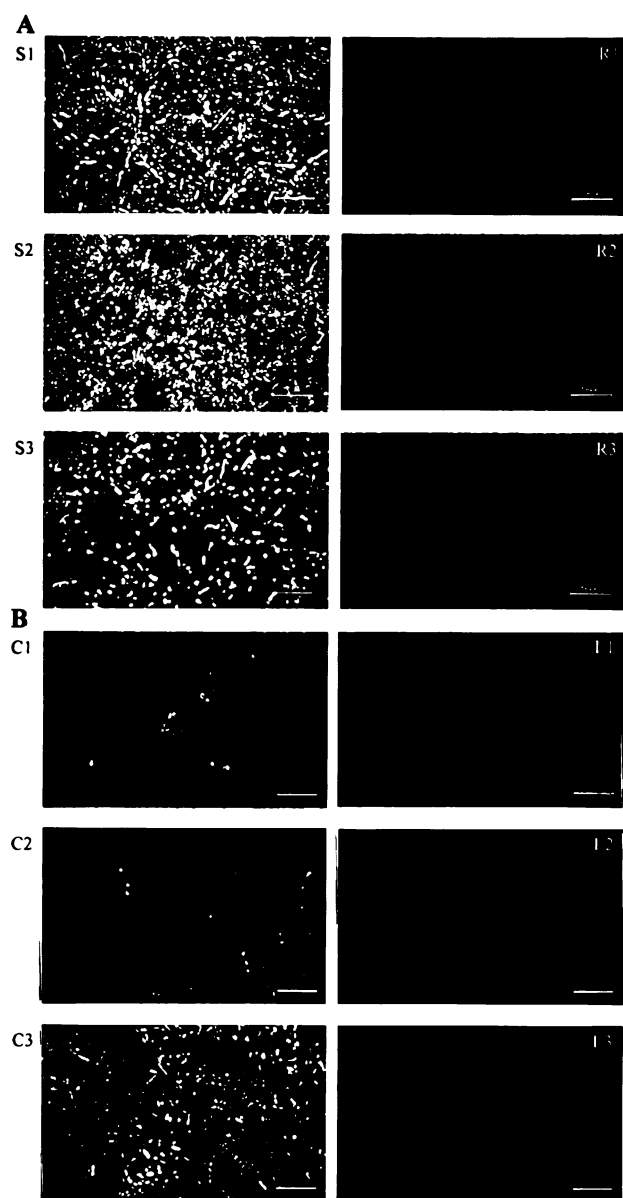


Figure 3.5.

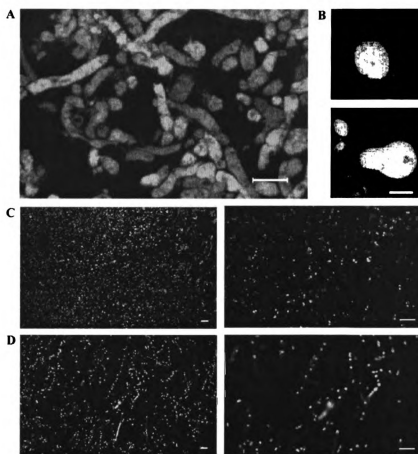


Figure 3.6. Protein localization using OmtA PAb and anti-SKL, and detection of nuclei using SYTOX Green. (A) Z-series overlay image of SU1 (fraction S2) immuno-labeled with OmtA PAb. The image consists of an overlay of ten consecutive optical sections taken at Z-interval of 800 nm (step size). (B) Fluorescence images of vesicles of conidiophores of SU-1 (fraction S1) immunolabeled with OmtA PAb. (C) Immuno-labeling of SU1 (fraction S2) with anti-SKL. The magnification for the left panel is 400X and for right panel is 2,000 X. (D) Fluorescence image of nuclei in SU1 (fraction S2) stained with SYTOX. The magnification for the left panel is 400X and for the right panel is 2,000 X. The bar in panels A, B, C, and D represents 10 μ m.

DISCUSSION

Because a close regulatory association between aflatoxin synthesis and conidiation has been demonstrated in several studies (7,9), we hypothesized a close temporal and spatial association between OmtA expression and conidiospore development. This study was designed to address this hypothesis. First, it was necessary to develop highly specific OmtA antibodies and a method for analysis of protein accumulation and distribution in cells and fungal colonies grown on solid growth medium.

We initially experienced specificity problems with PAb (15) raised to native OmtA that resulted in severe cross-reactivity in Western blot analysis and artifacts in protein localization (Figure 3.1.). Because aflatoxin enzymes are present at low concentration in the fungus (11), purification of OmtA from the fungus likely resulted in co-purification of at least trace amounts of other proteins that, although undetectable by SDS-PAGE, still possessed strong antigenicity.

To increase specificity, we generated PAb against affinity-purified MBP-OmtA and further purified them by affinity chromatography with a column carrying fungal proteins isolated from LW1432 (*omtA* knockout). This procedure helped eliminate cross-reactive antibodies. Specificity was demonstrated via Western blot analysis. OmtA could not be detected in either AFS10 or LW1432, strains that do not synthesize this protein. OmtA PABs did not detect OmtA after 24 h in YES liquid or solid media but did detect a protein of appropriate size (45kDa) at 48 and 72 h. This pattern of accumulation is similar to that observed for other aflatoxin proteins including Nor-1 (26), Ver-1 (13,14)

and VBS (unpublished data) suggesting that accumulation of these proteins is coordinately regulated. In addition, analysis of fungal extracts from SU-1, CS10, AFS10 and LW1432 did not show significant cross-reaction of OmtA PAb to other cellular proteins including DmtA; sequence identity between OmtA and DmtA was reported previously (18).

Time-dependent colony fractionation provided a practical method for monitoring protein accumulation and distribution in fungal tissues of different ages; similar information could not be obtained in liquid shake culture (batch fermentation). Knowledge of OmtA distribution was essential to identify fungal tissues that were rich in the target protein and allowed successful immuno-histochemistry in this study and immuno-electron microscopy in a study now underway. Since these protocols require very small quantities of fungal tissue (1mm³ for immunoelectron microscopy for example) one could easily miss the relevant protein if it was not uniformly distributed in a colony.

Using this colony fractionation protocol, OmtA PAb, and Western blot analysis, we observed OmtA in all fractions of a 72 h old colony (fractions S1, S2, and S3) grown on YES agar. The youngest colony fraction (S3; 0 to 24 h) contained mostly full-length OmtA, while fraction S1 (48 to 72 h) contained less full-length OmtA and more OmtA-derived peptides. In fraction C1 (CS10, 48 to 72 h) and the oldest fraction of SU-1 (48 to 72 h) grown on PDA medium, OmtA was almost undetectable. Similarly, OmtA was not observed in the oldest fraction of a 90 h old colony grown on YES medium. No OmtA protein was detected in 24 h old colonies grown on YES; OmtA was detected in 48 h old colonies on the same medium. Together the data suggest that OmtA biosynthesis in *A. parasiticus* SU1 grown on solid YES media initiates after 24 h. OmtA then accumulates

to relatively high levels in the youngest fraction, for example, in C3 and S3 (0 to 24 h) of a 72 h old colony. As cells in that fraction age (at 48 or 72 h), OmtA synthesis appears to decline, the protein is proteolytically cleaved, and disappears completely by 90 h. The rate of OmtA proteolysis appears to be age- and growth medium-dependent. OmtA proteolysis was not observed to the same extent in cells grown in liquid culture.

OmtA proteolysis may occur after “accidental” contact with fungal proteases released during mechanical disruption of fungal tissues. However, because the tissue is quickly frozen before disruption and because protease inhibitors are added to the extraction buffer, we hypothesize that OmtA proteolysis occurs as part of a natural process during fungal growth and development. To generate developmental structures in solid culture, fungi may require proteases to digest unneeded structures or metabolic proteins (20). For example, a mutation in one protease, subtilisin-related serine proteinase (ALP2), resulted in smaller conidiophore vesicles (50% reduction) and a lower number of conidia (80% reduction) in *A. nidulans* (20). We observed that SU-1 fungal colonies on PDA, in which colonies grew more slowly than on YES (smaller diameter), also had more severe OmtA proteolysis. Conidiophore structures also could be found in fraction C3 on YES whereas they were absent in S3 on YES.

Septal pores form “channels” between adjacent cells in the mycelium and appear to play an important role in cell-to-cell communication in filamentous fungi (3). Cytoplasm, mitochondria and nuclei migrate throughout the mycelium via septal pores (3,16). Because we do not see accumulation of OmtA in 24 h old colonies on YES but do see accumulation of OmtA in cells in the youngest fraction S3 (0 to 24 h) of a 72-h old fungal colony, we hypothesize that migration of OmtA together with cytoplasm and organelles occurs from older cells (fraction S2, 24 to 48 h) to younger cells (fraction S3, 0

to 24 h) on solid media. Alternatively, it is also possible that specific regulatory factor(s) involved in aflatoxin biosynthesis (eg. AflR) move from the aflatoxin producing cells in fraction S2 to fraction S3 inducing *omtA* expression in these younger tissues.

OmtA-specific PAb were also used in immuno-fluorescence microscopy. The data provided strong evidence that our purification strategy resulted in PAb that were sensitive and specific. Although the paraffin-embeddment procedure and sectioning technique have been used for microscopic analysis of a variety of organisms (4), this is the first reported use in the study of a fungus grown on solid media and the first application in a study of *Aspergillus parasiticus*. We previously utilized a fungal cell preparation technique for immuno-labeling that required digestion of the cell wall using Novozyme (8). However, in these early localization studies, variation in cell wall digestion resulted in significant artifacts. The paraffin-embedment and sectioning procedures developed and described in this study successfully preserved fungal mycelium, developmental structures, organelle structure, and protein antigenicity; they also eliminated the need for cell wall digestion, in turn generating consistent and reproducible immuno-labeling results. This technique provides a useful tool to localize proteins and possibly other compounds in fungal cells and colonies.

Despite the close regulatory relationship between sporulation and aflatoxin production, our data suggest that OmtA is not produced exclusively in conidiophores as hypothesized. On the contrary, CLSM micrographs showed that OmtA is distributed throughout the colony and in both conidiophores and vegetative hyphae. Western blot analysis indicated that abundant full-length OmtA was observed in fraction S3, even though conidiophores were nearly absent in this area. In fraction S2, the highest intensity of OmtA was detected under CLSM, and OmtA accumulated to similar levels in

vegetative hyphae and conidiophores.

Cells immuno-labeled with OmtA PAb and analyzed by CLSM showed patches of fluorescence within fungal cells suggesting that OmtA is confined to sub-cellular compartments. An alternative explanation is that OmtA is present in the cytoplasm and is thus excluded from cell organelles. To gain more information about sub-cellular localization, we labeled paraffin embedded sections to identify specific organelles; for example anti-SKL antibodies (10) were used to label peroxisomes and SYTOX Green was used to detect nuclei. Both probes generated small regularly shaped signals consistent with the expected organelles, indicating that the double- membrane bound nuclei as well as single-membrane bound microbodies were well-preserved. These observations strongly suggest that we have minimized artifacts due to poor sample preparation. Images using both probes were different than with OmtA PAb. The anti-SKL labeled organelles were recently demonstrated to be Woronin bodies by immuno-electron microscopy (data not shown).

There are some indirect data available that suggest that at least some aflatoxin proteins are localized in organelles. For example, in *A. parasiticus*, the aflatoxin enzyme OrdA was found to be membrane associated during protein purification (6). Based on amino acid sequence, another aflatoxin protein, AflJ, was predicted to contain a C-terminal microbody targeting signal, NRY, and three membrane-spanning regions (17). By comparing the protein sequence of purified OmtA with the predicted amino acid sequence derived from the OmtA cDNA, this protein was proposed to contain a leader sequence that apparently is processed to generate a 42-kDa protein (25). This leader sequence may be required for this enzyme to interact with membranes (25). Based on computer-assisted analysis (PSORT; prediction of protein localization sites Version 6.4:

<http://psort.nibb.ac.jp/psort>), we also speculate that putative peroxisomal targeting signals are present in aflatoxin proteins including Nor-1, AvnA, OmtA and OrdA (unpublished data). In contrast, OmtA (6) and Nor-1 (26) were observed in the post-microsomal cytoplasmic fraction in cell fractionation studies. Therefore, the distribution of aflatoxin enzymes within a fungal cell still is not clearly understood.

Localization to specific organelles has been demonstrated for enzymes involved in secondary metabolism. Penicillin is a secondary metabolite produced by several filamentous fungi including *A. nidulans*. The enzyme, 6-aminopenicillanic acid acyltransferase, which catalyzes the final step of penicillin biosynthesis in *Penicillium* was localized to a membrane bound organelle, the microbody (19); the authors suggested that penicillin is synthesized in this organelle. In a separate study, prehelminthosporol, a phytotoxin produced by *Bipolaris sorokinianawas*, was localized in the Woronin body (1) which is thought to be derived from the peroxisome (24). Prehelminthosporol has been shown to disrupt plant plasma membranes and inhibit growth of gram-positive bacteria. Detailed sub-cellular localization of OmtA and several other aflatoxin enzymes using immunoelectron microscopy should help clarify the cellular site of aflatoxin synthesis in *A. parasiticus*.

ACKNOWLEDGEMENTS

1. This work was supported by the Michigan Agricultural Experiment Station (MSU), the National Food Safety and Toxicology Center (MSU), the Center for Environmental Toxicology (MSU), and the National Institutes of Health (RO1 CA52003-11).
2. Data in chapter 2 and 3 were published in **Applied and Environmental Microbiology** entitled “**Function of native OmtA *in vivo* and expression/distribution of this protein in colonies of *Aspergillus Parasiticus***”.
3. The LSM images in Figure 5 and 6 were generated by Ching-Hsun Chiou.

REFERENCES

1. **Akesson, H., E. Carlemalm, E. Everitt, T. Gunnarsson, G. Odham, and H-B Jansson.** 1996. Immunocytochemical localization of phytotoxins in *Bioplaris sorokiniana*. Fungal Gene. Biol. **20**:205-216.
2. **Ausubel, F. M., R. Brent, E. Kingston, D. D. Moore, J. G. Seidman, J. A. Smith, and K. Struhl.** 2001. Current protocols in molecular biology. John Wiley and Sons, New York, NY.
3. **Belozerskaya, T. A.** 1998. Cell-to-cell communication in differentiation of mycelial fungi. Membr. Cell Biol. **11**: 831-840.
4. **Bratthauer, G.R.** 1999. In L.C. Javois (ed.), Methods in Molecular Biology. Human Press, Totowa, New Jersey.
5. **Cary, J., J. Linz, and D. Bhatnagar.** 2000 Aflatoxins: Biological significance and regulation of biosynthesis. In J. Cary, D. Bhatnagar. and J. Linz (eds.), Microbial foodborne disease: mechanisms of pathogenesis and toxin synthesis. Technomic Publishing, Lancaster, PA.
6. **Cleveland, T. E., A. R. Lax, L. S. Lee, and D. Bhatnagar.** 1987. Appearance of enzyme activities catalyzing conversion of sterigmatocystin to aflatoxin B1 in late-growth-phase *Aspergillus parasiticus* cultures. Appl. Environ. Microbiol. **53**:1711-3.
7. **Guzman-de-Pena, D. and J. Ruiz-Herrera.** 1997. Relationship between aflatoxin biosynthesis and sporulation in *Aspergillus parasiticus*. Fungal Genet. Biol. **21**:198-205.
8. **Harris, S. D., J. L. Morrell and J. E. Hamer.** 1994. Identification and characterization of *Aspergillus nidulans* mutants defective in cytokinesis. Genetics. **136**:517-532.
9. **Hicks J. K., J-H, Yu, N. P. Keller and T. H. Adams.** 1997. *Aspergillus* sporulation and mycotoxin production both require inactivation of the FadA G protein-dependent signaling pathway. EMBO J. **16**: 4916-4923.
10. **Keller, G-A., S. Krisans, S. J. Gould, J. M. Sommer, C. C. Wang, W. Schliebs, W. Kunau, S. Brody and S. Subramani.** 1991. Evolutionary conservation of a microbody targeting signal that targets proteins to peroxisomes, glyoxysomes, and glycosomes. J. Cell Biol. **114**:893-904.
11. **Keller, N. P., H. C. Dischinger, JR., D. Bhatnagar, T. E. Cleveland and A. H. J. Ullah.** 1993. Purification of a 40-kDa methyltransferase activity in the aflatoxin biosynthetic pathway. Appl. Environ. Microbiol. **59**:479-484.

12. **Liang, S.-H.** 1996. The function and expression of the *ver-1* gene and localization of the Ver-1 protein involved in aflatoxin B₁ biosynthesis in *Aspergillus parasiticus*. PhD Dissertation, Michigan State University, East Lansing.
13. **Liang, S.-H., C. D. Skory and J. E. Linz.** 1996. Characterization of the function of the *ver-1* and *ver-1B* genes, involved in aflatoxin biosynthesis in *Aspergillus parasiticus*. Appl. Environ. Microbiol. **62**:4568-4575.
14. **Liang, S.-H., T.-S. Wu, R. Lee, F. S. Chu and J. E. Linz.** 1997. Analysis of mechanism regulating expression of the *ver-1* gene, involved in aflatoxin biosynthesis. Appl. Environ. Microbiol. **63**:1058-1065.
15. **Liu, B. H., N. P. Keller, D. Bhatnagar, T. E. Cleveland and F. S. Chu.** 1993. Production and characterization of antibodies against sterigmatocystin O-methyltransferase. Food Agric. Immunol. **5**:155-164.
16. **Markham, P.** 1995. Organelles of filamentous fungi. p. 75-98. In N. A. R. Gow, and G. W. Gooday (ed), The growing fungus, 1st ed. Chapman & Hall, London, UK.
17. **Meyers, D. M., G. Obrian, W. L. Du, D. Bhatnagar and G. A. Payne.** 1998. Characterization of *afl J*, a gene required for conversion of pathway intermediates to aflatoxin. Appl. Environ. Microbiol. **64**:3713-7.
18. **Motomura, M., N. Chihaya, T. Shinozawa, T. Hamasaki and K. Yabe.** 1999. Cloning and characterization of the O-Methyltransferase I gene (*dmtA*) from *Aspergillus parasiticus* associated with the conversion of demethylsterigmatocystin to sterigmatocystin and dihydrodemethylsterigmatocystin to dihydrosterigmatocystin in aflatoxin biosynthesis. Appl. Environ. Microbiol. **65**:4987-4994.
19. **Muller, W. H., T. P. van der Krift, A. J. J. Krouwer, H. A. B. Wosten, L. H. M. van der Voort, E. B. Smaal and A. J. Verkleij.** 1991. Localization of the pathway of the penicillin biosynthesis in *Penicillium chrysogenum*. EMBO journal. **10**:489-495.
20. **Reichard, U., G. T. Cole, T. W. Hill, R. Ruchel and M. Monod.** 2000. Molecular characterization and influence on fungal development of ALP2, a novel serine proteinase from *Aspergillus fumigatus*. Int. J. Med. Microbiol. **290**:549-558.
21. **Skory, C. D., J. S. Horng, J. J. Pestka, and J. E. Linz.** 1990. Transformation of *Aspergillus parasiticus* with the homologous gene (*pyrG*) involved in pyrimidine biosynthesis. Appl. Environ. Microbiol. **56**:3315-3320.
22. **Skory, C. D., P.-K. Chang, J. Cary, and J. E. Linz.** 1992. Isolation and characterization of a gene from *Aspergillus parasiticus* associated with the conversion of versicolorin A to sterigmatocystin in aflatoxin biosynthesis. Appl. Environ. Microbiol. **58**:3527-3537.

23. **Trail, F., P-K. Chang, J. Cary and J. E. Linz.** 1994. Structural and functional analysis of the *nor-1* gene involved in the biosynthesis of aflatoxin by *Aspergillus parasiticus*. Appl. Environ. Microbiol. **60**:3315-3320.
24. **Valenciano, S., J.R. De Lucas, I. Van der Klei, M. Veenhuis, and F. Laborda.** 1998. Charatcerization of *Aspergillus nidulans* peroxisomes by immunoelectron microscopy. Arch. Microbiol. **170**:370-376.
25. **Yu, J., J. W. Cary, D. Bhatnagar, T. E. Cleveland, N. P. Keller, F. S. Chu.** 1993. Cloning and characterization of a cDNA from *Aspergillus parasiticus* encoding an O-methyltransferase involved in aflatoxin biosynthesis. Appl. Environ. Microbiol. **59**:3564-71.
26. **Zhou, R.** 1997. The function, accumulation, and localization of the Nor-1 protein involved in aflatoxin biosynthesis; the function of the *fluP* gene associated with sporulation in *Aspergillus parasiticus*. PhD Dissertation, Michigan State University, East lansing.

CHAPTER 4

Sub-cellular localization of aflatoxin biosynthetic enzymes in time-dependent fractionated colonies of *Aspergillus parasiticus*

INTRODUCTION

Aflatoxins are highly toxic and carcinogenic secondary metabolites produced by several filamentous fungi including *Aspergillus parasiticus*, *A. flavus*, *A. nomius*, and *A. tamarii* (12,23). Aflatoxins pose significant health and economic problems in the US and many other locations throughout the world because they frequently contaminate food and feed crops including corn, peanuts, tree nuts and cottonseed (9,12).

The biosynthesis of aflatoxin is a complex process that involves at least 17 enzyme activities (23). The distribution of these enzymes within fungal colonies and location within fungal cells remain unknown. The objective of this study was to investigate the distribution and sub-cellular location of representative enzymatic activities in the aflatoxin biosynthetic pathway. Toward this end, I focused attention on Nor-1 (29), Ver-1 (19) and OmtA (33) that catalyze early, middle and late enzymatic steps in the aflatoxin biosynthetic pathway, respectively. Nor-1 and Ver-1 are NADPH-dependent keto-reductases involved in the conversion of norsolorinic acid (NA) to averantin (AVN) and versicolorin A (VERA) to demethylsterigmatocystin (DMST), respectively; OmtA is a methyltransferase that converts sterigmatocystin (ST) to O-methylsterigmatocystin (OMST).

Specific secondary metabolites such as penicillin and prehelminthosporol are known to enhance the survival of the producing organism in the growth environment (5,1). However, the biological function of most secondary metabolites, including aflatoxin, is not clear. Characterization of the sub-cellular location of aflatoxin and/or its biosynthetic enzymes should provide important clues about the biological function and mechanisms that mediate intracellular transport, storage, and secretion of this toxic secondary metabolite by the producing fungus.

As a potential mechanism to protect fungal cells from the potential deleterious effects of aflatoxin accumulation in the mycelium, I hypothesized that aflatoxin enzymes are compartmentalized in a sub-cellular organelle(s). Further, I hypothesized that the end-product, aflatoxin, is synthesized within this organelle and then secreted directly into the extracellular environment. To address these hypotheses, I analyzed enzyme distribution in fungal colonies by Western blot analysis and immuno-fluorescence microscopy, and carried out *in situ* localization of aflatoxin enzymes within fungal cells using immuno-microscopic methods following cryofixation. For immuno-transmission electron microscopy (TEM), it had been shown previously that a sample preparation procedure that combines rapid freezing and freeze substitution is superior to chemical fixation in terms of ultrastructure and antigenicity (1). Therefore, I used a modification of published methods (32) to localize Nor-1, Ver-1 and OmtA in time-fractionated colonies. Nor-1 and Ver-1 enzymes were primarily localized to the cytoplasm in cells 24 to 48 h old (fraction 2) suggesting that they are cytosolic enzymes. OmtA was also detected in the cytoplasm. However, in cells located near the basal (substrate) surface of the colony, large quantities of OmtA were detected in organelles identified as vacuoles. Based on

current data, we hypothesize that the relative distribution of OmtA to cytoplasm or vacuoles depends on the age and/or physiological condition of the fungal cells.

MATERIALS AND METHODS

Fungal strains and time-dependent fractionation of fungal colonies. *A. parasiticus* SU1 (NRRL5862, ATCC 56775) is a wild-type, aflatoxin-producing strain. AFS10 (*aflR* via gene disruption) is a non-aflatoxin producing strain derived from *A. parasiticus* NR-1 (*niaD*) that in turn was derived from SU1 (7). Asexual conidiospores (5×10^5) of *A. parasiticus* SU1 and AFS10 were inoculated onto the center of YES agar medium (2% yeast extract, 6% sucrose, pH 5.8) overlaid with sterile cellophane membranes and incubated at 29° C in the dark. 72 h-old colonies of SU1 (S) and AFS10 (R) were fractionated into three concentric rings based on area covered at 24, 48, or 72 h of growth (fraction 1, 48-72 h old; fraction 2, 24-48 h, and fraction 3, 0-24 h) to generate fractions S1, S2, S3 and R1, R2, R3 respectively as described by Lee *et al.* (17). The harvested mycelia from appropriate sections of the colony were used in sample preparation for Western blot analysis and for fluorescence and electron microscopy.

Western blot analysis of proteins isolated from colony fractions. Sample preparation and Western blot analysis of *A. parasiticus* proteins isolated from colony fractions were conducted using methods described in Lee *et al.* (17). Each lane on the 12% SDS-PAGE gel contained 60µg protein. Nor-1, Ver-1 and OmtA polyclonal antibodies were raised against maltose binding protein fusions generated for each

aflatoxin protein (35,18,19,17). Anti-Nor-1 serum (rabbit No. 126) was generated in this study and used at a 1 to 5000 dilution. Anti-Ver-1 IgG was used at 2 µg per ml.

Immuno-fluorescence labeling and confocal laser scanning microscopy (CLSM). Preparation of paraffin-embedded fungal sections, immuno-labeling, and microscopic analysis via CLSM utilized methods described by Lee *et al.* (17). The samples were probed with primary antibodies against Nor-1 (1 to 500 dilution), Ver-1 (20 µg/ml) (19) or OmtA (20 µg/ml) (17), followed by secondary antibody conjugated to a fluorescent probe (goat anti-rabbit IgG- Alexa 488 conjugate [5 µg/ml]; Abs 495 nm/ Em 519 nm). Fluorescence image detection was performed on a Meridian INSIGHT plus laser-scanning microscope (Meridian Instruments, Inc., Okemos, MI) with a 488 nm laser line. The Alexa 488 green fluorescence was detected using a BP 530/30 barrier filter. All images were captured using a 40X Zeiss Plan-NEOFLUAR oil objective lens (N.A.=1.3) (Carl Zeiss Inc., Germany) with a 1X CCD cool-charged detector allowing analysis of a large number of cells in one 512 x 480 image. Fluorescence image analysis of strains SU1 and AFS10 was conducted using the same instrument parameter settings. For all AFS10 samples, bright field images were also generated to demonstrate the size and number of cells analyzed.

Quantitative fluorescence intensity analysis. Alexa 488 fluorescence was quantified using IQ Master Program (V2.31) image analysis software that accompanied the Meridian Insight laser-scanning microscope (Meridian Instruments, Inc., Okemos, MI). The CLSM images were acquired under the identical instrument settings for samples

analyzed in the same immuno-labeling experiments. For each colony fraction, twenty images were acquired for intensity analysis and the average pixel number was reported.

Sample preparation for immuno-electron microscopy. Three to five mm diameter circles of fungal tissue were obtained from fraction 2 of colonies of SU1 and AFS10 grown on YES agar plates. These circles were cut from the colony using sterile 200 μ l pipette tips with the end removed with a sterile razor blade to generate a cutting edge with the correct diameter. Samples were immediately cryofixed at -190° C in a commercial Jet-Freezer (RMC MF7200) and then transferred to a tube containing acetone that had been frozen by immersion in liquid nitrogen. The following substitution procedure was modified from a published method (32). Samples in frozen acetone were then stored at -80° C for 6 d. Samples were washed twice with fresh, ice-cold acetone (-20° C) and then immersed in fresh, ice-cold acetone (-20° C) containing 0.2% glutaraldehyde and stored at -20° C for 24 h. After washing with fresh, ice-cold acetone (-20° C) three times, acetone in samples was replaced with 100 % ethanol by a graded series of ethanol/acetone (35%, 50%, 75%, 90% [30 min each] and 100 % [two times, 30 min each]). Samples were then infiltrated with a graded series of LR White resin (Ted Pella, Inc., Redding, CA) /ethanol: 5, 10, 20, 40, 60% (3 h each), 90% for 24h and 100% (3 changes) for 2 d at -20° C. Polymerization was carried out under UV light (366 nm) at 4° C for 48 h.

Immuno-gold labeling and electron microscopy. Fungal sections for immuno-gold labeling were cut to 90 ~ 100 nm thickness using an MTX ultramicrotome (RMC, Tucson, Arizona). Sections were collected onto formvar-coated grids. Each grid

contained approximately 10-20 thin sections. For each labeling experiment, two grids each from SU1 and AFS10 tissues were used. For each antibody, at least three independent labeling experiments were performed. First, grids with sections were incubated with blocking solution (1% BSA plus 0.1% saponin in TBS) at 4° C overnight. Primary antibody treatment (purified OmtA IgG, 50 µg per ml; anti-Ver1 IgG, 140 µg per ml; anti-serum: anti-SKL serum, 1: 200; anti-Nor-1, 1: 500) was performed at room temperature for 4 h. Secondary antibody treatment (goat anti-rabbit conjugated with 10 nm gold; 1 to 30-fold dilution) (Ted Pella, Inc., Redding, CA) was performed at room temperature for 2 h. After each antibody incubation, grids were washed once with Tris-buffered saline (pH 7.5) containing 1% BSA and 0.1% saponin for 5 min followed by five washes with TBS for 25 min total. Finally, grids were washed with dd H₂O for 30 s and post stained with 3% uranyl acetate for 20 min. Sections were observed using a JEOL 100CX II transmission electron microscope (Tokyo, Japan) at 100 kV.

RESULTS

Western blot analysis of Nor-1 and Ver-1 isolated from colony fractions 1, 2, and 3 of *A. parasiticus* SU1 and AFS10 demonstrated the specificity of the antibody preparations used in microscopic analysis (Figure 4.1). Similar analysis was conducted previously on OmtA only, in which increasing quantities of proteolytically cleaved enzyme were detected in fractions 2 and 1 (17); the highest proportion of full-length protein was observed in fraction 2. In contrast, Nor-1 and Ver-1 in the current study appeared predominantly in full-length form in all colony fractions. The proteolytically cleaved forms of these two enzymes were not observed in cells grown on solid YES

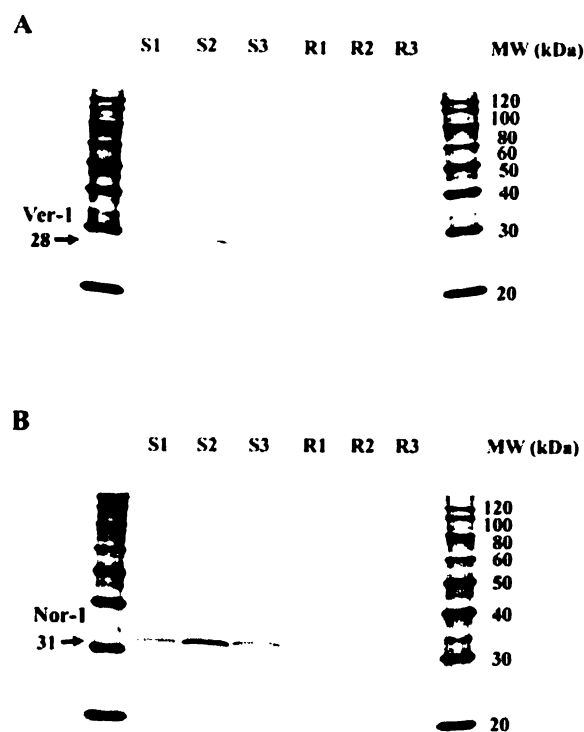


Figure 4.1. Western blot analysis of fungal protein extracts using Ver-1 and Nor-1 polyclonal antibodies. Proteins were extracted from time-fractionated colonies of SU1 and AFS10 grown on YES agar medium and were subjected to Western blot analysis with Ver-1 (Panel A) and Nor-1 (Panel B) polyclonal antibodies. 72 h-old colonies were fractionated into three concentric rings based on area covered at three time points: for S1 and R1, 48 to 72 h; S2 and R2, 24 to 48 h; S3 and R3, 0 to 24 h. The lanes to the left and right contain molecular mass standards. The molecular mass of standards are marked at the right of Panels A and B. The molecular masses of Ver-1 and Nor-1 (indicated by arrows at the left) are 28 kDa and 31 kDa, respectively.

medium. However, like OmtA, the highest quantity of Nor-1 and Ver-1 was observed in fraction 2 of SU1.

Immuno-fluorescence microscopy via CLSM confirmed the specificity of the Nor-1 and Ver-1 polyclonal antibodies for microscopic analysis. The specificity of the OmtA polyclonal antibody was confirmed in a previous study (17). Nor-1 and Ver-1 were detected in all colony fractions of SU1 (Figure 4.2a for Nor-1 and Figure 4.2d for Ver-1). Under the same instrument settings, very little signal was detected in AFS10 (Figure 4.2b for Nor-1 and Figure 4.2e for Ver-1). Therefore, bright field images of the AFS10 colony fractions are shown to illustrate the typical size and numbers of cells analyzed (Figure 4.2c and 2f). Quantitative analysis of the fluorescence intensity in the CLSM digital images using IQ Master Program (V2.31) image analysis software confirmed that the highest quantity of these three aflatoxin enzymes occurred in fraction 2 (Table 4.1). Therefore, we focused our immuno-TEM analysis on the proteins in this colony fraction.

Using our sample preparation, labeling, and imaging procedures, very few gold particles were observed on control sections of wild-type strain SU1 treated with secondary antibodies only (Figure 4.3A and B). Therefore, we interpreted an intense signal (black dots representing 10 nm gold particles) on sections treated with both primary and secondary antibodies to result from the specific interaction between primary antibodies and their target proteins immobilized within the cell. However, we occasionally detected labeling of the cell wall, especially for anti-Ver-1, in certain sections of both SU1 and AFS10 (no aflatoxin proteins produced), leading us to conclude that this was non-specific labeling (data not shown). It was reported previously that non-specific labeling may result either from non-specific binding of primary antibodies to the cell wall or from cell wall-reactive antibodies that arise in rabbits exposed to or

Figure 4.2. Immuno-fluorescence confocal microscopy of Nor-1 and Ver-1 in *A. parasiticus* SU1 and AFS10 (*aflR* knockout mutant) grown on YES agar for 72 h. Colonies of SU1 and AFS10 were divided into 3 fractions (see Material and Methods). The paraffin embedded fungal sections were immuno-labeled with anti-Nor-1 antiserum (Panel A) (1:500) or anti-Ver-1 IgG (Panel B) (20 µg/ml) followed by Alexa 488 conjugated goat anti-rabbit IgG. Fluorescence intensities of SU1 sections immuno-labeled with anti-Nor-1 and anti-Ver-1 are shown in Rows a and d, respectively; and of AFS10 sections in Rows b and e. The related bright field images of the AFS10 colony fractions are shown in Rows c and f (legends labeled in black). Bar, 100 µm.

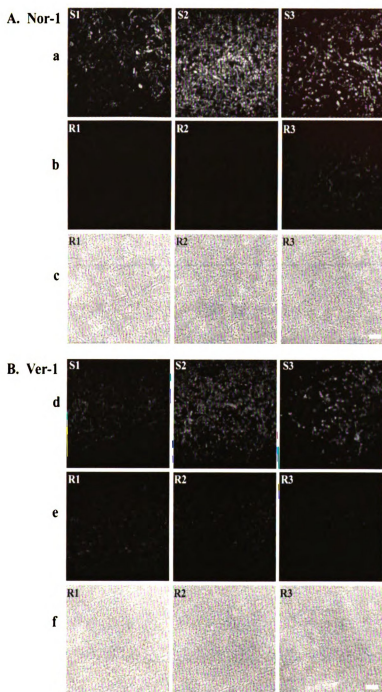


Figure 4.2.

Table 4.1. Quantative fluorescence intensity analysis of *A. parasiticus* SU1 and AFS10 immuno-fluorescence labeled with Nor-1, Ver-1 and OmtA antibodies.

(Fungal colony)	(SU-1)			(AFS10)		
<u>Protein / Colony fraction</u>	<u>S1</u>	<u>S2</u>	<u>S3</u>	<u>R1</u>	<u>R2</u>	<u>R3</u>
Nor-1	229.5	858.4	260.9	15.2	18.7	62.3
Ver-1	144.4	297.9	166.5	68.7	89.2	42.3
OmtA	120.0	940.1	146.7	4.3	3.9	21.6

* The data represent the average pixel number in 20 images from each colony fraction.

Figure 4.3. Immuno-gold labeling of *A. parasiticus* SU1 and AFS10. In Panels A and B, ultra-thin sections of fungal tissues of the aflatoxin producing strain SU1 were prepared for TEM and labeled with secondary antibodies only. Ultra-thin sections of fungal tissues of AFS10 (Panel C and E) and SU1 (Panel D and F) were labeled with primary antibodies against Nor-1 (Panel C and D) and Ver-1 (Panels E and F), followed by 10 nm gold beads conjugated to goat anti-rabbit IgG secondary antibodies (1 to 30 dilution) as described in Methods. Bars represent 500 nm in A and 250 nm in B, C, D, E and F. Abbreviations: **cw**, cell wall; **mb**, microbodies; **M**, mitochondria; **N**, nuclei; **V**, vacuole.

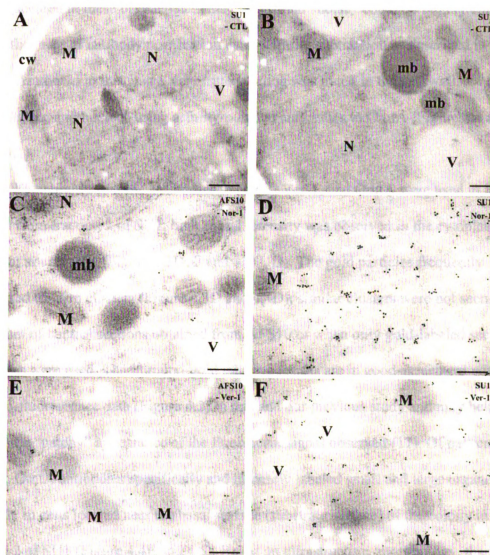


Figure 4.3.

infected by yeast or molds before or during antibody production (3, 4).

Widely scattered gold particles were also found occasionally associated with the nucleus and mitochondria in both AFS10 and SU1 labeled with Nor-1 and Ver-1 antibodies, suggesting that this was non-specific labeling or resulted from cross-reactive proteins located in these organelles. This background “noise” could be largely eliminated by a further step of antibody purification using affinity subtraction as described in Lee *et al.* (17). As shown in this study, very little labeling was noted in the cell wall, mitochondria, and nucleus using affinity-purified antibodies to OmtA (Figure 4.4 and Table. 4.1).

When highly specific antibodies to Nor-1, Ver-1, and OmtA were used to label sections from fraction 2 of SU1, high signal intensity was observed in the cytoplasm in many but not all cells (Figure 4.3D, F and 4.4C, D). The gold particles frequently aggregated to form clusters (Figure 4.3D and 4.4D); similar clusters were not seen in the cytoplasm of control sections obtained from AFS10 or when only gold-labeled secondary antibodies were used. The immuno-gold labeling results are in good agreement with immuno-fluorescence data (Figure 4.2) in this and our previous study and may help explain the “patchy” appearance of the fluorescent signal observed (17). Of particular interest, OmtA antibodies specifically and intensely labeled small and large organelles primarily in cells located near the basal surface (substrate surface) of the colony in fraction 2 of SU1 (Figure 4.4E and 4.5). Based on ultrastructure /morphology, these organelles have been identified as vacuoles (2). The labeling intensity suggested a high concentration of OmtA in these organelles. In contrast, antibodies against Nor-1 or Ver-1 did not label these organelles in sections from the same location (basal portion of fraction

Figure 4.4. Immuno-gold labeling of OmtA in *Aspergillus parasiticus* AFS10 and SU1. Ultra thin sections of fungal tissues of AFS10 (Panels A and B) and SU1 (Panels C and D) were labeled with primary antibodies against OmtA followed by gold-labeled secondary antibodies as described in Methods. Panel E is a schematic representation of the colony fractionation procedure and shows the cell distribution in a typical thin section. The specific location of OmtA in cells near the basal surface of the colony (shaded gray) is also shown in Panel E. Bars present 500 nm in panels A, C and E, and 250 nm in panels B and D. Abbreviations: cw, cell wall; M, mitochondria; N, nuclei; V, vacuole.

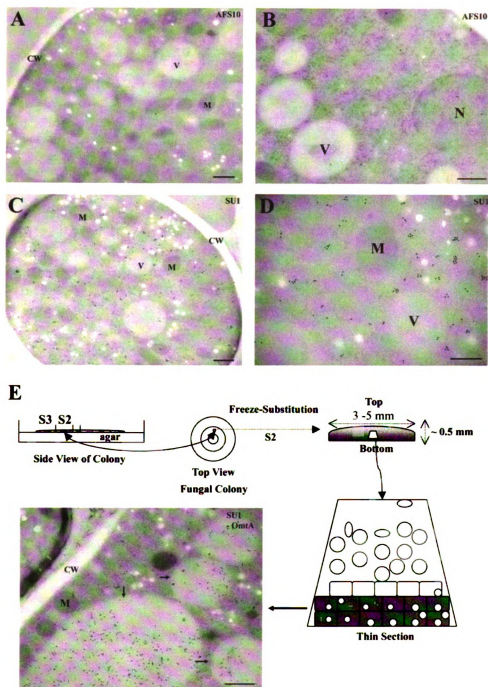


Figure 4.4.

Figure 4.5. Immuno-gold labeling of OmtA in *Aspergillus parasiticus* SU1.

Sections cut from the basal surface of the colony were labeled with primary antibodies against OmtA. The gold-labeled vacuoles inside of cells were numbered (1 to 8) and higher magnification images of these organelles are shown in Panels B, C, D and E. Bars present 2 μm in panels A and 1 μm in B, C, D and E. Abbreviations: **cw**, cell wall; **M**, mitochondria; **N**, nuclei; **V**, vacuole.

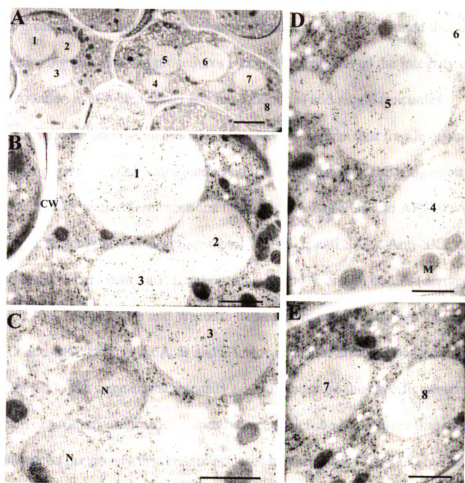


Figure 4.5.

2) (data not shown). Cells located above the basal region contained smaller organelles which were sporadically labeled by OmtA and not at all by antibodies to Nor-1 and Ver-1. Similar organelles in AFS10 did not label with polyclonal antibodies to any aflatoxin enzymes.

The gross ultrastructure of cells observed in thin sections suggested that our fixation, sectioning and labeling procedures successfully preserved the integrity of organelles bounded by double (nuclei and mitochondria) and single (vacuoles, microbodies, Woronin bodies) membranes. In order to confirm that fragile organelles bounded by single membranes could retain both ultrastructure and the antigenicity of internal proteins, we labeled some sections from fraction 2 of SU1 and AFS10 with antibodies against peroxisomal targeting signal 1 (PTS-1; anti SKL). Anti-SKL can label proteins exported to peroxisomes (microbodies; mb) and Woronin bodies (derived from microbodies; 30). Microbodies and Woronin bodies were specifically and intensely labeled with anti-SKL (Figure 4.6A, B and C). However, not all microbodies within one cell were labeled to the same signal intensity possibly because the specific protein concentration or protein composition varies between microbodies in the same cell. It has been demonstrated previously that certain proteins lacking PTS-1 can be localized in peroxisomes (21,27); these proteins should not be recognized by the anti-SKL preparation. In our studies, labeling of microbodies by Nor-1 and OmtA antibodies was rarely observed. However, we did observe that Woronin bodies but not other microbodies were labeled with anti-Ver-1 (Figure 4.6D and E). Woronin bodies in AFS10 were also labeled to a similar intensity, suggesting that this is non-specific labeling possibly due to a high antibody concentration used or that “contaminating” antibodies bound to cross-reactive proteins located in this organelle (Figure 4.6F and G).

Figure 4.6. Immuno-gold labeling using anti-SKL and anti-Ver-1 in *A. parasiticus* AFS10 and SU1. Ultra-thin sections of fungal tissues obtained from fraction 2 were labeled with primary antibodies to PTS-1 (anti-SKL) (Panels A, B, and C) or primary antibodies to Ver-1 (Panels, D, E, F and G) followed by gold-labeled secondary antibodies as described in Methods. Panels A, B, D, F, and G, represent ultra-thin sections prepared from fungal tissues of AFS10 and Panels C and E represent ultra-thin sections prepared from fungal tissues of SU1. Bars present 250 nm. Abbreviations: **cw**, cell wall; **mb**, microbodies; **wb**, woronin body; **st**, septum; **M**, mitochondria; **V**, vacuole.

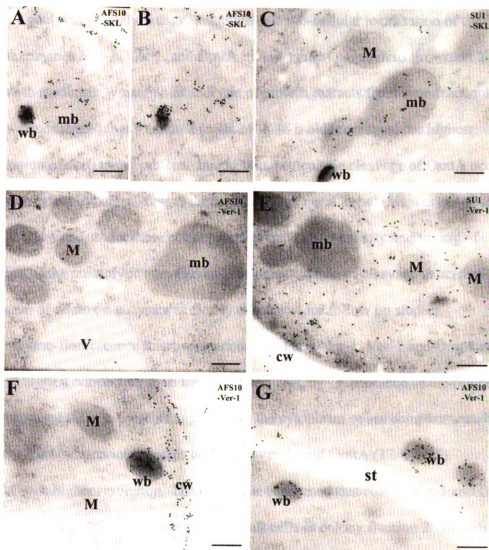


Figure 4.6.

DISCUSSION

My goal was to analyze the distribution and sub-cellular localization of the aflatoxin enzymes Nor-1, Ver-1, and OmtA in *Aspergillus parasiticus* grown on YES agar growth medium. Western blot analysis of protein extracts from time-fractionated colonies demonstrated that fraction 2 (cells 24 to 48 h old) contained the highest concentration of each target protein. In addition, proteolytic cleavage of OmtA occurred to a greater extent in “older” fungal tissues (fractions 1 and 2) but this was not observed for Nor-1 and Ver-1 under these culture conditions. The specificity and timing of expression of the proteolytic enzymes and the potential role of cleavage in activation/inactivation of aflatoxin enzymes is clearly of interest for follow up studies.

Immuno-fluorescence microscopy confirmed that Nor-1, Ver-1 and OmtA are present at highest concentration in fraction 2; the “patchy” appearance of the fluorescent signal suggested that the proteins aggregate in the cytoplasm or are compartmentalized consistent with our previous studies on Nor-1, Ver-1, and OmtA (17, 18, 35).

At even higher resolution, TEM analyses confirmed that Nor-1, Ver-1 and OmtA are present in the cytoplasm of many, but not all cells in colony fraction 2. In addition, most cells located near the basal surface of fraction 2 were closely packed and contained one to several large organelles heavily labeled with gold-labeled antibodies to OmtA. In some cells, the large and small organelles appeared to fuse together consistent with a model for vacuolar development in *Aspergillus* reported previously (22). To our knowledge, this is the first report of aflatoxin enzymes localizing to a specific cellular organelle.

The morphology and apparent developmental origin of the labeled organelles in fraction 2 prompted us to identify them as vacuoles. Vacuoles have been associated with several biological functions in fungi including degradation or recycling of proteins and whole organelles (2), storage of metabolites, ions and amino acids, enzyme maturation (e.g. aminopeptidase I) and pH homeostasis (15,28). Vacuoles are also the site for lipid degradation and glycerol production at specific stages of appressoria formation in *Magnaporthe grisea* (31). In yeast, the biological sulfonium compound, S-adenosyl-methionine (AdoMet), accumulates to high levels in vacuoles and cytoplasm (25,26,13). S-adenosyl-methionine is an important cofactor that provides the methyl group in the reaction catalyzed by OmtA. Based on the available data, it is difficult to determine if the vacuolar localization of OmtA occurs for protein recycling, for enzyme activation, or for some other purpose in *A. parasiticus*.

Although the data appeared quite convincing, it was possible that disruption of organelles occurred during sample preparation and was in part or fully responsible for the observed cytoplasmic location of Nor-1, Ver-1, and OmtA. To minimize this possibility, we demonstrated that the ultra-structure of Woronin bodies and microbodies (bounded by single membranes) and the antigenicity of their content proteins were preserved using our methods for sample preparation and microscopic analysis. These structures were intensely labeled by anti-SKL but not by antibodies to Nor-1 or OmtA. Some labeling of Woronin bodies did occur with anti-Ver-1, however, the observed labeling occurred in both AFS10 (control) and SU1 strains allowing us to interpret this as non-specific labeling. This interpretation appears to be likely because disruption of *afIR* in *A. parasiticus* (such as in AFS-10) results in loss of *nor-1*, *ver-1* and *omtA* gene transcripts

(6,7) and proteins (this study). Therefore, it is unlikely that Ver-1 exists at any location in AFS10.

Similarly, the ultrastructure of double-membrane bound organelles (nuclei and mitochondria) as well as other single-membrane bound organelles (vacuoles) were also maintained in this study. With the exception of vacuoles in the basal region of fraction 2 of SU1, these organelles did not label with antibodies against the aflatoxin enzymes. These results suggest that Nor-1, Ver-1, and OmtA do not localize to nuclei, mitochondria, Woronin bodies, or microbodies. Because the absence of signal in these organelles does not appear to be an artifact arising from organelle breakage, these data strongly support the specificity of labeling of the vacuoles observed in the basal region of fraction 2.

Two observations from this study are particularly noteworthy. First, intensely labeled, weakly labeled and unlabeled cells could be found adjacent to each other in the same thin section analyzed by TEM. It is known that cell components located under the surface of a section are unable to be labeled. However, the cytoplasm proteins such as Ver-1 and Nor-1 in these unlabeled cells were remainly unlabeled even in serial sections. These data suggest that the extent and timing of aflatoxin gene expression varies from cell to cell, even in an area of the colony that is presumably the same age. We propose that this variation may be related to the local concentration of available nutrients or the relative age of fungal cells (5,10,20). Second, OmtA appeared in the cytoplasm in certain cells and in the vacuole in other cells in the same colony fraction. In *Saccharomyces*, cytoplasmic proteins can be transported into vacuoles by at least two alternative pathways: 1) macroautophagy; and 2) the cytoplasm to vacuole targeting (cvt) pathway. The cvt pathway is regulated by the availability or limitation of specific nutrients (e.g.

glucose or ethanol) (15,16,28); to date, no pathway similar to the yeast cvt has been reported in filamentous fungi. However, we propose that transport of OmtA is similar to the cvt pathway in that a specific set of environmental changes (cell age, physiological conditions or nutrient availability) may trigger the transport of OmtA into the vacuole.

Based on data from this and previous studies, it is reasonable to assign two potential alternative roles for the vacuole in aflatoxin synthesis: 1) as a means to reduce or limit aflatoxin synthesis, OmtA is transported to and inactivated in vacuoles via proteolytic cleavage; 2) as a means to shield the cell from the potential toxic effects of aflatoxin in the mycelium, OmtA is transported to the vacuole together with the late aflatoxin pathway intermediate ST. In the vacuole, OmtA is activated and ST is converted to OMST and further converted to AFB₁ by OrdA (24,34) (catalyzes the final step of aflatoxin biosynthesis) localized in or on the same vacuole. These hypotheses form the basis for our future studies on aflatoxin synthesis.

ACKNOWLEDGEMENTS

Chapter 4 was submitted for publication in *Applied and Environmental Microbiology* (2003). Figure 4.2 and Table 4.1 were generated by Ching-Hsun Chiou. We also thank Dr. Shirley Owens for help in quantification of fluorescence intensity and Dr. Xudong Fan in operating the jet-freezer in Center of Advanced Microscopy at Michigan State University.

REFERENCES

1. **Akesson, H., E. Carlemalm, E. Everitt, T. Gunnarsson, G. Odham, and H-B Jansson.** 1996. Immunocytochemical localization of phytotoxins in *Bioplaris sorokiniana*. Fungal Gene. Biol. **20**:205-216.
2. **Amor, C., A. I. Dominguez, J. R. D. Lucas, and F. Laborda.** 2000. The catabolite inactivation of *Aspergillus nidulans* isocitrate lyase occurs by specific autophagy of peroxisomes. Arch. Microbiol. **174**:59-66.
3. **Atkin, A. L.** 1999. Preparation of yeast cells for confocal microscopy. Methods in Molecular Biology. **122**:131-139.
4. **Binder, M., A. Hartig, and T. Sata.** 1996. Immunogold labeling of yeast cells: an efficient tool for the study of protein targeting and morphological alterations due to overexpression and inactivation of genes. Histochem. Cell Biol. **106**:115-130.
5. **Calvo, A. M., R. A. Wilson, J. W. Bok, and N. P. Keller.** 2002. Relationship between secondary metabolism and fungal development. Microbiol. Mol. Biol. Rev. **66**:447-459.
6. **Cary, J. W., K. C. Ehrlich, M. S. Wright, P.-K. Chang and D. Bhatnagar.** 2000. Generation of *afIR* disruption mutants of *Aspergillus parasiticus*. Appl. Microbiol. Biotechnol. **53**: 680-684.
7. **Cary, J. W., M. D. John, K. C. Ehrlich, M. S. Wright, S-H. Liang and J. E. Linz.** 2002. Molecular and functional characterization of a second copy of the aflatoxin regulatory gene, *AflR*, from *Aspergillus parasiticus*. Biochim Biophys Acta. **1576**: 316-323.
8. **CAST.** 2003. Council for Agricultural Science and Technology. Mycotoxins: Risks in plant, animal, and human systems. Report 139.
9. **Chang, P.-K., J. Yu, D. Bhatnagar, and T. E. Cleveland.** 1998. Abstract. The USDA-ARS Aflatoxin Elimination Workshop.
10. **Chiou, C.-H., M. Miller, D. L. Wilson, F. Trail, and J. Linz.** 2002. Chromosomal location plays a role in regulation of aflatoxin gene expression in *Aspergillus parasiticus*. Appl. Environ. Microbiol. **68**:306-315.
11. **Cleveland, T. E., A. R. Lax, L. S. Lee, and D. Bhatnagar.** 1987. Appearance of enzyme activities catalyzing conversion of sterigmatocystin to aflatoxin B₁ in late-growth-phase *Aspergillus parasiticus* cultures. Appl. Environ. Microbiol. **53**:1711-3.

12. **Eaton, D. L. and J. D. Groopman (eds.).** 1994. The toxicology of aflatoxins: human health, veterinary, and agricultural significance. San Diego, CA: Academic.
13. **Farooqui, J. Z., H. W. Lee, S. Kim, and W. K. Paik.** 1983. Studies on the compartmentation of S-adenosyl-L-methionine in *Saccharomyces cerevisiae* and isolated rat hepatocytes. *Biochimica et Biophysica Acta.* **757**:342-352.
14. **Keller, N. P., H. C. Dischinger, JR., D. Bhatnagar, T. E. Cleveland and A. H. J. Ullah.** 1993. Purification of a 40-kDa methyltransferase activity in the aflatoxin biosynthetic pathway. *Appl. Environ. Microbiol.* **36**:270-3.
15. **Klionsky, D. J., P. K. Herman, and S. D. EMR.** 1990. The fungal vacuole: composition, function, and biogenesis. *Microbiol. Rev.* **54**: 266-292.
16. **Klionsky, D. J.** 1997. Protein transport from the cytoplasm into vacuole. *J. Membrane Biol.* **157**: 105-115.
17. **Lee, L.-W., C.-H., Chiou, and J. E. Linz.** 2002. Function of native OmtA *in vivo* and expression and distribution of this protein in colonies of *Aspergillus parasiticus*. *Appl. Environ. Microbiol.* **68**:5718-5727.
18. **Liang, S.-H.** 1996. The function and expression of the *ver-1* gene and localization of the Ver-1 protein involved in aflatoxin B₁ biosynthesis in *Aspergillus parasiticus*. PhD Dissertation, Michigan State University, East Lansing.
19. **Liang, S.-H., T.-S. Wu, R. Lee, F. S. Chu and J. E. Linz.** 1997. Analysis of mechanism regulating expression of the *ver-1* gene, involved in aflatoxin biosynthesis. *Appl. Environ. Microbiol.* **63**:1058-1065.
20. **Luchese, R.H., and W. F. Harrigan.** 1993. Biosynthesis of aflatoxin- the role of nutritional factors. *J. Applied Bacteriology.* **74**: 5-14.
21. **Maeting, I., G. Schmidt, H. Sahm, J. L. Revuelta, Y.-D. Stierhof, and K.-P. Stahmann.** 1999. Isocitrate lyase of *Ashbya gossypii*- transscriptional regulation and peroxisomal localization. *FEBS letters.* **444**:15-21.
22. **Ohsumi, K., M. Arioka, H. Nakajima, and K. Kitamoto.** 2002. Cloning and characterization of a gene (*avaA*) from *Aspergillus nidulans* encoding a small GTPase involved in vacuole biogenesis. *Gene.* **291**:77-84.
23. **Payne, G. A. and M. P. Brown.** 1998. Genetics and physiology of aflatoxin biosynthesis. *Annu. Rev. Phytopathol.* **36**:329-362.
24. **Prieto, R., and C. P. Woloshuk.** 1997. *ord1*, an oxidoreductase gene responsible for the conversion of *O*-methylsterigmatocystin to aflatoxin in *Aspergillus flavus*. *Appl. Environ. Microbiol.* **63**:1661-1666.

25. **Schwencke, J., and H. De Robichon-Szulmajster.** 1976. The transport of S-adenosyl-L-methionine in the isolated yeast vacuoles and spheroplasts. *Eur. J. Biochem.* **65**:49-60.
26. **Svihla, G., J. L. Dainko, and F. Schlenk.** 1969. Ultraviolet micrography of penetration of exogenous cytochrome c into the yeast cell. *J. Bacteriol.* **100**:498-504.
27. **Taylor, K. M., C. P. Kaplan, X. Gao, and A. Baker.** 1996. Localization and targeting of isocitrate lyases in *Saccharomyces cerevisiae*. *Biochem. J.* **319**:255-262.
28. **Thumm, M.** 2000. Structure and function of the yeast vacuole and its role in autophagy. *Microscopy Research and Technique.* **51**: 563-572.
29. **Trail, F., P.-K. Chang, J. Cary and J. E. Linz.** 1994. Structural and functional analysis of the *nor-1* gene involved in the biosynthesis of aflatoxin by *Aspergillus parasiticus*. *Appl. Environ. Microbiol.* **60**:3315-3320.
30. **Valenciano, S., J.R. De Lucas, I. Van der Klei, M. Veenhuis, and F. Laborda.** 1998. Characterization of *Aspergillus nidulans* peroxisomes by immunoelectron microscopy. *Arch. Microbiol.* **170**:370-376.
31. **Weber, R. W. S., G. E. Wakley, E. Thines, and N. J. Talbot.** 2001. The vacuole as element of the lytic system and sink for lipid droplets in maturing appressoria of *Magnaporthe grisea*. *Protoplasma.* **216**:101-112.
32. **Xu, H and K. Mendgen.** 1994. Endocytosis of 1,3- β -glucans by broad bean cells at the penetration site of the cowpea rust fungus (haploid stage). *Planta.* **195**:282-290.
33. **Yu, J., J. W. Cary, D. Bhatnagar, T. E. Cleveland, N. P. Keller, F. S. Chu.** 1993. Cloning and characterization of a cDNA from *Aspergillus parasiticus* encoding an O-methyltransferase involved in aflatoxin biosynthesis. *Appl. Environ. Microbiol.* **59**:3564-71.
34. **Yu, J., P.-K. Chang, K. C. Ehrlich, J. W. Cary, D. Bhatnagar, and T. E. Cleveland.** 1998. Characterization of the critical amino acids of *Aspergillus parasiticus* cytochrome P-450 monooxygenase encoded by *ordA* that is involved in the biosynthesis of aflatoxin B₁, G₁, B₂ and G₂. *Appl. Environ. Microbiol.* **64**:4834-4841.
35. **Zhou, R.** 1997. The function, accumulation, and localization of the Nor-1 protein involved in aflatoxin biosynthesis; the function of the *fluP* gene associated with sporulation in *Aspergillus parasiticus*. PhD Dissertation, Michigan State University, East Lansing.

CHAPTER 5

Detection of aflatoxin B₁ in fungal spores and colonies

INTRODUCTION

The biological function of aflatoxin in the producing fungus is still not clear. Since aflatoxins are secondary metabolites and synthesized primarily during stationary phase, they are not necessary for primary growth of the cell. It has been shown previously that the production of sterigmatocystin (ST) in *A. nidulus* and aflatoxin in *A. parasiticus* is closely associated with asexual sporulation (2), and positively regulated by FlbA (1). Although the details of the connection between production of aflatoxin and fungal sporulation are entirely not clear, the presence of aflatoxins in asexual conidiospores has been reported (4,6). Since spores are important structures involved in dispersal and colonization, one of the proposed function of aflatoxins is to provide the fungus with a survival advantage by overcoming environmental threats (e.g. resistance to UV light). The aflatoxin concentrations in spores harvested from different media were estimated. Wicklow and Shotwell (1982) reported that conidiospores harvested from Czapek agar cultures (grown in the dark at 28° C for 21 days) contained 1,106 to 54,300 ppb (ng/g) of AFB₁ in four *A. parasiticus* strains and 36 to 97,400 ppb in five *A. flavus* strains. Palmgren and Lee (1986) reported that conidiospores harvested from *A. parasiticus* (SRRC-2004) cultured on autoclaved rice at 25°C for 7 days contained 166,000 ppb of AFB₁. In contrast to aflatoxin distribution in wild-type strains, the distribution of the

aflatoxin intermediate, Nosolorinic acid (NA), in a *nor-1* mutant is mainly in vegetative mycelia.

In the present study, I wanted to compare: 1) the distribution of aflatoxin between colony and substrate (agar); and 2) the aflatoxin concentration in spores harvested under wet and dry conditions. Although the aflatoxin gene cluster contains an *aflT* gene, which may function as a toxin transporter, no data in the literature have demonstrated that a specific secretion system including AflT is used to transport aflatoxin into the environmental media. In this study, I measured the aflatoxin concentration in time fractionated colonies grown for different total times and compared the aflatoxin distribution between fungal colonies and the substrate media. My results showed that, in YES cultures ranging from 2 days to 5 days of age, the ratio of aflatoxin in the fungal mycelium and total aflatoxin produced decreased with culture time. However, for an unknown reason, the ratio increased at days 6 and 7. In addition, culture media affected the distribution of aflatoxin in the mycelium. Compared with 60% in YES culture, only 20% of the total aflatoxin was detected in fungal mycelium cultured on PDA agar. Based on the current data, the nature of the specific transport system for aflatoxin can not be determined yet. My data also showed that there is a 10-fold difference in aflatoxin concentration between conidiospores isolated under wet and dry conditions. The higher concentration obtained from spores harvested under wet conditions is due to absorption of aflatoxin from water used for harvest onto the surface of the spores.

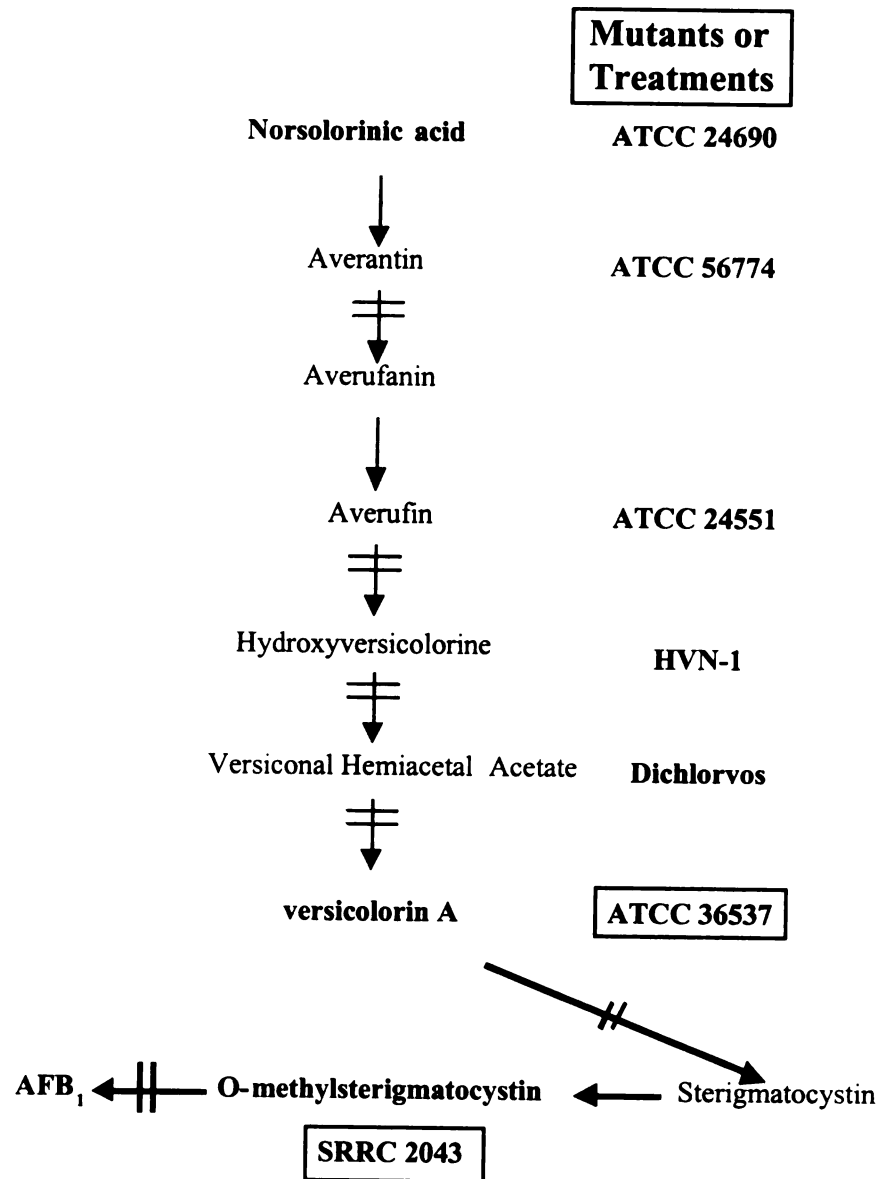


Figure 5.1. Mutants in the aflatoxin biosynthetic pathway.

MATERIAL AND METHODS

Fungal strains. *A. parasiticus* SU1(NRRL5862, ATCC 56775) is a wild-type, aflatoxin-producing strain. *A. parasiticus* RHN1 (SRRC2043; *ordA*) accumulates the aflatoxin intermediate OMST and ATCC36537 (*ver-1*) accumulates VA (Figure 5.1).

Aflatoxin distribution in time-dependent fractionated colonies of SU1 grown on solid medium. To determine the accumulation and distribution of aflatoxin in fungal colonies grown on solid culture media, conidiospores (2×10^5) of *A. parasiticus* SU1 were inoculated onto the center of YES or PDA agar overlaid with sterilized cellophane membranes and incubated at 29° C in the dark. Colonies were analyzed after 2, 3, 4, 5, 6 and 7 d of growth. The 2 d-old colonies were harvested directly without fractionation. Colonies older than 2 d were marked at the edge every 24-h as an indicator for future cutting. For example, the 3 d-old colony was fractionated into two concentric rings (ring-1 and 2) based on area covered at the two time points: Ring-1 (48 h) contained mycelia from the colony center out to a distance of 2.5 cm (24 to 72 h) and Ring-2 (0 to 24 h) contained mycelia from 2.5 to 4.2 cm (0 to 24 h) (Figure 5.2 and Table 5.1). The harvested mycelia from appropriate fractions were weighed and extracted with chloroform. The chloroform extracts were evaporated and resuspended in methanol. In the same culture, the substrate (agar) and membrane were also analyzed for aflatoxin levels. The aflatoxin concentrations were determined by ELISA (5)

Spores harvested by water (wet conditions). 1) In early experiments, the fungus was grown on a nylon membrane on PDA agar plates at 29° C in the dark for 7 d.

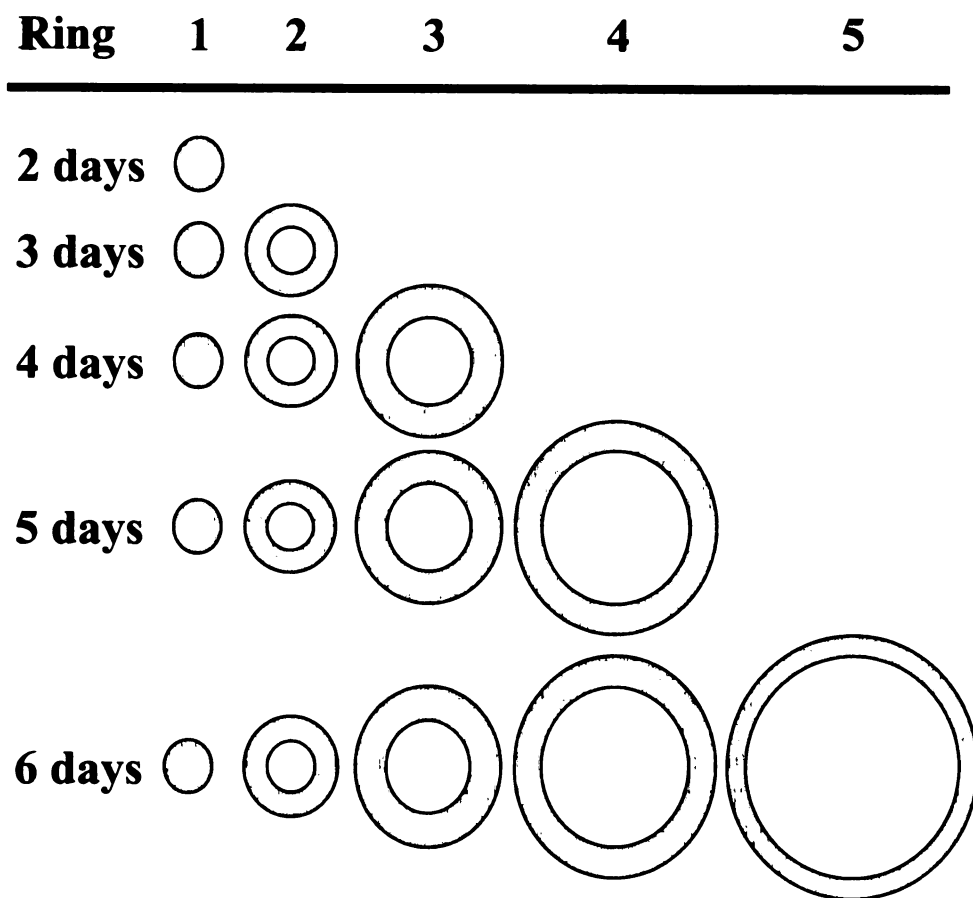


Figure 5.2. Diagram of colony fractionation.

Table 5.1. Fractionation of fungal colonies at different ages.

Age\Diameter (cm)	2.5	2.5-4.2	4.2-5.0	5.0-6.5	6.5-8.0
2d	Ring-1				
3d	Ring-1	Ring-2			
4d	Ring-1	Ring-2	Ring-3		
5d	Ring-1	Ring-2	Ring-3	Ring-4	
6d	Ring-1	Ring-2	Ring-3	Ring-4	Ring-5

Spores were released from conidiophores into water (harvest water) by mechanical force. Colonies with membranes were immersed into the water and the surface of the colony was scraped with a spatula. The water containing spores was passed through glass wool to remove any hyphal fragments. Spores were pelleted from the water by centrifugation at 3,000 x RPM for 20 min. Both water and spores were measured for aflatoxin concentrations. 2) In later experiments, fungal strains, including SU1, RHN1 (SRRC2043) and ATCC36537, were grown on cellophane membranes laid onto PDA agar plates and incubated at 29°C in the dark for 7 d. For spore isolation, the whole colony was removed from the cellophane into a 50-ml conical tube and 35 ml of water was dispensed into the tube. Spores were released into the harvest water by rocking the tube back and forth for 1 min. The spore-containing water was then filtered through glass wool. Spores were pelleted by centrifuged at 20,000 x g for 15 min and resuspend in 1 ml of H₂O. The resulting spore pellet and the harvest water were used in binding assays as described in the following section to test their ability to absorb aflatoxin (AFB₁ and G₁) and aflatoxin intermediates (OMST and VA) contained in the harvest water. The AFB₁ and G₁ or OMST-containing water used in the binding experiment were further filtered through 0.22 µm or 0.45 µm filters to eliminate any contaminating spores. In addition, to make sure that the aflatoxin and pathway intermediates would not block the filter membrane, the filtered water and only centrifuge-treated water (without passing through filter) were examined under a microscope and analyzed by TLC analysis in parallel. No spores were observed in the filtered water, but a small quantity of spores were observed in the centrifuge-treated water. In both treatments, AFB₁, AFG₁ and OMST were all detected in harvest water by TLC analysis (Figure 5.3).

Binding of AFB₁, AFG₁, OMST, and VA in harvest water by spores. Spores isolated from the non-aflatoxin producing strain RHN1 (accumulates only OMST) were used to study the binding of AFB₁ and AFG₁ in harvest water. Spores isolated from aflatoxin-producing strain SU-1 (accumulates only AFB₁ and G₁) were used to study the binding of OMST and VA in harvest water. The same numbers of spores (2×10^7) were used in the binding assay and for extraction of aflatoxin and OMST for comparison.

The RHN1 spores were mixed with harvest water (1 ml) containing AFB₁ and G₁ (saved from a SU-1 spore preparation) for 10 min and then spun down at 20,000 x g for 15 min. The spores were washed once with 1 ml of pure water and spun down again (same conditions). Spores were finally resuspended in 1 ml of water and extracted with 0.5 ml of chloroform. 10 µl of spore extracts was analyzed in parallel with other extracts, including the harvest water, spores before binding, and toxin extracted from a whole colony, by TLC. The same procedure was applied to the binding of OMST and VA from harvest water by SU-1 spores.

Spores harvested by cotton-tipped applicators. A method to harvest spores under dry conditions was developed. The colony surface was gently swabbed with cotton-tipped applicators and the spores attached to the applicator were then released into water by stirring the applicator in the water. A new applicator was used each time to touch the colony surface. In this dry-harvested method, water was never directly in contact with the colony during spore harvest. The spore-containing water (total 8 ml) was then filtered through glass wool. Spores were pelleted by centrifugation as described above. The water was saved for future aflatoxin measurement. The spore pellet was dried under vacuum with heat (60 °C) for 4 h. The AFB₁ concentrations were determined by ELISA.

RESULTS

Aflatoxin distribution in time-dependent fractionated colonies of SU1 grown on solid medium. The total aflatoxin produced by a colony increased with time during the first 4 days, declined at d 5, and then increased at d 6 and 7 (Table 5.2). The total aflatoxin in the mycelium also reached a peak at d 4 and then decreased at d 5 (Table 5.2). A similar pattern was observed in the agar (Table 5.2). These results suggest that, for unknown reasons, the detectable aflatoxin decreased between d 4 and 5. The ratio of aflatoxin in the mycelium to total AFB1 tended to decline with time until d 5 (Table 5.2) and then increased at d 6 (40 and 46 %) and d 7 (61%). By monitoring dry weight in the same fraction isolated from different age of colonies, the results suggest that the fungus is not only growing outward (two-dimensions) but also growing upward (three dimensions) with increased time (Table 5.3). As shown by dry weights measured in Ring-2, the regular rate of growth is 0.12 g per d (Table 5.3). Approximately 10 µg of aflatoxin were detected in the Ring 2 (0-24 h-old) of a 72 h-old colony. Over the next 24 h (24-48 h-old), aflatoxin in Ring 2 rapidly accumulated (6-fold increase in concentration) and the accumulation then declined (Table 5.4). The aflatoxin concentrations in each fraction isolated from two 6-d colonies varied even they were cultured at the same time (Table 5.4 and 5.5). This variation may be explained by the observation that a part of the edge of colony-No. 2 made contact with the Petri dish. That contact may affect a normal fungal growth and the normal physiology of the fungal cells. Similarly for 7-d old colony, the colony margin reached the edge of plate, which appeared to result in an increase in aflatoxin content.

Table 5.2. Total aflatoxin detected in a colony, agar and membrane from different aged colonies.

Day of sample and Colony No.	Membrane (µg)	Agar (µg)	Mycelium (µg)	Total (µg)	Mycelium / Agar /Total (%)	
YES						
2 d-1	0.1	8	8	16	100	50
2	0.1	7	10	17	140	59
3	1	10	16	27	160	59
3 d-1	2	63	94	159	150	59
2	6	98	87	191	90	46
4 d-1	2	155	143	300	90	48
2	9	191	133	333	70	40
5 d-1	2	138	77	217	60	35
2	7	153	80	240	60	33
6 d	11	286	218	515	80	42
7 d	14	257	420	691	160	61
PDA						
7 d-1	19	301	86	406	30	21
2	25	460	67	552	10	12

Table 5.3. Dry weight (g) of fractionated mycelium from different aged colonies.

Age/Fraction	Ring 1 g	Ring 2 g	Ring 3 g	Ring 4 g	Ring 5 g	Total g
YES						
2 d	0.128					0.128
3 d	0.200	0.135				0.335
4 d	0.238	0.250	0.216			0.704
5 d	0.247	0.374	0.300	0.217		1.138
6 d-1	0.407	0.502	0.438	0.548	0.327	2.222
-2	0.306	0.369	0.420	0.551	1.273	2.919
7 d						3.107
PDA						
7 d-1						1.263
-2						1.328

Table 5.4. Total aflatoxin (μg) in fractionated mycelium from different aged colonies.

Age/Fraction	Ring 1	Ring 2	Ring 3	Ring 4	Ring 5
	μg	μg	μg	μg	μg
2 d	16				
3 d	75	12			
4 d	46	74	13		
5 d	35	29	13	3	
6 d-1	47	60	37	19	4
-2	54	87	57	59	12

Table 5.5. Normalized aflatoxin levels (μg of aflatoxin/g dry weight mycelium) in fractionated mycelium from different aged colonies.

Age/Fraction	Ring 1	Ring 2	Ring 3	Ring 4	Ring 5	Total/w.t
	$\mu\text{g/g}$	$\mu\text{g/g}$	$\mu\text{g/g}$	$\mu\text{g/g}$	$\mu\text{g/g}$	$\mu\text{g/g}$
YES						
2 d	125					125
3 d	375	89				260
4 d	193	296	60			189
5 d	142	78	43	14		70
6 d-1	115	120	84	35	12	75
-2	176	236	136	107	9	92
7 days						135
PDA						
7 d-1						68
-2						50

Binding of AFB₁ and pathway intermediates in water by spores. Spores harvested under wet conditions (by water) contained 10-fold higher AFB₁ concentration (1350 ng/mg) than under dry conditions (by cotton-tipped applicator) (average 114 ng/mg) (Table 5.6). Based on TLC analysis, the explanation for the higher concentration in wet-harvested spores is that they absorb aflatoxin from water used in spore harvest—this presumably arises from the mycelium. This is supported by the binding assay. In this experiment, SU1 spores were demonstrated to bind OMST from water used to harvest RHN-1 spores and RHN-1 spores bound AFB₁ and AFG₁ from water used to harvest SU1 spores. Before the binding assay, TLC analysis showed that only AFB₁ and G₁ were detected in extracts of SU1 spores and water used to harvest SU-1 spores, and only OMST was detected in extracts of RHN1 spores and water used to harvest RHN-1 spores (Figure 5.3 and Fig. 5.4, lane 3 and 4). After binding, AFB₁, G₁, and OMST were detected in an extract of RHN1 spores (Figure 5.4, lane 5 and 6); and were also detected in extracts of SU1 spores (Figure 5.6, lane 4). The AFB₁ and AFG₁ concentrations detected on RHN1 spores were very similar to the amount detected on SU-1 spores suggesting efficient binding (Figure 5.4). VA was not detected in extracts of ATCC36537 spores and water used to harvest spores but was detected in extracts of the whole colony (Figure 5.5). Because VA was not detected in the water used to harvest spore, it is not surprising that it was also not detected in extracts of SU-1 and RHN1 spores after the binding assay (Figure 5.5 and Figure 5.6, lane 2, 3, 6 and 7). Possible explanations for the lack of detectable VA in water used to harvest spores are the solubility of VA in water is very low or the quantity of VA secreted on the colony surface is very low.

Table 5.6. Aflatoxin detected in conidiospores isolated under wet and dry conditions from *A. parasiticus* grown on YES and PDA agar.

	Spore			Water		
	Wt ^b . (mg)	Total (ng)	Conc. ^c (ng/mg)	Vol. ^d (ml)	Total (ng)	Conc. (ng/ml)
Dry^a						
YES	3.0	156	52			
	1.3	226	174	8	194	24
PDA	1.0	135	135	8	72	9
	3.0	351	117	8	74	9
Wet						
PDA	10.0	16215	1622			
	10.0	14177	1418			
	9.9	11621	1174	50	63000	1260
	8.5	10140	1193	50	42400	848

a: Water used in dry spore-harvest did not directly contact the colony. **b:** Dry weight. **c:** Concentration. **d:** Volume.

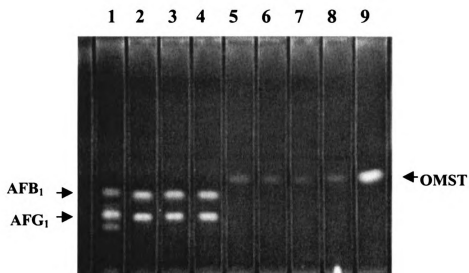


Figure 5.3. Thin layer chromatography of aflatoxin and OMST in water used for spore harvest.

Lane 1. AFB₁, B₂, G₁, G₂ standards. Lane 2. Water used to harvest SU1 spores (centrifuged to remove spores). Lane 3. Water used to harvest SU1 spores (0.22 μ m filtrate). Lane 4. Water used to harvest SU1 spores (0.45 μ m filtrate). Lane 5. Water used to harvest RHN1 spores (centrifuged to remove spores). Lane 6. Water used to harvest RHN1 spores (0.22 μ m filtrate). Lane 7. Water used to harvest RHN1 spores (0.45 μ m filtrate). Lane 8. Fluid (brown color) collected from the surface of RHN1 colony. Lane 9. OMST standard.

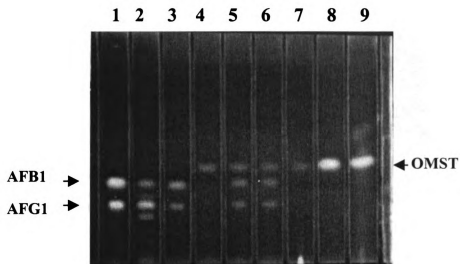


Figure 5.4. Thin layer chromatography of RHN1 spore extracts.

Lane 1. SU1 whole colony extract. Lane 2. AFB₁, B₂, G₁ and G₂ standards. Lane 3. SU1 spore extract. Lane 4. RHN1 spore extract. Lane 5. RHN1 spores mixed with water used to harvest SU1 spores (0.22 um filtrate). Lane 6. RHN1 spores mixed with water used to harvest SU1 spores (0.45 um filtrate). Lane 7. Fluid (brown color) collected from the surface of RHN1 colony. Lane 8. OMST standard. Lane 9. RHN1 whole colony extract.

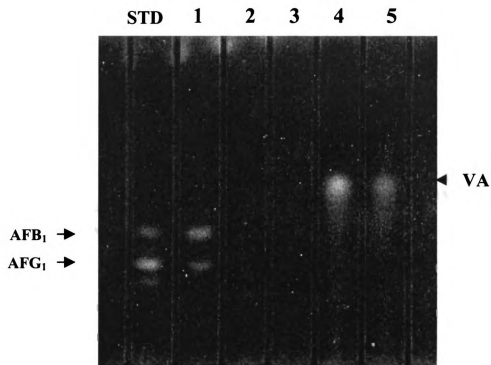


Figure 5.5. Thin layer chromatography of SU1 and ATCC36537 spore extracts.

Lane 1. SU1 spore extract. Lane 2. ATCC 36537 spore extract. Lane 3. ATCC 36537 spore extract. Lane 4. ATCC 36537 whole colony extract. Lane 5. VA standard.

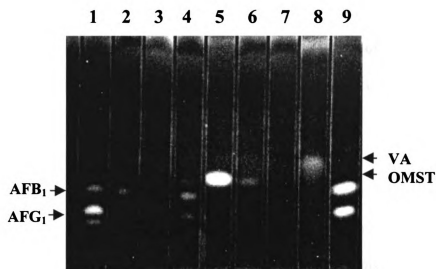


Figure 5.6. Thin layer chromatography of SU1 and RHN1 spore extracts after binding with water used to harvest ATCC36537 spores.

Lane 1. AFB₁, B₂, G₁ and G₂ standards. Lane 2. Extract of SU1 spores mixed with water used to harvest ATCC36537 spores (0.22 μ m filtrate). Lane 3. Extract of ATCC36537 spores. Lane 4. Extract of SU1 spores mixed with water used to harvest RHN1 spores (0.22 μ m filtrate). Lane 5. OMST standard. Lane 6. Extract of RHN1 spores mixed with water used to harvest ATCC36537 spores (0.22 μ m filtrate). Lane 7. Water used to harvest ATCC36537 spores (0.22 μ m filtrate). Lane 8. VA standard. Lane 9. SU1 whole colony extract.

AFB₁ concentrations in spores harvested under dry condition. The AFB₁ concentrations in spores were also measured in spores harvested under dry conditions (Table 5.6). Spores harvested from two cultures (PDA and YES) contained concentrations from 50 to 174 ng of aflatoxin per mg of spores, which is about 10 fold lower than the results using a wet harvest method. Only 73 to 194 ng of aflatoxin was detected in water used to release spores from cotton tips of applicators.

DISCUSSION

In preliminary experiments, *Aspergillus* was cultured on nylon membranes on which the mycelia was firmly attached; the bottom portion of the mycelia could not be completely recovered for analysis and, therefore, this caused difficulty in estimating the aflatoxin concentration in the colony. This problem was solved by replacing the nylon membrane with a cellophane membrane; the mycelia could be fractionated and completely removed from the cellophane membrane

The colony fractionation results showed that, from day 2 to day 5, the ratio of aflatoxin in the fungal mycelium to total aflatoxin produced by the colony decreased. However, the ratio then increased at day 6 and 7. One possible explanation is that the colony edge made contact with the Petri dish at day 6. This possibly could be a signal to the fungus that the space and nutrients are limited, resulting in a change in the normal physiological conditions to promote aflatoxin production. Another possible explanation is a pH change in the medium. As reported by Mellon *et al.*, the pH in the medium dropped to be its lowest value at day 5 (under their culture conditions), possibly stimulating higher levels of aflatoxin synthesis in the mycelium (3).

The media used was observed to affect the distribution of aflatoxin within and outside of the fungal colony. Whereas 80% of the aflatoxin was released into the medium when cultured on PDA agar for 7 days, more than 50% of the aflatoxin was found in the mycelium cultured on YES agar. The reason for this is not clear but may be related to the level of sporulation. I can observe two major differences in colony morphology on PDA: more green spores and less mycelial mass. Although it has been previously hypothesized that aflatoxin synthesis and asexual sporulation are tightly associated (2,4,6), no estimation was conducted on the relative distribution of aflatoxin in the fungal mass and the culture medium. Researchers previously measured aflatoxin in the medium only or in whole culture extracts (mycelium and medium). I hypothesize that, since spores are important structures for dispersal and colonization, if aflatoxin is harmful (carcinogen) to the fungus, then the ability to reduce aflatoxin concentration inside of fungal mycelium prior to and during spore production could be necessary to prevent mistakes in DNA replication caused by DNA adduct formation. Therefore, a related hypothesis is that the substrate mycelium is still highly active in aflatoxin production but the toxin is secreted outside of the mycelium to prevent toxin accumulation. This mechanism could enhance the precise production of spores by conidiophores.

It is obvious that spores harvested under dry conditions have a much lower aflatoxin concentration than those collected under wet conditions (with water). The water used to harvest spores contains high aflatoxin concentrations and is responsible for the higher aflatoxin detected in spores as compared to mycelium. Under dry harvest conditions, the water used to release the spores from the cotton-tipped applicator contained very low but detectable amounts of aflatoxin. The traces of aflatoxin in this water may come from the fluid on the colony surface, absorbed by applicator and released

into water. In support of this notion the brown-colored liquid collected from the colony surface of RHN1 contained significant levels of OMST (Figure 4, lane 7). We believe this fluid on the colony surface was secreted by fungal cells.

It has been demonstrated previously that the variation in spore aflatoxin concentration between strains was high and was affected by the culture conditions and spore-harvest methods (4,6). Wicklow and Shotwell (1982) reported that conidiospores harvested from Czapek agar cultures (in the dark at 28° C for 21 days) using water contained a range of 1,106 to 54,300 ppb (ng per g) of AFB₁ in four *A. parasiticus* strains and a range of 36 to 97,400 ppb in five *A. flavus* strains. Palmgren and Lee (1986) reported that the conidia harvested from *A. parasiticus* (SRRC-2004) cultured on autoclaved rice and incubated at 25°C for 7 days contained 161,000 ppb (161 ng per mg) of AFB₁. In this report, the spores were harvested by vacuum (dry conditions). Based on our data, we suspect that the real aflatoxin concentration in spores in Wicklow (1982) was likely 10-fold lower than that reported because Czapek agar media is not a good aflatoxin-inducing media. In addition, the method used to harvest the spores (similar to the wet condition reported in our study), caused an artificially high concentration of aflatoxin detected in spores; the aflatoxin extracted from the colony bound to the spore surface. The results reported by Palmgren (4) were similar to ours (proximately 126 ng per mg); we believe these data generated using a dry-harvest method more closely represent the actual concentration in spore.

My current data show that both fungal hyphae and spores isolated from aflatoxin-producing strains contain aflatoxin. However, for a *nor-1* mutant, spores (harvested by vacuum) contained very low amount of NA (280 ng per g of spores) as compared with mycelia (760 ug per g) (4). This observation prompts us to propose that aflatoxin is

synthesized in the mycelium and then needs to be transported to spores. In this regard, it will be interesting to determine if all aflatoxin intermediates or only certain pathway-intermediates can be accumulated in spores.

REFERENCES

1. **Adams T. H. and J-H. Yu.** 1998. Coordinate control of secondary metabolite production and asexual sporulation in *Aspergillus nidulans*. *Curr Opin Microbiol.* **1**: 674-677.
2. **Guzman-de-Pena D and J. Ruiz-Herrera.** 1997. Relationship between aflatoxin biosynthesis and sporulation in *Aspergillus parasiticus*. *Fungal Genet Biol.* **21**:198-205.
3. **Mellon, J. E., P. J. Cotty, and M. K. Dowd.** 2000. Influence of lipids with and without other cottonseed reserve materials on aflatoxin B₁ production by *Aspergillus flavus*. *J. Agric. Food Chem.* **48**:3611-3615.
4. **Palmgren M.S. and L.S. Lee.** 1986. Separation of mycotoxin-containing sources in grain dust and determination of their mycotoxin potential. **66**:105-108.
5. **Pestka, J. J., P. K. Gaur, and F. S. Chu.** 1980. Quantitation of aflatoxin B₁ and aflatoxin B₁ antibody by an enzyme-linked immunosorbent microassay. *Appl. Environ. Microbiol.* **40**:1027-1031.
6. **Wicklowsky, D. T., and O. L. Shotwell.** 1983. Intrafungal distribution of aflatoxins among conidia and sclerotia of *Aspergillus flavus* and *Aspergillus parasiticus*. *Can. J. Microbiol.* **29**:1-5.

CHAPTER 6

Future Studies

Based on the current data, it is difficult to determine if the vacuolar localization of OmtA occurs for protein recycling, for enzyme activation, or for some other purpose in *A. parasiticus*. The compartment for storage of aflatoxin B₁ in the fungus was also not determined in this study. We propose three alternative models for synthesis and export of aflatoxin from fungal cells that are consistent with data from this and previous studies. We propose these models as a primary means to design future research directions (Figure 6.1).

Model 1. Aflatoxin enzymes aggregate in large complexes in the cytoplasm to carry out sequential reactions efficiently. Aflatoxins are synthesized in the cytoplasm and are transported to the extra-cellular environment via AflT (with identity to a transproter protein), via another transporter, or via direct release into the extra-cellular environment when cells die. To fine tune the level of (reduce or limit) aflatoxin synthesis, aflatoxin enzymes (OmtA in particular) are transported to and inactivated in vacuoles by proteolytic cleavage.

Model 2. Aflatoxin enzymes form complexes in the cytoplasm to generate the late pathway intermediate sterigmatocystin (ST); the intermediates in the pathway upstream from ST are passed directly from one active site to the next in the enzyme complex limiting the quantity of free intermediates in the cytoplasm. OmtA is synthesized and participates as one enzyme in the complex but it is present in inactive form. As ST bound to OmtA accumulates in the complexes, OmtA carries ST into

vacuoles in cells near the basal surface of the colony. Proteolytic cleavage activates OmtA that then converts ST to OMST. OrdA, also localized to the vacuole, converts OMST to AFB₁ that accumulates in the vacuole. As it fills, the vacuole fuses with the cell membrane and releases AFB₁ into the external environment at the basal surface (substrate surface) of the fungal colony. Purified native OmtA has a molecular weight about 40 kDa. Based on the nucleotide sequence of the cDNA, OmtA has a predicted molecular mass of 45 kDa suggesting that a 5 kDa peptide is cleaved from its N-terminus. This cleavage could inactivate OmtA as proposed in Model 1 or activate OmtA as proposed in Model 2. In support of this idea, Western blot analysis demonstrated that OmtA is cleaved in fungal cells and the first cleavage releases a peptide of the predicted size.

Model 3. This model is similar to Model 2 except OmtA is functional in the cytoplasm. OmtA and its product, OMST, are transported together to the vacuole where OMST is converted to AFB₁ by OrdA.

Three experiments will be conducted in the future to allow discrimination between these models: 1) co-immunoprecipitation, 2) subcellular fractionation, 3) *in situ* localization of OrdA by immunoelectron microscopy (IEM). Results from Experiment 1 will answer the question whether aflatoxin proteins can form protein aggregates to carry out several reactions together. Results from Experiment 2 and 3 will answer the question regarding where OrdA (60 kDa) and aflatoxins are compartmentalized. The purified organelles will be used to test their ability to convert OMST to AFB₁ in feeding experiments; they will also be freeze-substituted and immunolabeled to confirm protein localization. The protein content extracted from isolated organelles will be assayed to determine their aflatoxin protein profile using Western blot analysis. To assist in these experiments, the required OrdA antibody was generated using similar procedure as

described in Chapter 3. The specificity of this antibody was tested by Western blot analysis, and the results are shown in Figure 6.2. In addition, a MBP-AflJ fusion protein and AflJ antibody were also produced (Figure 6.3). These reagents will be used in Experiment 1 to test the possibility that the protein-protein interaction between AflJ (47 kDa) and AflR (and other transcription factors) or proteins involved in microbody targeting pathway.

The primers used in PCR to clone *ordA* cDNA were: 5'- ATG ATT TCTAGA ATA ATT ATT TGT GCG G-3' and 5'- GTA AAGCTT TCA AAT CAT CTG ATT-3'. The primers used to clone *aflJ* cDNA were: 5'- TCC TCTAGA ATG ACC TTG ACT GAC CTA G-3' and 5'- CAT AAGCTT TTA ATA TCG GTT GTC ATC G -3'. (XbaI restriction sequence: TCT AGA; HindIII: AAG CTT).

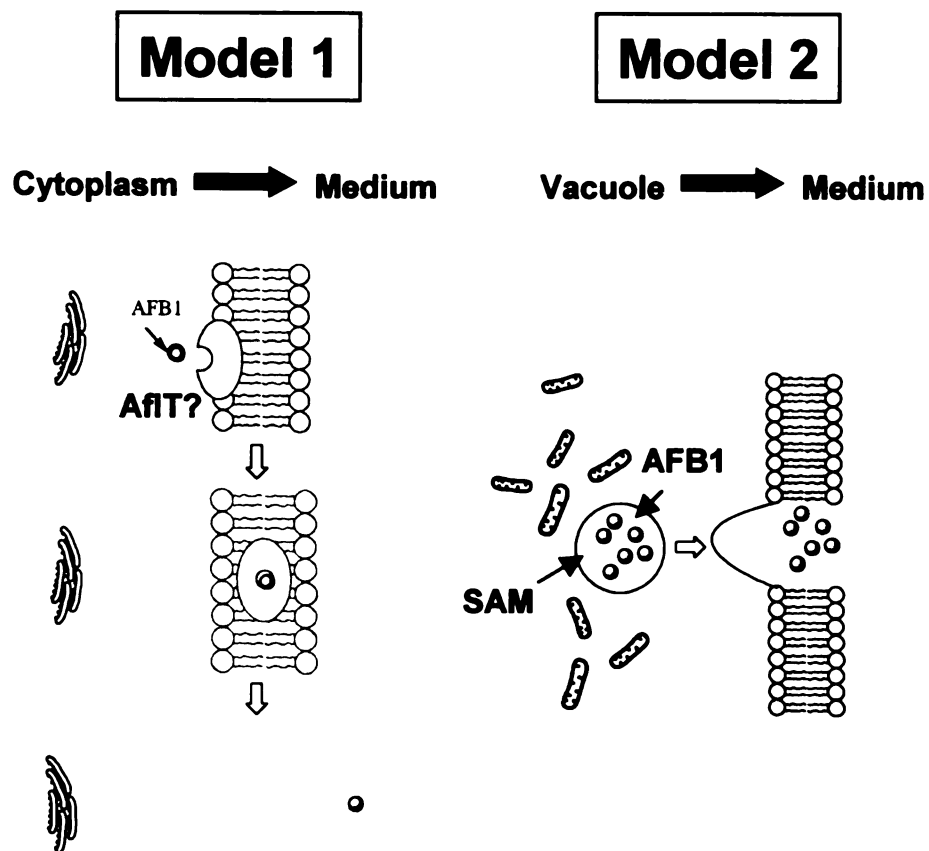


Figure 6.1. Proposed models for synthesis and export of aflatoxin from fungal cells.

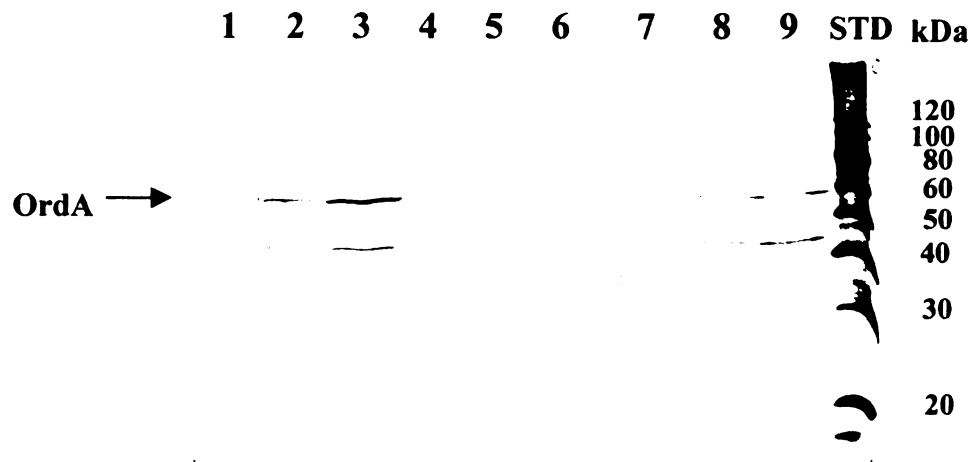


Figure 6.2. Western blot analysis of fungal protein extracts using affinity-purified OrdA PAb. Proteins were extracted from time-fractionated colonies of SU-1 and AFS10 grown on YES agar medium. 60 μ g of protein was loaded in each lane on SDS-PAGE. OrdA antibody (#137) was purified by a column packed with AFS10 (*afIR* knockout) protein. OrdA antibody was used at a concentration of 6 μ g per ml in the experiment. Lane 1, S1 fraction; 2, S2 fraction; 3, S3 fraction; 4, R1 fraction; 5, R2 fraction; 6, R3 fraction; 7, S_{2cm} fraction; 8, S_{4cm} fraction; 9, S_{6cm} fraction. Lane STD contains molecular mass standards; mass of standards is shown at the right side of blot. S_{2cm}, S_{4cm}, and S_{6cm} are fractions isolated from SU-1 colonies grown for 90-h and were fractionated according to their diameters. S_{2cm} covers from center to 2cm; S_{4cm}, 2 to 4 cm; S_{6cm}, 4 to 6 cm.

Figure 6.3. Production of MBP-AflJ fusion protein and AflJ antibody.

(A) SDS-PAGE of IPTG- induced bacterial crude extracts containing MBP-AflJ. Lane 1, Non-induced bacterial crude extract; 2, IPTG- induced bacterial crude extract; 3, Molecular mass standards; molecular mass is indicated to the right of the gel.

(B) SDS-PAGE of affinity purified MBP-AflJ. Lanes 1, Affinity-purified MBP-AflJ; 2, Molecular mass standards; molecular mass is indicated to the right of the gel.

(C) Western blot analysis of fungal protein extracts using AflJ PAb (#124). Proteins were extracted from time-fractionated colonies of SU-1 and AFS10 grown on YES agar medium. 60 µg of protein was loaded in each lane on SDS-PAGE. AflJ antibody was used at 1 to 1000 dilution in the experiment. Lane 1, Molecular mass standards; mass of standards is shown at the left side of blot; 2, S1 fraction; 3, S2 fraction; 4, S3 fraction; 5, R1 fraction; 6, R2 fraction; 7, R3 fraction.

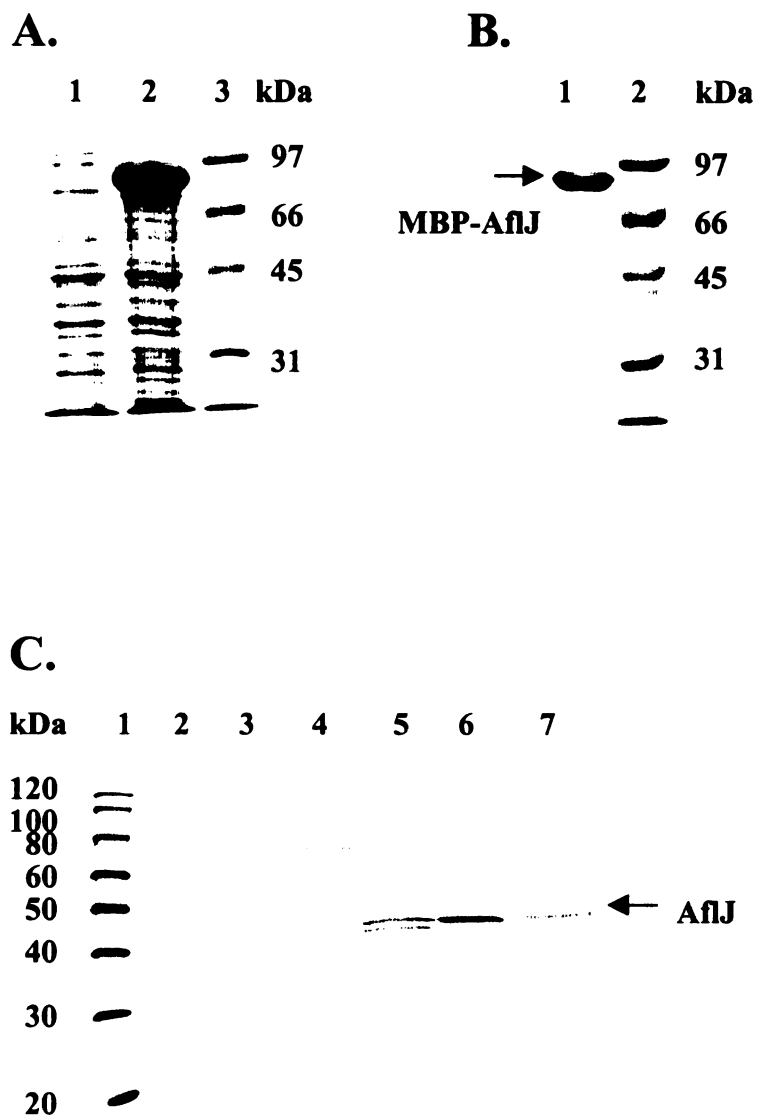


Figure 6.2